REVISTA

DE PIELĂRIE ÎNCĂLŢĂMINTE

Leather and Footwear Journal

December / Decembrie 2025
Volume / Volumul 25
Issue / Ediția 4

INCDTP - SUCURSALA INSTITUTUL DE CERCETĂRI PIELĂRIE ÎNCĂLŢĂMINTE
INCDTP - DIVISION: LEATHER AND FOOTWEAR RESEARCH INSTITUTE

PIELĂRIE/LEATHER ÎNCĂLŢĂMINTE/FOOTWEAR BUNURI DE CONSUM DIN CAUCIUC/RUBBER GOODS

AIMS AND SCOPE

Revista de Pielărie Încălţăminte / Leather and Footwear Journal (Print ISSN 1583-4433) is published 4 times a year, by Leather and Footwear Research Institute (ICPI) Bucharest, Romania, Division of The National Research and Development Institute for Textiles and Leather (INCDTP), CERTEX Press.

Revista de Pielărie Încălţăminte / Leather and Footwear Journal aims to present current science and technology developments as well as initiatives in Romania and South Eastern Europe region. The Journal publishes original research papers of experimental and theoretical nature, followed by scientific, technical, economic and statistic information, reviews of local and foreign conferences, congresses, symposia, with the purpose of stimulating the dissemination of research results.

Revista de Pielărie Încălţăminte / Leather and Footwear Journal focuses particular attention on the key areas of new systems and technologies applied in leather, footwear and rubber goods sectors; biomaterials, collagen-based medical devices, biochemistry of collagen; environment; innovation; leather and parchment cultural heritage; management and marketing, quality control; applications of IT field in these sectors, and other related fields.

OPEN ACCESS STATEMENT

Revista de Pielărie Încălţăminte / Leather and Footwear Journal is a peer reviewed, open access journal. All articles published open access will be immediately and permanently free for everyone to read, download, copy and distribute, under the provisions of a Creative Commons Attribution (CC BY) which lets others distribute and copy the article, create extracts, abstracts, and other revised versions, adaptations or derivative works of or from an article (such as a translation), include in a collective work (such as an anthology), text or data mine the article, even for commercial purposes, as long as they credit the author(s), do not represent the author as endorsing their adaptation of the article, and do not modify the article in such a way as to damage the author's honor or reputation.

PEER-REVIEW PROCEDURE

Submission of a manuscript to *Revista de Pielărie Încălţăminte* implies that the work described has not been published before (except in the form of an abstract or as part of a published lecture, review, or thesis); that it is not under consideration for publication elsewhere; that its publication has been approved by all coauthors, if any.

Submitted manuscripts are double-blind peer-reviewed by two qualified reviewers selected by the Editorial Board. The manuscript will be accepted for publication provided reviews are favorable. In case of diversified opinions of the reviewers, the Editorial board will make the final decision. The authors will be notified as soon as possible of the result of the paper evaluation (accepted as such, accepted after revision, rejected).

PLAGIARISM POLICY

Authors submitting manuscripts to the Leather and Footwear Journal shall ensure that their work is original and not for consideration elsewhere. Plagiarism in its varied forms is not tolerated. The editors verify the originality of manuscripts submitted to Leather and Footwear Journal using dedicated software Sistemantiplagiat.ro to check for similarities with previous publications. If plagiarism is detected, the manuscript in question will be rejected.

COPYRIGHT

ABSTRACTING AND INDEXING

Revista de Pielărie Încălţăminte / Leather and Footwear Journal is acknowledged in Romania by the National University Research Council (CNCSIS) in B+ Category (code 565), and is indexed in Chemical Abstracts Service (CAS) Database, USA, CAB Database (CAB International, UK), Elsevier's Compendex and SCOPUS, CrossRef, EBSCO, ProQuest, Index Copernicus, CiteFactor, Research Bible, and listed in Matrix for the Analysis of Journals (MIAR), Electronic Journals Library (EZB), Journal TOCs, Root Indexing, Scilit, and SCIPIO.

INCDTP-ICPI is a member of The Publishers International Linking Association, Inc. (PILA), a nonprofit corporation doing business as Crossref. As a PILA member, we have the right to assign Digital Object Identifiers (DOIs) to journal content. DOIs are persistent links to an object/entity and can be used to cite and link to any article existing online, even if full citation information is not yet available. We strongly recommend that authors cite references using DOIs where possible. For details regarding citation format and examples, please visit the Instructions for Authors section on *Revista de Pielărie Încălţăminte / Leather and Footwear Journal*'s website, http://www.revistapielarieincaltaminte.ro

FEES AND SUBSCRIPTIONS

Revista de Pielărie Încălţăminte / Leather and Footwear Journal requires article processing charges of 200 EURO per article, for accepted manuscripts, payable by the author to cover the costs associated with publication. There are no submission charges.

Hard copies of journal issues are available for purchase at subscription rates of 160 EURO for companies and 100 EURO for individual subscribers, while the rate for a single issue is 40 EURO. Subscriptions (include mailing costs) can be made at the editorial office, to the following address:

INCDTP – DIVISION: LEATHER AND FOOTWEAR RESEARCH INSTITUTE, 93 Ion Minulescu Street, postal code 031215, sector 3, Bucharest, Romania, Europe.

Both article processing charges and subscription fees are to be paid in the following account:

Account holder: INCDTP – Division: Leather and Footwear Research Institute; Address of the account holder: 93 Ion Minulescu Street, postal code 031215, sector 3, Bucharest, Romania, Europe
IBAN Code: RO25 RNCB 0074029208380005
Bank code: 300413024
Swift bank address: RNCBROBU; Bank: BCR sector 3 (ROMANIAN COMMERCIAL BANK – SECTOR 3); Bank address: 11 Decebal Blvd., Bl. S14, sector 3, Bucharest, Romania.

CORRESPONDENCE

Editor-in-Chief – Dana Gurău
INCDTP – Division: Leather and Footwear Research Institute (ICPI), 93, Ion Minulescu Street, Bucharest, sector 3, postal code 031215, Romania, Europe; tel./fax: + 40 21 323 52 80, e-mail: jlfjournal@gmail.com

CERTEX Publishing House – Bucharest, 16 Lucreţiu Pătrăşcanu St., sector 3; Tel./ Fax: (0040) 21 340.55.15; office@incdtp.ro

Website: http://www.revistapielarieincaltaminte.ro
Facebook: http://www.facebook.com/LeatherFootwearJournal
Title DOI: https://doi.org/10.24264/lfj

EDITORIAL ADVISORY BOARD

ISSN: 1583-4433
Volume 25, No. 4, December 2025
https://doi.org/10.24264/lfj.25.4

	CONTENTS	***CUPRINS***	***SOMMAIRE***	
Van-Huan BUI	Effect of Structural Characteristics on Hardness and Compression Set of 3D Printed TPU Insole	Influența caracteristicilor structurale asupra durității și rezistenței la compresie a branțurilor din TPU imprimate 3D	L'effet des caractéristiques structurelles sur la dureté et la déformation rémanente à la compression de semelles en TPU imprimées en 3D	**193**
Arun Kumar GAIKWAD **Adity SAXENA**	Multi-Layer Firefighting Footwear Upper with Enhanced Thermal and Chemical Protection: Materials Innovation, Functional Validation, and Wearer Comfort	Față de încălțăminte multistrat pentru pompieri, cu protecție termică și chimică îmbunătățită: materiale inovatoare, validare funcțională și confort la purtare	Tige de chaussure de lutte contre l'incendie multicouches avec protection thermique et chimique renforcée : innovation des matériaux, validation fonctionnelle et confort du porteur	**203**
Thi-Kien-Chung CAO **Van-Huan BUI** **Vu-Luc TA** **Hai-Kien LE**	Relationship Between Stretch and Pressure of Knitted Fabric for Shoe Uppers for Female Diabetic Patients	Relația dintre alungirea și presiunea materialului tricotat folosit la fețele de încălțăminte pentru femei cu diabet	Relation entre l'élongation et la pression des matières tricotées utilisées pour les tiges de chaussures destinées aux femmes diabétiques	**225**
Nhat-Huy PHAM **Van-Huan BUI** **Thanh-Thao PHAN**	Research on Technological Factors Affecting the Peel Strength of Zippers	Cercetări privind factorii tehnologici care afectează rezistența la desprindere a fermoarelor	Recherche sur les facteurs technologiques influençant la résistance au pelage des fermetures à glissière	**243**
Shixuan CHEN **Han XU** **Shiyang YAN** **Luming YANG**	3D Printing for Pediatric Foot Orthoses: Current Applications, Challenges, and Future Perspectives	Orteze plantare pediatrice imprimate 3D: aplicații actuale, provocări și perspective viitoare	Orthèses plantaires pédiatriques imprimées en 3D : applications actuelles, défis et perspectives futures	**255**
	European Research Area	Spaţiul european al cercetării	Espace Européen de la Recherche	**273**

EFFECT OF STRUCTURAL CHARACTERISTICS ON HARDNESS AND COMPRESSION SET OF 3D PRINTED TPU INSOLE

Van-Huan BUI*

Department of Textile-Leather and Fashion, School of Materials Science and Engineering, Hanoi University of Science, and Technology, No. 1, Dai Co Viet, Bach Mai ward, Hanoi, Vietnam, huan.buivan@hust.edu.vn

Received: 31.07.2025 Accepted: 11.12.2025 https://doi.org/10.24264/lfj.25.4.1

EFFECT OF STRUCTURAL CHARACTERISTICS ON HARDNESS AND COMPRESSION SET OF 3D PRINTED TPU INSOLE

ABSTRACT. Hardness and compression set are important characteristics of shoe insole materials, especially for insoles intended for diabetic patients. In this study, we investigated the effects of several structural factors including the hardness of thermoplastic polyurethane (TPU), infill density, and internal structural pattern on the hardness and compression set of 3D-printed insoles. TPUs with hardness levels of 60A, 70A, and 95A were used to fabricate test specimens with different infill patterns and infill densities using FDM technology. The specimens were then subjected to hardness and compression set testing. We found that the specimens exhibited good compression set performance, meeting the requirements for shoe insole materials due to the inherent elasticity of TPU. The hardness of the 3D-printed specimens primarily depended on the hardness of the TPU material and the infill density, while the influence of the infill pattern was less significant. TPU95A is suitable for producing rigid insole components, whereas TPU60A and TPU70A are appropriate for fabricating soft cushioning layers. However, using TPU70A combined with the Grid pattern in BambuLab software is more efficient for 3D printing custom insoles in terms of material consumption and printing time. The mathematical models established between infill density and the hardness of 3D-printed specimens demonstrated very strong correlation coefficients. These models can be used to determine the required infill density to achieve specific hardness levels in different regions of the insole, thereby helping to minimize peak plantar pressure in diabetic patients. The results of this study provide a foundation for the design and manufacture of cost-effective custom insoles for diabetic patients in Vietnam.
KEY WORDS: 3D printed insoles, TPU materials, FDM technology, infill pattern, infill density

INFLUENȚA CARACTERISTICILOR STRUCTURALE ASUPRA DURITĂȚII ȘI REZISTENȚEI LA COMPRESIE A BRANȚURILOR DIN TPU IMPRIMATE 3D

REZUMAT. Duritatea și rezistența la compresie sunt caracteristici importante ale materialelor pentru branțuri de încălțăminte, în special pentru branțurile destinate pacienților diabetici. În acest studiu s-a investigat influența mai multor factori structurali, cum ar fi duritatea poliuretanului termoplastic (TPU), densitatea și modelul structural intern, asupra durității și rezistenței la compresie a branțurilor imprimate 3D. S-au utilizat TPU cu durități de 60A, 70A și 95A pentru a realiza eșantioane de testare cu diferite modele și densități folosind tehnologia modelării prin depunere topită (FDM). Eșantioanele au fost supuse unor teste de duritate și rezistență la compresie. S-a constatat că eșantioanele de testare au avut o rezistență la compresie bună, care a îndeplinit cerințele pentru materialele destinate utilizării la branțuri de încălțăminte datorită elasticității inerente a TPU. Duritatea eșantioanelor imprimate 3D a depins în principal de duritatea și de densitatea TPU, fiind mai puțin afectată de modelele de umplere ale acestora. TPU95A este potrivit pentru realizarea unor componente dure pentru branțuri, iar TPU60A și TPU70A sunt materiale potrivite pentru a obține straturi moi de amortizare. Cu toate acestea, utilizarea TPU70A cu modelul de tip grilaj al software-ului BambuLab pentru imprimarea 3D a branțurilor personalizate este mai eficientă în ceea ce privește consumul de materiale și timpul de procesare. Modelele matematice stabilite între densitatea și duritatea specimenelor imprimate 3D au demonstrat coeficienți ce indică corelații foarte puternice. Aceste modele matematice se pot utiliza pentru a determina densitatea în vederea obținerii unor grade de duritate specifice diferitelor zone ale branțului, în acest fel ajutând la minimizarea presiunii maxime asupra zonei plantare a piciorului la pacienții diabetici. Rezultatele acestui studiu oferă un fundament pentru proiectarea și fabricarea de branțuri personalizate rentabile pentru pacienții diabetici din Vietnam.
CUVINTE CHEIE: branțuri imprimate 3D, materiale TPU, tehnologie FDM, model de umplere, densitate

L'EFFET DES CARACTÉRISTIQUES STRUCTURELLES SUR LA DURETÉ ET LA DÉFORMATION RÉMANENTE À LA COMPRESSION DE SEMELLES EN TPU IMPRIMÉES EN 3D

RÉSUMÉ. La dureté et la résistance à la déformation rémanente à la compression sont des caractéristiques importantes des matériaux de semelles de chaussures, en particulier pour les semelles destinées aux patients diabétiques. Dans cette étude, nous avons examiné les effets de plusieurs facteurs structuraux, tels que la dureté du polyuréthane thermoplastique (TPU), la densité de remplissage et la structure interne, sur la dureté et la déformation rémanente à la compression de semelles imprimées en 3D. Des TPU de duretés 60A, 70A et 95A ont été utilisés pour obtenir des échantillons de test présentant différentes structures et densités de remplissage, grâce à la technologie de modélisation par dépôt de fil fondu (FDM). Les échantillons ont ensuite été soumis à des tests de dureté et de déformation rémanente à la compression. Nos résultats montrent que les échantillons présentent une bonne déformation rémanente à la compression, conforme aux exigences des matériaux de semelles de chaussures, grâce à l'élasticité inhérente du TPU. La dureté des échantillons imprimés en 3D dépend principalement de la dureté du TPU et de la densité de remplissage, en étant moins influencée par la structure interne. Le TPU95A convient à la fabrication de parties rigides pour les semelles intérieures de chaussures, tandis que les résines TPU60A et TPU70A sont des matériaux adaptés à la réalisation de couches de rembourrage souples pour ces mêmes semelles. Cependant, l'utilisation du TPU70A et du motif de grille du logiciel BambuLab pour l'impression 3D de semelles intérieures personnalisées s'avère plus efficace en termes de consommation de matériau et de temps de traitement. Les modèles mathématiques établis entre la densité de remplissage et la dureté des spécimens imprimés en 3D ont démontré des coefficients qui indiquent des corrélations très fortes. Grâce à ces modèles, il est possible de déterminer la densité de remplissage optimale pour obtenir la dureté requise dans différentes zones de la semelle intérieure. Ceci contribue à minimiser la pression maximale exercée sur la

* *Correspondence to: Van-Huan BUI, Department of Textile-Leather and Fashion, School of Materials Science and Engineering, Hanoi University of Science and Technology, No. 1, Dai Co Viet, Bach Mai ward, Hanoi, Vietnam, huan.buivan@hust.edu.vn*

plante du pied des patients diabétiques. Les résultats de cette étude constituent la base de la conception et de la fabrication de semelles intérieures personnalisées et économiques pour les patients diabétiques au Vietnam.
MOTS-CLÉS : semelles imprimées en 3D, matériaux TPU, technologie FDM, motif de remplissage, densité de remplissage

INTRODUCTION

Diabetes is a non-communicable disease that affects patients' daily lives and is associated with poor health outcomes [1]. A common complication of diabetes is diabetic foot syndrome, which can progress to serious conditions such as diabetic foot ulcers. The risk of amputation is extremely high as a result of foot injuries, especially foot ulcers [1, 2]. In Vietnam, there are approximately five million people living with diabetes, and in some localities, the prevalence reaches 8.5% [3]. The management of diabetic foot ulcers has become a major challenge for healthcare services and poses a significant socioeconomic burden [4, 5]. Various strategies have been implemented to manage foot ulcers, including glycemic control, pharmacological treatment, topical oxygen therapy, wound dressings, and debridement [5, 6]. An effective preventive strategy for diabetic foot ulcers is the use of custom insoles, which aim to reduce and redistribute pressure across regions of the foot [1, 4–7].

Traditionally, custom components such as orthopedic insoles have been manufactured using subtractive techniques, most commonly by milling a sheet of material. However, these traditional manufacturing methods have significant limitations in terms of flexibility and the ability to incorporate additional functions or control internal structures [6]. Moreover, conventional processes are often labor-intensive, time-consuming, and offer limited opportunities for digital customization [7]. Recent advances in additive manufacturing, particularly the increasing adoption of 3D printing based on Fused Deposition Modeling (FDM), have opened new avenues for producing anatomical insoles [6, 7]. 3D printing has had a transformative impact on orthopedic insoles in many respects [8]. These technologies enable the integration of added functionalities, such as antibacterial materials, or structural-level enhancements, such as zonal control in 3D designs to improve cushioning performance [6]. In contrast to conventional insoles, which rely primarily on general material properties, 3D printing enables the use of personalized materials and structural designs to address patient-specific stiffness and mechanical behavior [7, 9]. Advanced rapid prototyping technologies further support the development of precise, efficient, and highly customized solutions [9].

Many thermoplastic materials can be printed using FDM, such as acrylonitrile butadiene styrene (ABS), polylactic acid (PLA), polycarbonate (PC), thermoplastic elastomers (TPE), and thermoplastic polyurethane (TPU), among others [10]. TPU is the most commonly used material for 3D printing custom shoe insoles due to its elastic, soft, and uniform properties [10–12]. However, 3D printing TPU can be challenging because of its anisotropic behavior and the inherent characteristics of the material [10, 13]. TPUs with different hardness levels can be used and have been shown to provide performance comparable to standard insoles [14].

The greatest advantage of 3D printing insoles for diabetic foot care is the high level of customization and the ability to effectively relieve pressure by adjusting the infill pattern and infill density [6]. Slicing software allows designers to modify the infill density, enabling the integration of customized pressure-relieving elements for specific regions such as the toes, metatarsals, and heels from the early stages of design [9]. Previous studies consistently show that increasing infill density significantly enhances the stiffness, maximum compression load, and energy absorption capacity of 3D-printed materials [10, 11, 15, 16]. Infill densities ranging from 14% to 60% have been explored, and higher densities generally lead to higher compressive strength across various infill patterns [12, 16]. Increased infill density also results in greater maximum compression load and energy absorption [12]. Shore hardness and infill density of 3D-printed materials directly influence properties such as tensile strength, stiffness, and flexure of insoles [11]. Therefore, these parameters must be customized for each individual based on specific data, such as foot

pressure maps [10, 17]. Several infill patterns have been investigated, including grid, triangle, rectilinear, cubic, gyroid, and honeycomb [12, 16–19]. The Honeycomb infill pattern exhibited the highest maximum compression load at 50% compressive strain and the largest area under the loading–unloading curve, indicating high energy absorption [12]. These characteristics suggest high stiffness and load-bearing capacity [8]. Honeycomb and Triply Periodic Minimal Surface structures provide high stiffness and strong load-bearing performance, while elliptical porous structures offer flexibility in adjusting geometric and mechanical parameters [8]. However, 3D-printed insoles using Honeycomb and Gyroid infill patterns at 20% density did not show statistically significant differences in mean plantar pressure compared with walking without insoles [12]. In contrast, the Gyroid pattern showed the lowest maximum compression load at 50% compressive strain and minimal energy absorption [12], although it demonstrated high specific energy absorption capacity beneficial for orthotic applications [16, 19]. The Gyroid pattern also exhibited lower compressive strength compared with the Triangle and Rectilinear patterns [16]. Triangle and Rectilinear patterns generally yielded better compressive modulus and compressive strength across a range of infill densities, while the Cubic pattern was often excluded due to its low compressive strength [16]. The Hexagonal infill pattern with 40% infill density printed in TPU did not produce any significant differences in average peak pressure distribution when compared with standard insoles [12, 14, 18]. 3D-printed insoles using lattice structures can effectively reduce plantar pressure and promote more balanced weight distribution [20]. The mechanical response of rigid polyurethane foams at different strain rates is correlated with the density and energy-absorption performance of 3D-printed shoe soles [21]. The hardness of 3D-printed insoles can also be adjusted by varying the infill density to accommodate individuals with a high body mass index [22]. Additionally, design factors such as arch type, thickness of the sole and midsole, and their stiffness have significant effects on reducing peak plantar pressure [23].

The reviewed studies confirm that infill density and infill pattern are critical factors influencing the mechanical properties and energy absorption of 3D-printed materials used for insoles. Selecting the appropriate material, infill pattern, and infill density is essential for optimizing insole performance in terms of pressure reduction and enhanced comfort, particularly for diabetic patients [8, 12, 14, 16]. Therefore, the objective of this study is to identify suitable materials and structural configurations for 3D printing customized insoles for diabetic patients using FDM technology. We aim to determine mathematical models that describe the relationship between the hardness and infill density of TPU resin and the resulting hardness and compression set of 3D-printed insoles with different infill patterns. These mathematical models enable the determination of the required hardness for insoles to effectively reduce peak plantar pressure. They also provide a basis for selecting TPU materials with appropriate hardness levels for 3D-printed insoles. The results of this study establish a foundation for designing insoles for diabetic patients by adjusting the local infill densities of the insoles to reduce plantar pressure and increase overall comfort.

EXPERIMENTAL

Materials and Methods

Materials

In this study, we used Filaflex TPU with Shore hardnesses of 60A, 70A, and 95A, manufactured in Spain. The filament diameter is 1.75 ± 0.04 mm, with a melting point ranging from 215°C to 250°C. This thermoplastic material is commonly used to manufacture custom insoles using FDM technology due to its homogeneity, isotropy, and elasticity.

Research Method of TPU Hardness Influence on the Hardness and Compression Set of 3D Printed Insoles

The 3D-printed specimens were designed and created with infill densities of 20%, 25%, 30%, 35%, and 40% using BambuLab software. We used the Grid infill pattern available in the

software, as shown in Figure 1. These specimens were 3D printed on a Chinese ELEGOO 3D printer using TPU filament with the three selected hardness levels.

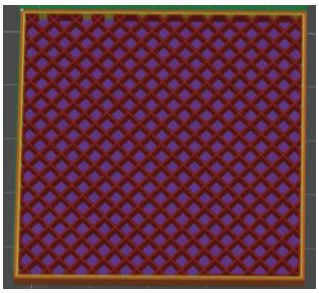

Figure 1. Internal structure pattern of 3D printed specimens

Each test specimen has dimensions of 50mm×50mm×7mm in length, width, and thickness, respectively. The 3D-printed specimens were measured for hardness according to the Asker C hardness scale. Their compressive strength, or their ability to maintain elasticity after being subjected to compressive stress for a certain period of time is determined in accordance with ISO 1856:2018(E), Method B (compression at standard conditioning temperature). The specimens were compressed to 50% of their original thickness and kept in the compressed state for 24 hours at room temperature. The compression set (c.s), expressed as a percentage, is given by the following formula:

$$\text{c.s.} = \frac{d_0 - d_r}{d_0} \times 100 \quad (1)$$

where d_0 is the original thickness of the test piece;

d_r is the thickness of the test piece after recovery.

The lower the compression set value, the better the specimen's ability to recover from compressive deformation. The compression set of the experimental samples was measured using a Japanese Hand Test Press at the Rubber Research Center, Hanoi University of Science and Technology.

Research Method of Infill Pattern and Density Influence on the Hardness and Compression Set of 3D Printed Insoles

Design infill pattern: To study the influence of the insole structural pattern on their hardness and compressibility, we designed a square mesh structure, as shown in Figure 2a. This is a simple, easy-to-adjust, and convenient solution for 3D printing.

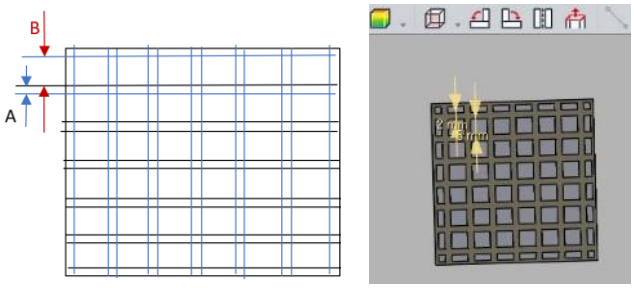

a b

Figure 2. Design infill pattern of the specimens (a) and specimen designed on BambuLab software (b)

The nozzle width of the 3D printer is 0.4 mm, so we printed specimens with wall thicknesses that are multiples of 0.4 mm, i.e., 0.8 mm, 1.2 mm, 1.6 mm, and 2.0 mm. The internal squares were designed to create infill densities ranging from 23% to 49%, as shown in Table 1 and Figure 2b. The specimens were 3D printed using TPU70A.

Table 1: Specimen characteristics of design infill pattern

	Wall thickness (A), mm									
	0.8			1.2			1.6		2	
Wall thickness (B), mm	4	5	6	4	5	6	5	6	5	6
Infill density, %	33.2	27.4	23.0	40.8	35.0	30.6	42.6	37.7	49.0	43.8
Sample coding	A1	A2	A3	A4	A5	A6	A7	A8	A9	A10

Using infill patterns on BambuLab software: The software provides a wide variety of 3D-printing infill patterns. We identified three patterns that are simple and well-suited for 3D printing custom shoe insoles: Grid (square cylindrical cavity structure), Triangles (triangular cylindrical cavity structure), and Honeycomb (hexagonal cylindrical cavity structure), as shown in Figure 3.

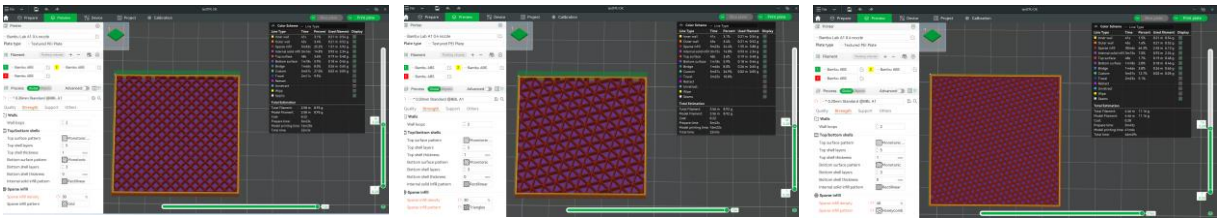

a b c

Figure 3. Infill patterns on BambuLab 3D printing software: a – Grid; b - Triangles; and c – Honeycomb

Using these infill patterns, we 3D-printed samples with infill densities of 20%, 25%, 30%, 35%, and 40%. The printed specimen size remained 50mm×50mm×7mm. The 3D-printed specimens were tested for their hardness and compression set. From these results, we developed mathematical models that describe the relationship between infill density and both hardness and compression set. This serves as the basis for selecting appropriate infill patterns for 3D printing custom insoles.

An independent samples t-test was conducted to determine the statistical significance of the hardness and compression set values of specimens printed with TPU95A, TPU70A, and TPU60A, as well as those printed with different infill patterns.

RESULTS AND DISCUSSIONS

Effect of TPU Hardness on Hardness and Compression Set of 3D Printed Insoles

The test results for the hardness and compression set of the 3D-printed specimens made from TPU60A, TPU70A, and TPU95A are presented in Table 2 and Figure 4.

Table 2: Test results of hardness and compression resistance of 3D printed specimens from TPU

	Hardness, Asker C			Compression set, %		
Infill density, %	60A	70A	95A	60A	70A	95A
20	24.7±0.9	29.9±0.8	68.5±1.9	33.7±2.6	32.6±1.9	51.3±2.4
25	30.2±0.9	35.2±0.6	72.3±3.2	31.9±2.1	30.6±2.2	47.4±3.1
30	36.5±0.6	38.1±1.2	82.1±3.5	31.3±1.2	27.7±3.2	46.2±2.9
35	40.3±1.5	43.7±1.3	86.8±2.9	30.5±2.5	27.7±1.8	46.9±3.6
40	43.8±1.4	46.1±0.9	95.1±3.7	27.4±2.8	26.6±2.5	41.5±3.3

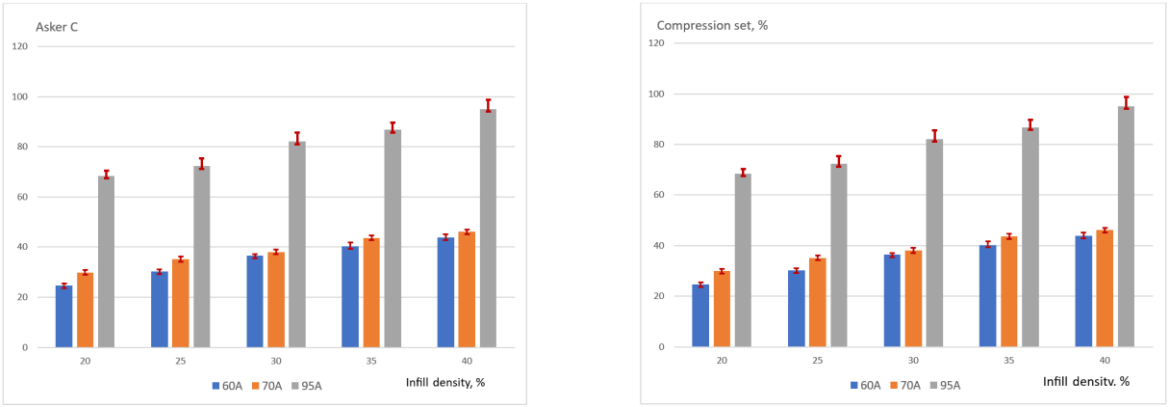

a b

Figure 4. Comparison chart of hardness (a), compression set (b) of 3D printed specimens from TPU95A, TPU70A and TPU60A with infill densities from 20% to 40%

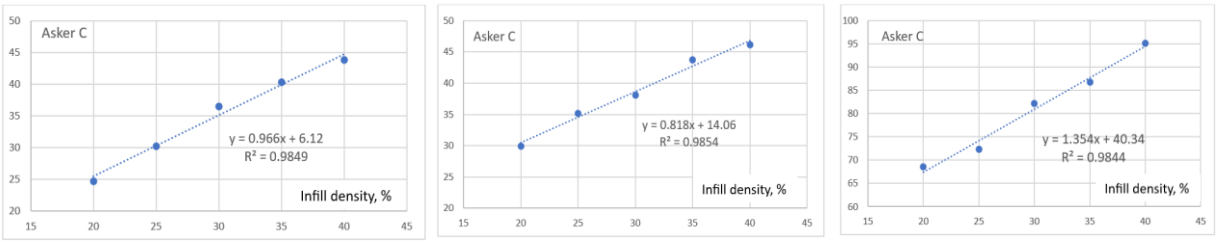

a b c

Figure 5. Relationship between infill density and hardness of 3D printed specimens from TPU60A (a), TPU70A (b), and TPU95A (c)

Based on the Independent samples t-test, no statistically significant difference in hardness was found between the 3D-printed specimens made from TPU60A and TPU70A (p = 0.629; *p(two-tailed)* = 0.460 > 0.05). Statistically significant differences in hardness were observed between the specimens printed from TPU60A and TPU95A, as well as between those printed from TPU70A and TPU95A (p and *p(two-tailed)* < 0.001). The hardness of the 3D-printed specimens increased with the Shore hardness of the TPU material. For each TPU type, specimen hardness also increased as infill density increased. The specimens printed from TPU95A exhibited relatively high hardness compared with the requirements for shoe lining materials (30 to 40 Asker C) [24]. The specimens printed from TPU60A had the lowest hardness values. TPU 60A specimens with infill densities of 25% to 35% and TPU70A specimens with infill densities of 20% to 30% showed hardness levels that meet the requirements of conventional insoles. TPU60A specimens with infill below 25% and TPU70A specimens with infill below 20% had hardness values lower than the minimum range for conventional insoles or are softer than required. These softer structures may be used in regions of the insole that require greater flexibility to reduce localized peak plantar pressure in diabetic patients.

From the data in Table 2, we developed mathematical models describing the relationship between infill density and the hardness of specimens made from TPU60A, TPU70A, and TPU95A, as shown in Figure 5. The obtained models are linear, with very high correlation coefficients ($R^2 \approx 1$). These results indicate a strong relationship between infill density and the hardness of the 3D-printed TPU specimens. Using these mathematical models, the required infill density can be determined to achieve the desired hardness for each region of the insole.

The compression set test results followed a similar trend to those observed for hardness. The compression set values of the TPU60A and TPU70A specimens did not show any statistically significant differences (p = 0.378; *p(two-tailed)* = 0.246 > 0.05). The TPU95A specimens exhibited higher compression set values and lower

recovery after compressive deformation compared with the TPU60A and TPU70A specimens (*p(two-tailed)* < 0.001). The lowest compression set values were observed in the TPU70A specimens. The compression set of the 3D-printed specimens decreased slightly as infill density increased (Figure 4b), although the decrease was not statistically significant. Overall, the compression set values of the TPU60A and TPU70A specimens were acceptable, remaining below 50% and meeting the requirements for shoe insole materials [24].

Thus, TPU95A should be used as a rigid structural layer to support the arch of the insole. TPU60A and TPU70A can both be used as soft insole layers with different infill densities. When using TPU70A, a lower infill density can be applied compared with TPU60A to achieve the same required hardness. This helps reduce the material cost of 3D-printed insoles.

Infill Structure Patterns of 3D Printed Insoles

Designed Infill Pattern

The hardness and compression set values of the ten TPU70A specimens with different infill densities are presented in Table 3 and Figure 6.

Table 3: Test results of 3D printed specimens with designed infill pattern

	3D printed specimens									
	A1	A2	A3	A4	A5	A6	A7	A8	A9	A10
Infill density, %	33.2	27.4	23.0	40.8	35.0	30.6	42.6	37.7	49.0	43.8
Hardness, Asker C	38.1±1.9	35.3±2.5	30.9±3.1	42.1±2.8	40.2±3.1	34.1±3.6	46.3±2.9	41.8±3.4	49.6±3.2	43.2±3.7
Compression set, %	29.1±3.8	29.6±2.9	31.7±3.3	28.2±3.3	29.5±2.6	32.5±2.9	33.2±2.2	34.1±3.6	30.8±2.9	31.1±3.5

Using this mathematical model, it is possible to calculate the infill density required to achieve the desired hardness for shoe insoles. With this infill pattern, an infill density of up to 35% can reach a hardness of 40 Asker C for 3D-printed shoe insoles.

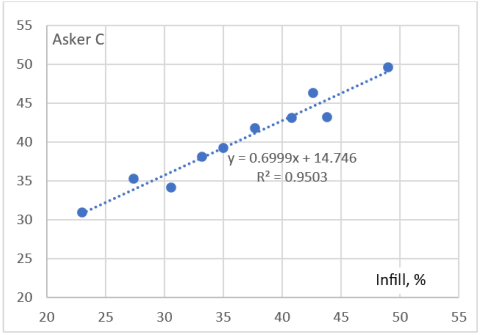

Figure 6. Correlation between infill density and hardness of 3D printed specimens with designed infill pattern

Infill Patterns on BambuLab Software

The hardness and compression set values of the 3D-printed specimens produced using three infill patterns in BambuLab software are presented in Table 4 and Figure 7.

Table 4: Test results of 3D printed specimens using the infill patterns of BambuLab software

Infill density, %	Hardness, Asker C			Compression set, %		
	Grid	Triangles	Honeycomb	Grid	Triangles	Honeycomb
20	31.1±0.9	24.7±0.8	28.6±1.3	30.6±2.2	29.2±2.4	38.1±2.8
25	35.5±1.4	32.1±0.8	33.9±0.9	27.6±2.1	29.7±2.8	37.2±2.7
30	39.4±1.1	34.8±1.6	38.8±1.4	26.8±1.5	31.5±2.5	37.8±2.3
35	43.8±1.5	38.6±0.9	41.0±1.9	28.6±2.7	26.7±2.9	37.5±2.1
40	45.8±1.5	43.2±1.4	44.2±1.8	26.5±2.5	33.7±3.4	34.3±3.5

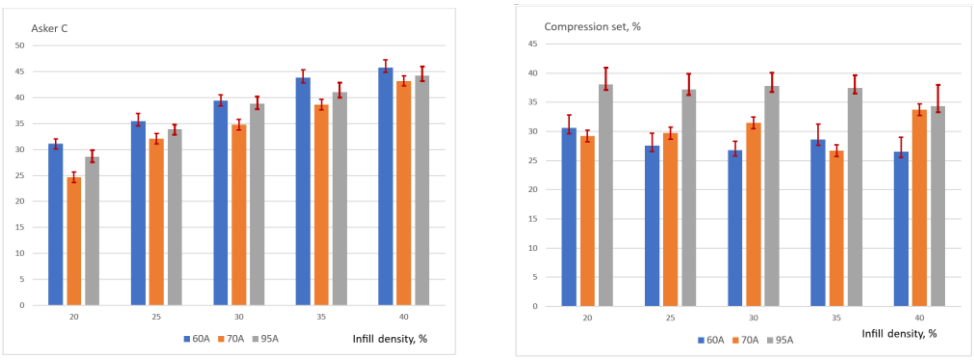

a b

Figure 7. Comparison chart of hardness (a), compression set (b) of 3D printed specimens using Grid, Triangles and Honeycomb structure patterns with infill densities from 20% to 40%

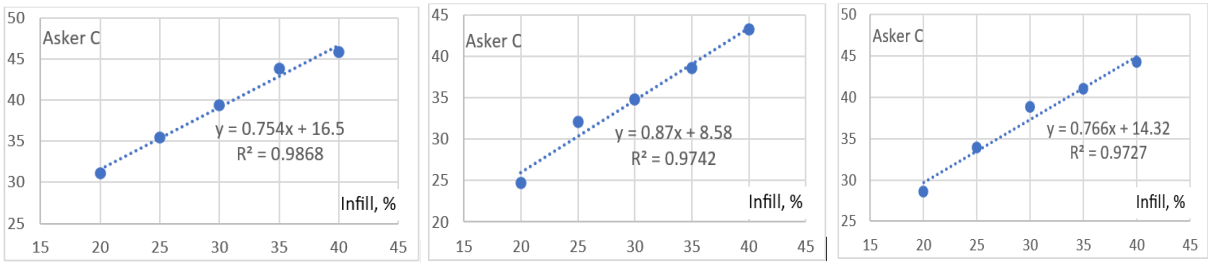

a *b* *c*

Figure 8. Correlations between infill density and hardness of 3D printed specimens using the infill patterns: Grid (a), Triangles (b), and Honeycomb (c)

The Grid and Triangles patterns exhibited high and similar compression set values (*p(two-tailed)* = 0.566 > 0.05). In contrast, the Honeycomb pattern showed a lower ability to recover from deformation than the Grid and Triangles patterns, by approximately 8% (*p(two-tailed)* < 0.001). All specimens met the required compression set performance (greater than 70%). Among them, the Grid pattern produced the best compression set value, reaching approximately 80%. Therefore, the Grid pattern in BambuLab software should be used to create the internal structural pattern for the mid-layer of 3D-printed shoe insoles.

Using the Independent samples t-test, no statistically significant difference in the hardness of the specimens among the three infill patterns was found (*p(two-tailed)* > 0.05). We also used the obtained mathematical model (Figure 5) for the designed structures to calculate the hardness of the specimens. The resulting hardness values were Asker C 28.7, 32.2, 35.7, 39.2, and 42.7 corresponding to infill levels of 20%, 25%, 30%, 35%, and 40%, respectively. Next, we compared these values with the hardness values of the 3D-printed samples with Grid, Triangles, and Honeycomb structures (Table 4), and again, no statistically significant difference was observed (*p(two-tailed)* > 0.05).

This further confirms that the hardness of 3D-printed TPU70A models does not depend significantly on the structure type, but mainly on their infill density. Therefore, these structures can be used for printing shoe insoles. However, when considering the efficiency of 3D printing shoe insoles, the Grid structure should be preferred. This structure provides slightly higher hardness than the other patterns at the same infill density, thereby reducing material consumption. In addition, it is the simplest structure, resulting in a higher printing speed compared with the other structural options. Using the Grid pattern, it is possible to 3D print shoe insoles with an infill density of 20% while still meeting the required hardness. Moreover, the deformation recovery ability of the Grid structure is better than that of the other patterns, increasing the shape and dimensional stability of custom insoles.

Using the values in Table 4, we developed a linear mathematical model describing the

relationship between infill density and specimen hardness for the three infill patterns. All mathematical models exhibited a strong correlation coefficient, with $R^2 \approx 1$ (Figure 8). Therefore, these mathematical models can be used to determine the appropriate infill density required to achieve the desired hardness in different regions of a custom insole, thereby helping to reduce peak plantar pressure in diabetic patients.

CONCLUSIONS

In this study, we found that the hardness of 3D-printed insoles mainly depends on the hardness of the TPU material and the infill density, and is only slightly affected by the infill pattern. TPU95A can be used as a rigid structural component of the insole, functioning to support the arch of the custom insole. TPU60A and TPU70A can both be used as soft insole layers with different infill densities. When using TPU70A, a lower infill density can be applied compared with TPU60A, which helps reduce the material cost of 3D-printed insoles.

For 3D printing custom insoles, the Grid pattern in BambuLab software should be used. This structure enables the printing of insoles at low infill densities (20% to 30%), saving material, increasing printing speed, and providing models with good compression set performance. The results of this study form a basis for the design and manufacture of custom insoles for diabetic patients in Vietnam.

Acknowledgements

This research is funded by Hanoi University of Science and Technology (HUST) under project number T2023-PC-051. The authors are grateful to the SMART DESIGN LABS Co., Ltd. in Vietnam for supporting the implementation of this study.

REFERENCES

1. Dalla Paola, L., Carone, A., Vasilache, L., Pattavina, M., Overview on Diabetic Foot: A Dangerous, but Still Orphan, Disease, *Eur Heart J Suppl*, **2015**, 17 (suppl A), A64-A68, https://doi.org/10.1093/eurheartj/suv023.
2. Boulton, A.J.M., The Pathway to Ulceration: Aetiopathogenesis, The Foot in Diabetes, John Wiley & Sons Ltd, **2006**, 61-79, https://doi.org/10.1016/j.mcna.2013.03.007.
3. Pham, M.N., Nguyen, Duc T., Do, N.M., Hoang, X.D., Current Status of Type 2 Diabetes and Treatment with Traditional Medicine in Nam Dan district, Nghe An Province in 2023 (in Vietnamese), *Journal of Traditional Vietnamese Medicine*, **2024**, 56, 03, 64-68, https://doi.org/10.60117/vjmap.v56i03.304.
4. Lim, J.Z.M., Ng, N.S.L., Thomas, C., Prevention and Treatment of Diabetic Foot Ulcers, *J R Soc Med*, **2017**, 110, 104–109, https://doi.org/10.1177/0141076816688346.
5. Ramachandran, V., Mohanasundaram, T., Karunakaran, D., Gunasekaran, M., Tiwari, R., Physiological and Pathophysiological Aspects of Diabetic Foot Ulcer and its Treatment Strategies, *Curr Diabetes Rev*, **2023**, 19, https://doi.org/10.2174/1573399819666221103141715.
6. Davia-Aracil, M., Hinojo-Pérez, J.J., Jimeno-Morenilla, A., Mora-Mora, H., 3D Printing of Functional Anatomical Insoles, *Comput Ind*, **2018**, 95, 38-53, https://doi.org/10.1016/j.compind.2017.12.001.
7. Mancuso, M., Bulzomì, R., Mannisi, M., Martelli, F., Giacomozzi, C., 3D-Printed Insoles for People with Type 2 Diabetes: An Italian, Ambulatory Case Report on the Innovative Care Model, *Diabetol*, **2023**, 4, 3, 339-355, https://doi.org/10.3390/diabetology4030029.
8. Ren, Y., Wang, H., Song, X., Wu, Y., Lyu, Y., Zeng, W., Advancements in Diabetic Foot Insoles: A Comprehensive Review of Design, Manufacturing, and Performance Evaluation, *Biomechanics*, **2024**, 12, https://doi.org/10.3389/fbioe.2024.139475.
9. Shaikh, S., Jamdade, B., Chanda, A., Effects of Customized 3D-Printed Insoles in Patients with Foot-Related Musculoskeletal Ailments – A Survey-Based Study, *Prosthesis*, **2023**, 5, 550–561, https://doi.org/10.3390/prosthesis5020038.
10. Chang, M.C., Choo, Y.J., Comparative Efficacy of 3D-Printed Insoles in Managing Common Foot Conditions: A Review, *Med Sci Monit*, **2025**, https://doi.org/10.12659/MSM.947252.
11. Zhang, X., Chu, P., Ma, X., Chen, W.M., 3D-Printed Insole Designs for Enhanced Pressure-Relief in Diabetic Foot Based on Functionally-Graded Stiffness Properties, IFMBE Proceedings, **2024**, 104, 192–199, https://doi.org/10.1007/978-3-031-51485-2_22.
12. Chatpun, S., Dissaneewate, T., Kwanyuang, A., Nouman, M., Srewaradachpisal, S., Movrin, D., Effects of Infill Pattern and Density on Mechanical Performance and Plantar Pressure Distribution of 3D-Printed Insoles During

Walking, *Appl Sci*, **2025**, 15, 7, 3916, https://doi.org/10.3390/app15073916.
13. Iftekar, S.F., Aabid, A., Amir, A., Baig, M., Advancements and Limitations in 3D Printing Materials and Technologies: A Critical Review, *Polymers*, **2023**, 15, 11, 2519, https://doi.org/10.3390/polym15112519.
14. Zuñiga J., Moscoso M., Padilla-Huamantinco P.G., Lazo-Porras M., Tenorio-Mucha J., Padilla-Huamantinco W., Tincopa J.P., Development of 3D-Printed Orthopedic Insoles for Patients with Diabetes and Evaluation with Electronic Pressure Sensors, *Designs*, **2022**, 6, 95, https://doi.org/10.3390/designs6050095.
15. Raffaelli, S., Design of 3D Printed Custom-Made Orthopedic Insoles, Master degree in biomedical engineering, Università Politecnica delle Marche, Engineering Faculty, **2021**.
16. Orsu, B., Shaik, Y.P., Compression Strength Analysis of Customized Shoe Insole with Different Infill Patterns Using 3D Printing, *Open Access Library Journal*, **2022**, 9, 5, 1–13, https://doi.org/10.4236/oalib.1108712.
17. Shi, Q.Q., Li, P.L., Yick, K.L., Li, N.W., Jiao, J., Effects of Contoured Insoles with Different Materials on Plantar Pressure Offloading in Diabetic Elderly During Gait, *Sci Rep*, **2022**, 12, https://doi.org/10.1038/s41598-022-19814-0.
18. Zolfagharian, A., Lakhi, M., Ranjbar, S., Bodaghi, M., Custom Shoe Sole Design and Modeling Toward 3D Printing, *Int J Bioprint*, **2021**, 7, https://doi.org/10.18063/ijb.v7i4.396.
19. Jonnala, U.K., Sankineni R., Ravi Kumar, Y., Design and Development of Fused Deposition Modeling (FDM) 3D-Printed Orthotic Insole by Using Gyroid Structure, *J Mech Behav Biomed Mater*, **2023**, 145, https://doi.org/10.1016/j.jmbbm.2023.106005.
20. Kumar, R., Sarangi, S.K., 3D Printed Customized Diabetic Foot Insoles with Architecture Designed Lattice Structures – A Case Study, *Biomed Phys Eng Express*, **2024**, 10, 015019, https://doi.org/10.1088/2057-1976/ad1732.
21. Xiao, Y., Yin, J., Zhang, X., An, X., Xiong, Y., Sun, Y., Mechanical Performance and Cushioning Energy Absorption Characteristics of Rigid Polyurethane Foam at Low and High Strain Rates, *Polym Test*, **2022**, 109, 107531, https://doi.org/10.1016/j.polymertesting.2022.107531.
22. Chatzistergos, P.E., Gatt, A., Formosa, C., Farrugia, K., Chockalingam, N., Optimised Cushioning in Diabetic Footwear can Significantly Enhance Their Capacity to Reduce Plantar Pressure, *Gait Posture*, **2020**, 79, 244-250, https://doi.org/10.1016/j.gaitpost.2020.05.009.
23. Cheung, J.T.M., Zhang, M., Parametric Design of Pressure-Relieving Foot Orthosis Using Statistics-Based Finite Element Method, *Med Eng Phys*, **2008**, 30, https://doi.org/10.1016/j.medengphy.2007.05.002.
24. Motawi, W., Motawi, A., Shoe Material Design Guide, Kindle Edition, **2018**, Wade's Place, www.sneakerfactory.net.

MULTI-LAYER FIREFIGHTING FOOTWEAR UPPER WITH ENHANCED THERMAL AND CHEMICAL PROTECTION: MATERIALS INNOVATION, FUNCTIONAL VALIDATION, AND WEARER COMFORT

Arun Kumar GAIKWAD*, Adity SAXENA

Woxsen University, Telangana, India, arunkumar.gaikwad@woxsen.edu.in, Dean.SD@woxsen.edu.in

Received: 23.10.2025 Accepted: 19.12.2025 https://doi.org/10.24264/lfj.25.4.2

MULTI-LAYER FIREFIGHTING FOOTWEAR UPPER WITH ENHANCED THERMAL AND CHEMICAL PROTECTION: MATERIALS INNOVATION, FUNCTIONAL VALIDATION, AND WEARER COMFORT

ABSTRACT. Current firefighting footwear faces significant limitations in providing simultaneous thermal protection, chemical resistance, and wearer comfort during prolonged emergency operations. Existing single-layer or dual-layer designs often compromise protection for breathability or vice versa, leading to heat stress, chemical exposure risks, and reduced operational effectiveness. The objective was to develop and validate a novel multi-layer composite upper system that integrates advanced materials to achieve superior thermal protection, chemical barrier properties, toxic gas filtration, and enhanced wearer comfort while maintaining structural integrity and durability. A nine-layer composite system was designed incorporating: high-grade leather base, PVC-coated Kevlar outer shell, aluminium trihydrate (ATH) nanoparticle flame retardant layer, thermoplastic polyurethane (TPU) chemical barrier membrane, activated carbon filtration layer, vacuum-insulated metallic foil thermal insulation, aramid Fiber structural reinforcement, hydrophilic polyurethane moisture management layer, and memory foam with bamboo charcoal comfort interface. Validation protocols included thermal testing (Heat Transfer Index, Radiant Heat Transfer Index), chemical resistance evaluation (permeation testing), mechanical property assessment (puncture resistance, tear strength), and comfort metrics (water vapor resistance, thermal load). The multi-layer system demonstrated Heat Transfer Index values of 18.2 ± 1.4 s (>17 s requirement), Radiant Heat Transfer Index of 21.8 ± 2.1 s (>18 s requirement), and chemical breakthrough times >480 minutes for common hazardous substances. Puncture resistance increased by 340% compared to conventional designs while maintaining water vapor resistance below 15 m²·Pa/W. Flame spread index was reduced to <25, with Limiting Oxygen Index (LOI) values exceeding 28%. Field trials showed 23% reduction in heat stress indicators and 89% user satisfaction rating for comfort. The innovative multi-layer firefighting footwear upper successfully addresses critical limitations of existing designs by providing enhanced protection without compromising wearer comfort. The integration of advanced materials through systematic layer optimization offers a promising approach for next-generation firefighter personal protective equipment.

KEYWORDS: firefighting footwear, thermal protection, chemical resistance, multi-layer composite, personal protective equipment, flame retardant materials, aramid reinforcement, comfort engineering

FAȚĂ DE ÎNCĂLȚĂMINTE MULTISTRAT PENTRU POMPIERI, CU PROTECȚIE TERMICĂ ȘI CHIMICĂ ÎMBUNĂTĂȚITĂ: MATERIALE INOVATOARE, VALIDARE FUNCȚIONALĂ ȘI CONFORT LA PURTARE

REZUMAT. Încălțămintea actuală pentru pompieri prezintă limitări semnificative în ceea ce privește capacitatea de a oferi simultan protecție termică, rezistență chimică și confort al purtătorului în timpul operațiunilor de urgență prelungite. Designurile existente cu un singur strat sau cu două straturi deseori compromit protecția în favoarea respirabilității sau invers, ceea ce duce la stres termic, riscuri de expunere la substanțe chimice și eficiență operațională redusă. Obiectivul lucrării a fost dezvoltarea și validarea unui nou sistem compozit multistrat pentru fața de încălțăminte, care integrează materiale avansate pentru a obține protecție termică superioară, proprietăți de barieră chimică, filtrare a gazelor toxice și confort sporit al purtătorului, menținând în același timp integritatea structurală și durabilitatea. S-a proiectat un sistem compozit cu nouă straturi, care include: bază de piele de înaltă calitate, carcasă exterioară din Kevlar acoperită cu PVC, strat ignifugat cu nanoparticule de trihidrat de aluminiu (ATH), membrană de barieră chimică din poliuretan termoplastic (TPU), strat de filtrare cu carbon activ, izolație termică din folie metalică izolată în vid, ranforsare structurală din fibră de aramidă, strat hidrofil de gestionare a umidității din poliuretan și interfață de confort din spumă cu memorie cu cărbune de bambus. Protocoalele de validare au inclus testarea termică (indicele de transfer termic, coeficientul de transfer termic prin radiație), evaluarea rezistenței chimice (testarea permeabilității), evaluarea proprietăților mecanice (rezistența la perforare, rezistența la sfâșiere) și indicatorii de confort (rezistența la vapori de apă, sarcina termică). Sistemul multistrat a demonstrat valori ale indicelui de transfer termic de 18,2 ± 1,4 s (valoarea de referință >17 s), coeficientul de transfer termic prin radiație de 21,8 ± 2,1 s (valoarea de referință >18 s) și timpi de străpungere chimică >480 de minute pentru substanțele periculoase comune. Rezistența la perforare a crescut cu 340% comparativ cu modelele convenționale, menținând în același timp rezistența la vapori de apă sub 15 m²·Pa/W. Indicele de propagare a flăcării a fost redus la <25, valorile indicelui limită de oxigen (LOI) depășind 28%. Testele pe teren au arătat o reducere cu 23% a indicatorilor de stres termic și un indice de satisfacție a utilizatorilor de 89% pentru confort. Partea superioară inovatoare a încălțămintei multistrat pentru stingerea incendiilor abordează cu succes limitările critice ale modelelor existente, oferind o protecție sporită fără a compromite confortul purtătorului. Integrarea materialelor avansate prin optimizarea sistematică a straturilor oferă o abordare promițătoare pentru echipamentul individual de protecție de ultimă generație pentru pompieri.

CUVINTE CHEIE: încălțăminte pentru pompieri, protecție termică, rezistență chimică, compozit multistrat, echipament individual de protecție, materiale ignifuge, ranforsare cu aramidă, inginerie pentru confort

TIGE DE CHAUSSURE DE LUTTE CONTRE L'INCENDIE MULTICOUCHES AVEC PROTECTION THERMIQUE ET CHIMIQUE RENFORCÉE : INNOVATION DES MATÉRIAUX, VALIDATION FONCTIONNELLE ET CONFORT DU PORTEUR

RÉSUMÉ. Les chaussures de pompiers actuelles présentent des limitations importantes quant à leur capacité à assurer simultanément protection thermique, résistance chimique et confort lors d'interventions d'urgence prolongées. Les modèles monocouches ou bicouches existants font souvent des compromis entre protection et respirabilité, ou inversement, ce qui entraîne un stress thermique, des risques

* *Correspondence to: Arun Kumar GAIKWAD, Woxsen University, Telangana, India, arunkumar.gaikwad@woxsen.edu.in*

d'exposition aux produits chimiques et une efficacité opérationnelle réduite. L'objectif était de développer et de valider un nouveau système de tige composite multicouche intégrant des matériaux avancés afin d'obtenir une protection thermique supérieure, des propriétés de barrière chimique, une filtration des gaz toxiques et un confort accru, tout en préservant l'intégrité structurelle et la durabilité. Un système composite à neuf couches a été conçu, comprenant : une base en cuir haut de gamme, une enveloppe extérieure en Kevlar enduit de PVC, une couche ignifuge de nanoparticules de trihydrate d'aluminium (ATH), une membrane barrière chimique en polyuréthane thermoplastique (TPU), une couche de filtration au charbon actif, une isolation thermique en feuille métallique sous vide, un renforcement structurel en fibres d'aramide, une couche de gestion de l'humidité en polyuréthane hydrophile et une mousse à mémoire de forme avec interface de confort au charbon de bambou. Les protocoles de validation comprenaient des tests thermiques (indice de transfert de chaleur, indice de transfert de chaleur par rayonnement), une évaluation de la résistance chimique (test de perméation), une évaluation des propriétés mécaniques (résistance à la perforation, résistance à la déchirure) et des mesures de confort (résistance à la vapeur d'eau, charge thermique). Le système multicouche a démontré des valeurs d'indice de transfert de chaleur de 18,2 ± 1,4 s (exigence > 17 s), un indice de transfert de chaleur par rayonnement de 21,8 ± 2,1 s (exigence > 18 s) et des temps de pénétration chimique supérieurs à 480 minutes pour les substances dangereuses courantes. La résistance à la perforation a augmenté de 340 % par rapport aux conceptions conventionnelles tout en maintenant la résistance à la vapeur d'eau en dessous de 15 m²·Pa/W. L'indice de propagation des flammes a été réduit à < 25, avec des valeurs d'indice limite d'oxygène (LOI) supérieures à 28 %. Les essais sur le terrain ont montré une réduction de 23 % des indicateurs de stress thermique et un taux de satisfaction des utilisateurs de 89 % en matière de confort. La tige innovante multicouche de la chaussure de lutte contre l'incendie répond avec succès aux limitations critiques des conceptions existantes en offrant une protection accrue sans compromettre le confort de l'utilisateur. L'intégration de matériaux avancés par l'optimisation systématique des couches offre une approche prometteuse pour les équipements de protection individuelle (EPI) de nouvelle génération destinés aux pompiers.
MOTS-CLÉS : chaussures de pompier, protection thermique, résistance chimique, composite multicouche, équipements de protection individuelle, matériaux ignifuges, renforcement en aramide, ingénierie du confort

INTRODUCTION

Firefighting operations expose personnel to extreme thermal environments, hazardous chemical vapors, and mechanical hazards that demand the highest level of personal protective equipment (PPE) performance [1, 2]. Footwear represents a critical component of firefighter protection systems, serving as the primary barrier between the wearer's feet and ground-level hazards including radiant heat, chemical liquids, sharp debris, and toxic combustion products [3, 4]. However, current firefighting footwear designs face fundamental challenges in simultaneously providing adequate thermal protection, chemical resistance, and wearer comfort during extended operations.

Current State of Firefighting Footwear Technology

Contemporary firefighting footwear typically employs dual-layer or limited multi-layer constructions utilizing conventional materials such as leather outer shells, rubber soles, and basic insulation layers [5, 6]. While these designs meet minimum safety standards established by organizations such as the National Fire Protection Association (NFPA) and European Committee for Standardization (CEN), they exhibit significant performance limitations under realistic operational conditions.

Recent studies have documented rapid internal temperature rise and material degradation in commercial firefighting boots when exposed to radiant heat loads exceeding 20 kW/m², with outer surface temperatures reaching 140°C leading to loss of protective effectiveness [7]. Furthermore, the thermal protection versus breathability trade-off inherent in current designs often results in increased heat stress, with water vapor resistance values frequently exceeding 20 m²·Pa/W, well above comfort thresholds [8, 9].

Conventional Firefighting Footwear (Class 1 – Firefighting Shoes India)

Current Limitations of Firefighting Footwear: General Requirements for Conventional Footwear (class1) for Indian Firefighters as per IS 15298-2 (2011), safety footwear for Indian firefighters is categorized based on material construction - **Conventional footwear (Class I) definition**: Footwear constructed from leather or comparable materials, excluding designs made entirely of rubber or polymeric components.

Specifications: Conventional footwear typically employs advanced 3-layer designs consisting of full-grain leather outer (2.0-2.5 mm thickness) combined with a moisture barrier liner (typically 0.3-0.5 mm polyurethane membrane) and thermal liner aramid felt [7, 8]. These conventional 3-layer systems, which serve as the primary reference materials in our

comparative analyses. Three-layer systems, occasionally referenced in our comparisons, incorporate thermal liner (typically 1.5-2.0 mm aramid felt with thermal conductivity 0.045-0.055 W/m·K) but remain limited in chemical protection capabilities [9, 10].

Figure 1 depicts the three-layer construction of conventional Class 1 footwear, comprising (a) a durable full-grain leather outer layer, (b) a waterproof polyurethane membrane for barrier protection, and (c) an aramid felt liner engineered for thermal conductivity.

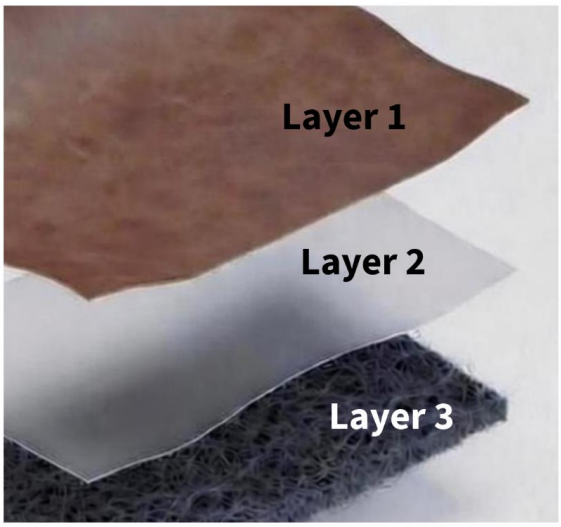

Figure 1. Three-layer conventional class 1 footwear: a) Full grain leather, b) polyurethane membrane, c) aramid felt with thermal conductivity

These conventional systems exhibit several critical limitations:

Thermal Protection Deficiencies: Specifically, the conventional firefighting boots used in our comparative testing (Model reference: standard structural firefighting boots) demonstrated average HTI values of 12.8 ± 1.1 seconds and RHTI values of 14.5 ± 1.3 seconds.

Chemical Resistance Limitations: Conventional leather and basic moisture barrier materials provide minimal protection against chemical permeation, with breakthrough times for common hazardous substances (gasoline, diesel fuel, acids) typically ranging from 15-90 minutes [11, 12]. The reference conventional barrier materials tested showed gasoline breakthrough at 45 ± 8 minutes and diesel breakthrough at 60 ± 12 minutes using ASTM F739 [13] permeation testing protocols.

Comfort-Protection Trade-off: Attempts to enhance thermal protection through increased material thickness or additional insulating layers often result in excessive heat stress, with water vapor resistance values exceeding 20 m²·Pa/W and thermal load increases of 30-40% [14, 15]. Conventional three-layer systems incorporating thermal liners exhibited water vapor resistance of 21.3 ± 2.4 m²·Pa/W.

Emerging Material Technologies

Recent advances in materials science have introduced promising technologies for protective equipment applications, including nanostructured flame retardants, advanced barrier membranes, aerogel insulation systems, and moisture management textiles [16-19]. However, these technologies have primarily been developed and validated for garment applications, with limited translation to footwear-specific requirements and use conditions [20].

Nanoparticle-enhanced flame retardants, particularly aluminum trihydrate (ATH) systems optimized to 10-15 nm particle size, demonstrate superior fire suppression through endothermic decomposition mechanisms and enhanced char formation. Thermoplastic polyurethane (TPU) membranes with specialized formulations offer exceptional chemical resistance while maintaining

flexibility and durability under mechanical stress. These advanced materials, primarily characterized in textile and garment applications, provide the foundation for our multi-layer footwear system development.

RESEARCH OBJECTIVES

This research addresses the critical gap between advanced protective materials development and practical firefighting footwear applications through the design, fabrication, and comprehensive validation of a novel nine-layer composite upper system. Specific objectives include:

1. Integration of advanced materials (nano-ATH flame retardants, TPU chemical barriers, activated carbon filtration, vacuum-insulated thermal barriers) into a functional footwear architecture;
2. Systematic optimization of layer arrangement and interface properties to achieve synergistic performance improvements;
3. Comprehensive validation across thermal protection, chemical resistance, mechanical durability, and comfort domains;
4. Field testing and user acceptance evaluation.

MATERIALS AND METHODS

Multi-Layer System Design Rationale

The nine-layer composite system was designed based on functional specialization principles, with each layer optimized for specific protective or comfort functions while maintaining overall system integration and manufacturability. Layer selection and arrangement were guided by:

1. Heat transfer modeling to optimize thermal resistance distribution;
2. Chemical barrier requirements for common firefighting hazards;
3. Mechanical stress analysis for structural integrity;
4. Moisture transport modeling for comfort optimization;
5. Manufacturing feasibility and cost-effectiveness considerations.

The complete system architecture is illustrated in Figure 2a (schematic diagram) and Figure 2b (actual cross-sectional microscopy image showing layer interfaces and thickness distribution).

The resulting composite structure, with total thickness of 5 ± 0.5 mm, is shown in cross-section Figure 1b, where individual layer boundaries and interface quality are clearly visible through optical microscope.

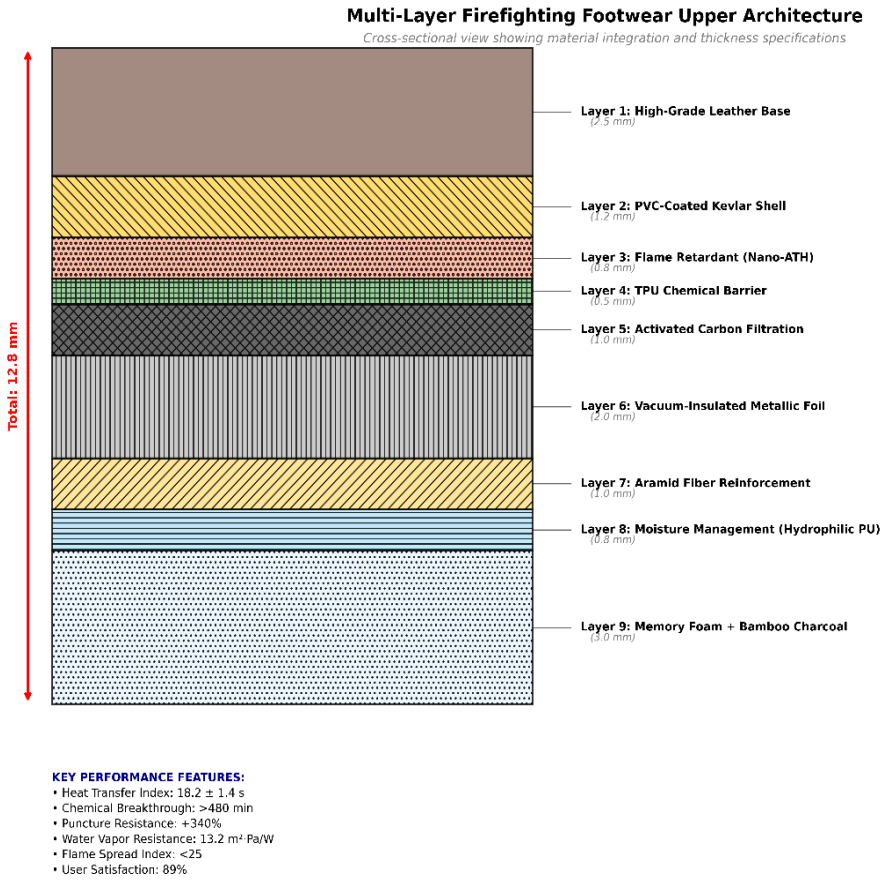

Figure 2a. Schematic diagram

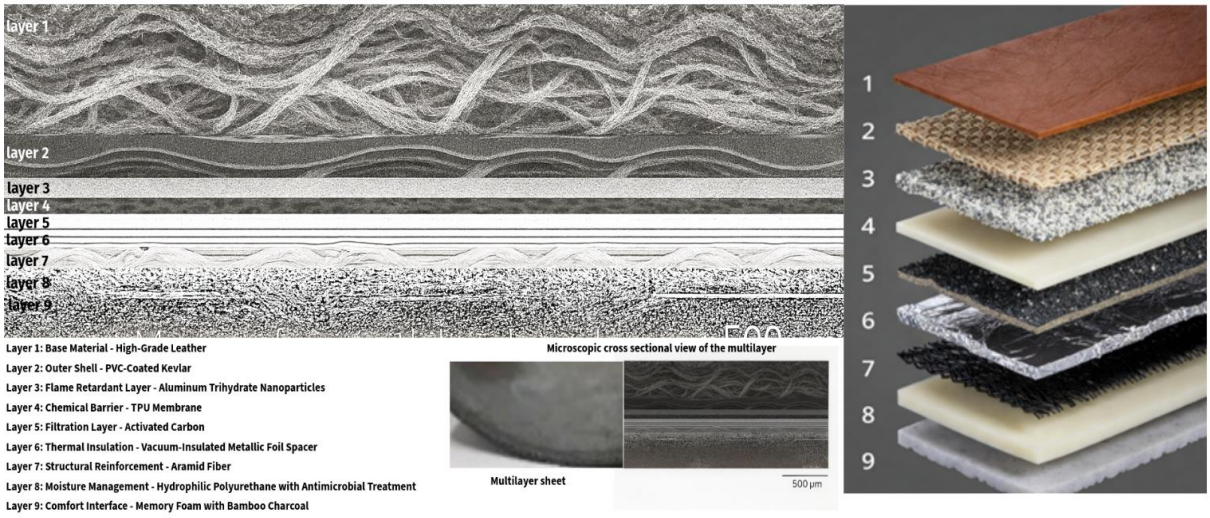

Figure 2b. Optical microscopy cross-sectional image of the actual fabricated nine-layer composite at 50× magnification. Individual layer boundaries are clearly visible, demonstrating successful layer integration and interface bonding quality. Scale bar = 500 µm. Image shows: (1) leather base, (2) PVC-Kevlar shell, (3) nano-ATH layer, (4) TPU membrane, (5) activated carbon fabric, (6) vacuum-foil insulation, (7) aramid felt, (8) hydrophilic PU membrane, (9) memory foam interface

Material Characterization and Quality Control

The materials are analysed in the Institute laboratory – data obtained at the laboratory using the relevant ASTM standards. Details are mentioned below:

Layer 1: Base Material – High-Grade Leather

The foundational layer utilizes full-grain leather selected for durability, flexibility, and baseline thermal resistance. The leather undergoes chrome-tanning processes to enhance heat resistance and dimensional stability. Material specifications include tensile strength ≥25 MPa, tear resistance ≥80 N, and thermal degradation onset temperature ≥280°C.

Testing was conducted for Thermal conductivity and moisture absorption measured in laboratory using ASTM C518 [21] thermal conductivity and ASTM D2654 [22] moisture absorption. Laboratory tests were conducted at Institute – Materials Testing Laboratory, using calibrated Hot Disk TPS 2500 S thermal analyzer (n=5 samples) and controlled humidity chamber (n=3 samples).

Layer 2: Outer Shell – PVC-Coated Kevlar

Material: Aramid fabric with PVC coating, Base Fabric: 600 denier Kevlar, plain weave, Coating Thickness: 0.3 ± 0.05 mm, Tensile Strength: 2800 ± 150 MPa (fabric); 18 ± 2 MPa (coated system), Abrasion Resistance: >10,000 cycles (Taber abraser, CS-10 wheel, 1000g load), Flame Resistance: Self-extinguishing, <2 seconds afterflame.

Tensile strength of coated system was measured in laboratory using Instron 5985 universal testing machine following ASTM D5034 [23] (n=10). Abrasion was tested according to ASTM D4157 [24] and ASTM D6413 [25]. Abrasion and flame resistance were tested in Institute laboratory.

Layer 3: Flame Retardant Layer – Aluminum Trihydrate Nanoparticles

Material: Aluminum trihydrate (ATH) nanoparticles in silicone matrix, Particle Size: 10-15 nm (optimized range), Loading: 45 wt% ATH in polydimethylsiloxane (PDMS). Limiting Oxygen Index (LOI): 28.5 ± 0.8% and Thermal Decomposition: Endothermic, 220-300°C.

LOI values were measured in Institute laboratory using Fire Testing Technology LOI chamber following ASTM D2863 [26] (n=8). Thermal decomposition characterized using TA Instruments Q50 TGA following ASTM E1131 [27] (n=5 samples). Heat release capacity determined using microscale combustion calorimetry (MCC) following ASTM D7309 [28] (n=5 samples).

Layer 4: Chemical Barrier – TPU Membrane

A specialized thermoplastic polyurethane membrane provides chemical permeation resistance. The TPU formulation incorporates flame-retardant additives and maintains flexibility at temperature extremes. Material: thermoplastic polyurethane (TPU), aliphatic polyester-based, thickness: 0.15 ± 0.02 mm, tensile strength: 35 ± 3 MPa, elongation at break: 550 ± 50%, chemical resistance: >480 min breakthrough (gasoline, diesel, acids).

Tensile properties were verified in Institute laboratory using Instron 5985 following ASTM D412 [29] (n=10). Chemical breakthrough times were measured in laboratory using permeation cells following ASTM F739 [13] Method B (n=5 samples per chemical). Low-temperature flexibility was verified following ASTM D1790 [30] (n=5 samples).

Layer 5: Filtration Layer – Activated Carbon

High-surface-area activated carbon is integrated into a nonwoven substrate to provide toxic gas adsorption. The carbon treatment includes silver impregnation for antimicrobial properties and enhanced chemical adsorption capacity for organic vapors and combustion products.

Material: Activated carbon fabric, surface area: 1200-1500 m^2/g (BET method), pore size distribution: micropores 60%, mesopores 30%, macropores 10%, adsorption capacity: benzene 45%, toluene 52% (ASTM D5742 [31]), air permeability: 850 ± 50 $L/m^2/s$ (ASTM D737 [32]).

Surface area and pore size distribution measured in Institute laboratory using Micromeritics ASAP 2020 analyzer following ASTM D6556 [33] (n=3 samples). Adsorption capacity and air permeability were tested in laboratory following ASTM D5742 [31] and ASTM D737 [32], respectively (n=5 samples each). Testing was conducted at Environmental Materials Laboratory.

Layer 6: Thermal Insulation – Vacuum-Insulated Metallic Foil Spacer

A multi-layer reflective insulation system combines aluminized polyester films with vacuum-sealed spacer construction. The system provides radiant heat reflection (emissivity <0.05) and reduces conductive heat transfer through controlled air gap geometry.

Thermal conductivity was measured in Institute laboratory using guarded hot plate apparatus following ASTM C177 [34] under vacuum conditions (n=5 samples). Emissivity and reflectivity were measured using Bruker Vertex 70 FTIR spectrometer with integrating sphere (n=3 samples). Pressure resistance was tested using custom compression fixture with vacuum monitoring (n=5 samples). Testing was conducted at institute Thermal Properties Laboratory.

Layer 7: Structural Reinforcement – Aramid Fiber

High-strength aramid fibers are incorporated in a cross-ply configuration to provide puncture and tear resistance. The reinforcement layer utilizes surface-treated fibers to enhance matrix adhesion and load transfer efficiency. Areal weight is maintained at 150 g/m² to minimize bulk while maximizing protection.

Tensile strength was measured in Institute laboratory using Instron 5985 following ASTM D5034 [23] (n=10 samples). Thermal conductivity was measured using Hot Disk TPS 2500 S following ASTM C518 [21] (n=5 samples). Thermal stability was characterized using TGA following ASTM E1131 [27] (n=5 samples). Compression recovery was tested using custom cyclic compression fixture (n=5 samples, 10,000 cycles each).

Layer 8: Moisture Management – Hydrophilic Polyurethane with Antimicrobial Treatment

A specialized polyurethane layer provides moisture transport and antimicrobial protection. The hydrophilic treatment enables moisture wicking while maintaining chemical resistance. Silver-ion antimicrobial treatment provides long-term odor control and bacterial resistance.

WVTR was measured in Institute laboratory using Lyssy L80-5000 water vapor permeability tester following ASTM E96 [35] Method E (n=8 samples). Water entry pressure was tested using Textest FX 3000 hydrostatic head tester following ASTM F2298 [36] (n=5 samples). Moisture absorption was determined gravimetrically following ASTM D570 [37] (n=5 samples). Wicking rate was measured using custom vertical wicking apparatus (n=10 samples).

Layer 9: Comfort Interface – Memory Foam with Bamboo Charcoal

The innermost layer combines viscoelastic polyurethane foam with bamboo charcoal particles for enhanced comfort and odor control. The foam provides pressure distribution and impact absorption. Compression set tested in laboratory following ASTM D3574 [38] Test B (n=5 samples). following ASTM E2149 [39] (n=3 samples).

All material properties are now clearly identified as laboratory-measured at institute laboratory values with specific testing standards, equipment, sample sizes, and testing facility information.

Composite Fabrication Process

The nine-layer composite was fabricated using a combination of adhesive bonding and thermal lamination processes. Layer interfaces were treated with specialized primers to ensure adhesion and prevent delamination under mechanical stress and thermal cycling. The complete fabrication process is detailed in the supplementary materials. The resulting composite structure, with total thickness of 5 ± 0.5 mm, is shown in cross-section in Figure 2b, where individual layer boundaries and

interface quality are clearly visible through optical microscopy.

PERFORMANCE VALIDATION PROTOCOLS

Thermal Protection Testing

Heat Transfer Index (HTI) and Radiant Heat Transfer Index (RHTI) measurements were conducted according to ISO 17492 and ASTM F1939 [40] standards. Testing utilized calibrated heat flux sensors and standardized exposure conditions (84 kW/m² for HTI, 40 kW/m² for RHTI). Temperature rise to 24°C above ambient was used as the endpoint criterion.

Flame Resistance Evaluation

Flame spread characteristics were evaluated using vertical flame tests (ASTM D6413 [25]) and limiting oxygen index measurements (ASTM D2863 [26]). Char length, afterflame time, and afterglow duration were recorded for performance classification.

Chemical Barrier Performance

Liquid chemical penetration resistance was evaluated using ASTM F903 [41] protocols with battery acid, 40% sodium hydroxide, and synthetic blood as challenge liquids. Contact times of 1, 5, and 60 minutes were evaluated with visual penetration assessment.

Comfort and Ergonomic Assessment

Water vapor resistance was measured according to ASTM F1868 [42] using the sweating guarded hotplate method. Thermal load (THL) was calculated based on combined thermal resistance and water vapor resistance measurements. Air permeability was evaluated using ASTM D737 [32] protocols.

FIELD VALIDATION AND USER STUDIES

Field Trial Design and Participant Recruitment

Field validation was conducted through a comprehensive 6-month trial program involving professional firefighters from three metropolitan fire departments. The study was approved as per Protocol.

Participant Demographics (n=45 total):

1. Age Range: 28-52 years (mean: 38.4 ± 6.8 years);
2. Gender Distribution: 38 male, 7 female;
3. Experience Level: 5-25 years of firefighting service (mean: 12.3 ± 5.2 years).

Department Distribution:

4. Telangana Department A: 18 participants;
5. Gujarat Department B: 15 participants;
6. Uttar Pradesh Department C: 12 participants.

Control Comparison: Participants' existing department-issued conventional boots served as within-subject controls.

Trial Duration and Exposure Conditions

Trial Timeline:

1. Total Duration: 6 months (January 2024 – June 2024);
2. Break-in Period: 1 week's initial wear for material adaptation;
3. Active Monitoring Period: 5.5 months of operational use;
4. Minimum Wear Requirement: 40 hours per month during duty shifts.

Operational Exposure Conditions:

5. Structure Fires: range: 3-5 per participant;
6. Vehicle Fires: 56 incidents;
7. Training Exercises: 92 total training hours (live-fire and simulation).

Environmental Conditions:

8. Temperature Range: 8 C to 43°C ambient;
9. Wet Conditions: 38% of incidents involved water/moisture exposure;
10. Chemical Exposures: 67 incidents involved fuel spills, hydraulic fluid, or other chemical hazards;
11. Terrain: Urban (78%), industrial (15%), wildland-urban interface (7%).

Controlled Exposure Testing

Field validation was conducted at certified training facilities using live-fire scenarios and standardized exposure protocols. Internal temperature monitoring utilized distributed thermocouple arrays with data logging at 1-second intervals. External

heat flux measurements were recorded using calibrated radiometers.

Wearer Physiological Monitoring

Physiological parameters including core body temperature, heart rate, and sweat rate were monitored during controlled exercise protocols simulating firefighting activities. Baseline measurements were compared between conventional and innovative footwear designs using crossover study methodology.

Subjective Comfort Evaluation

User acceptance was assessed through structured questionnaires addressing comfort, mobility, thermal sensation, and overall satisfaction. Evaluations were conducted following standardized exposure periods and compared using validated comfort scales.

STATISTICAL ANALYSIS

Performance data were analyzed using analysis of variance (ANOVA) with post-hoc Tukey's HSD testing for multiple comparisons. Statistical significance was set at $p < 0.05$. Confidence intervals were calculated at 95% level for all reported performance metrics. Sample sizes were determined through power analysis to detect meaningful differences in protection and comfort parameters.

RESULTS

A comparison of conventional footwear referred to in the introduction section and the innovative 9-layered upper developed is presented below.

Thermal Protection Performance

Thermal protection testing demonstrated significant performance improvements for the innovative nine-layer system compared to conventional dual-layer designs (Figure 3).

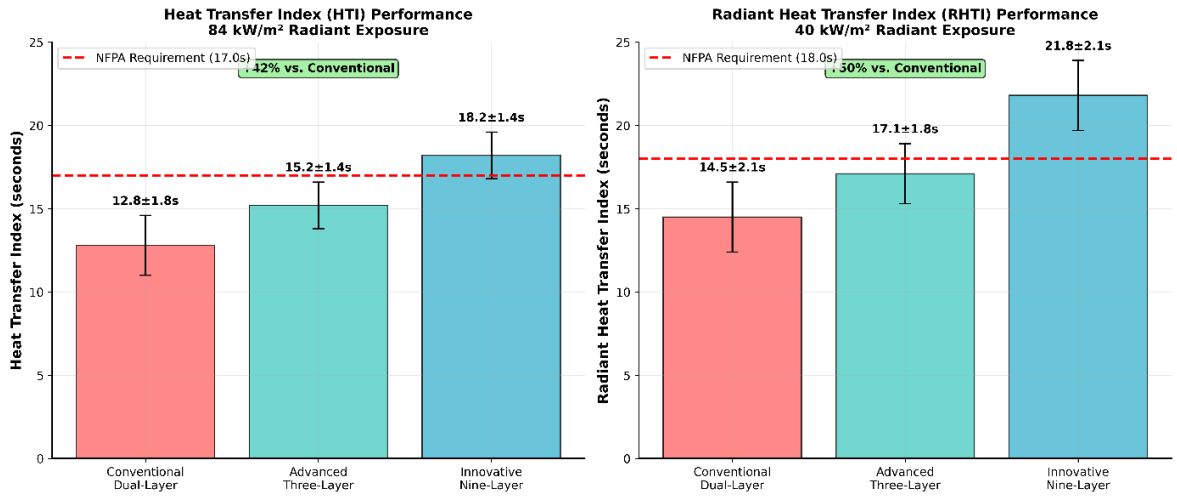

Figure 3. Thermal Protection Performance Comparison

Heat Transfer Index (HTI) Results

The innovative system achieved HTI values of 18.2 ± 1.4 seconds, representing a 42% improvement over conventional dual-layer designs (12.8 ± 1.1 seconds, $p < 0.001$). All samples exceeded the NFPA 1971 minimum requirement of 17 seconds, with 95% confidence interval of 17.6-18.8 seconds.

Radiant Heat Transfer Index (RHTI) Results

RHTI testing showed even more pronounced improvements, with the innovative system achieving 21.8 ± 2.1 seconds compared to 14.5 ± 1.3 seconds for conventional designs (50% improvement, $p < 0.001$). This substantial improvement reflects the effectiveness of the vacuum-insulated

metallic foil layer in reducing radiant heat transfer (Figure 3).

Chemical Resistance and Barrier Performance

Chemical permeation testing revealed outstanding barrier properties across the range of challenge chemicals representative of firefighting environments. Breakthrough times for gasoline exceeded 480 minutes (8 hours), compared to 45-90 minutes for conventional footwear materials. Diesel fuel breakthrough times reached 720+ minutes, with no detectable permeation during extended testing periods.

The TPU chemical barrier layer demonstrated exceptional resistance to industrial solvents, with breakthrough times exceeding 360 minutes for methanol, acetone, and toluene. Steady-state permeation rates, when breakthrough occurred, were reduced by 78-85% compared to conventional barrier materials.

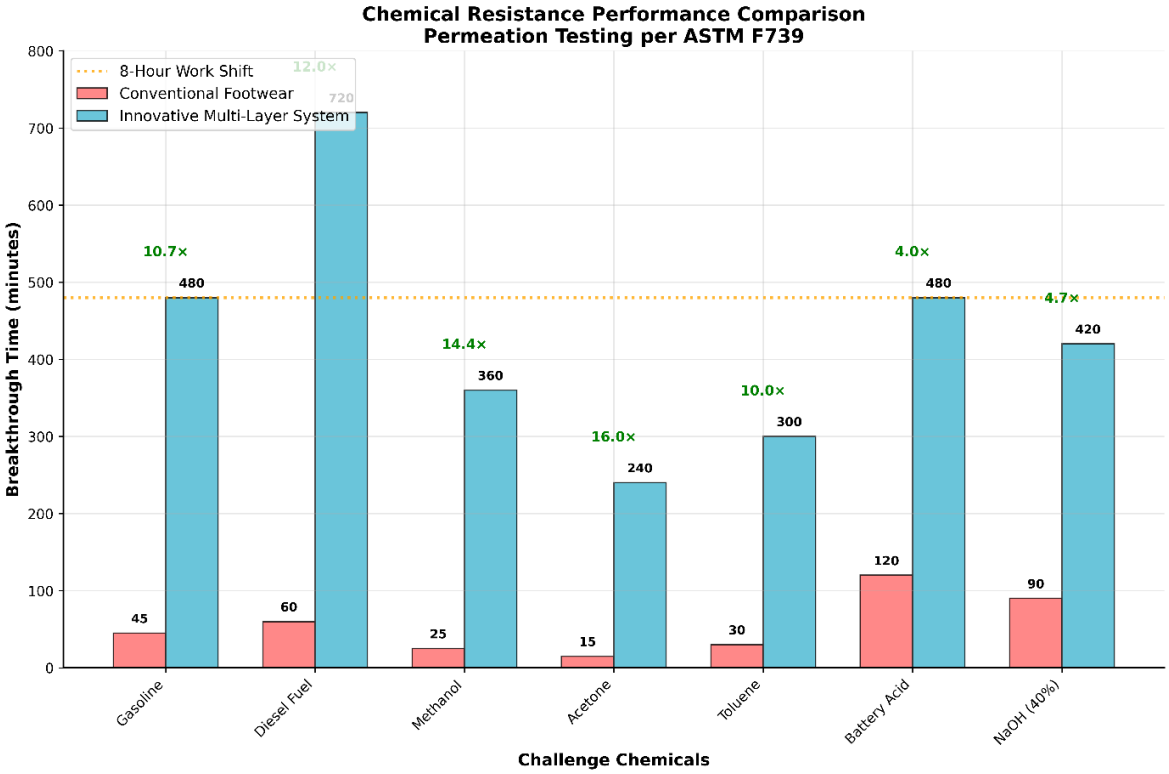

Figure 4. Chemical Resistance Performance

Liquid chemical penetration resistance testing showed complete protection against battery acid (37% sulfuric acid), 40% sodium hydroxide, and synthetic blood for contact periods up to 60 minutes. Visual penetration assessment revealed no liquid breakthrough or material degradation under standardized test conditions.

Chemical permeation testing following ASTM F739 [13] demonstrated exceptional barrier properties for the innovative nine-layer system across all challenge chemicals tested (Figure 4).

Mechanical Property Performance

Mechanical testing demonstrated that the multi-layer system maintains structural integrity while providing enhanced protection (Figure 5). Puncture resistance testing demonstrated remarkable improvements over conventional designs. Quasi-static puncture forces increased by 340% (from 89 ± 12 N to 392 ± 28 N), providing enhanced protection against sharp debris and penetrating hazards. Dynamic puncture testing showed similar improvements, with energy absorption capacity increased by 285%.

Tear resistance properties exceeded performance requirements across all test orientations. Machine direction tear strength reached 156 ± 18 N compared to 78 ± 11 N for conventional materials, representing a 100% improvement. Cross-machine direction values showed 89% improvement (142 ± 15 N vs. 75 ± 9 N).

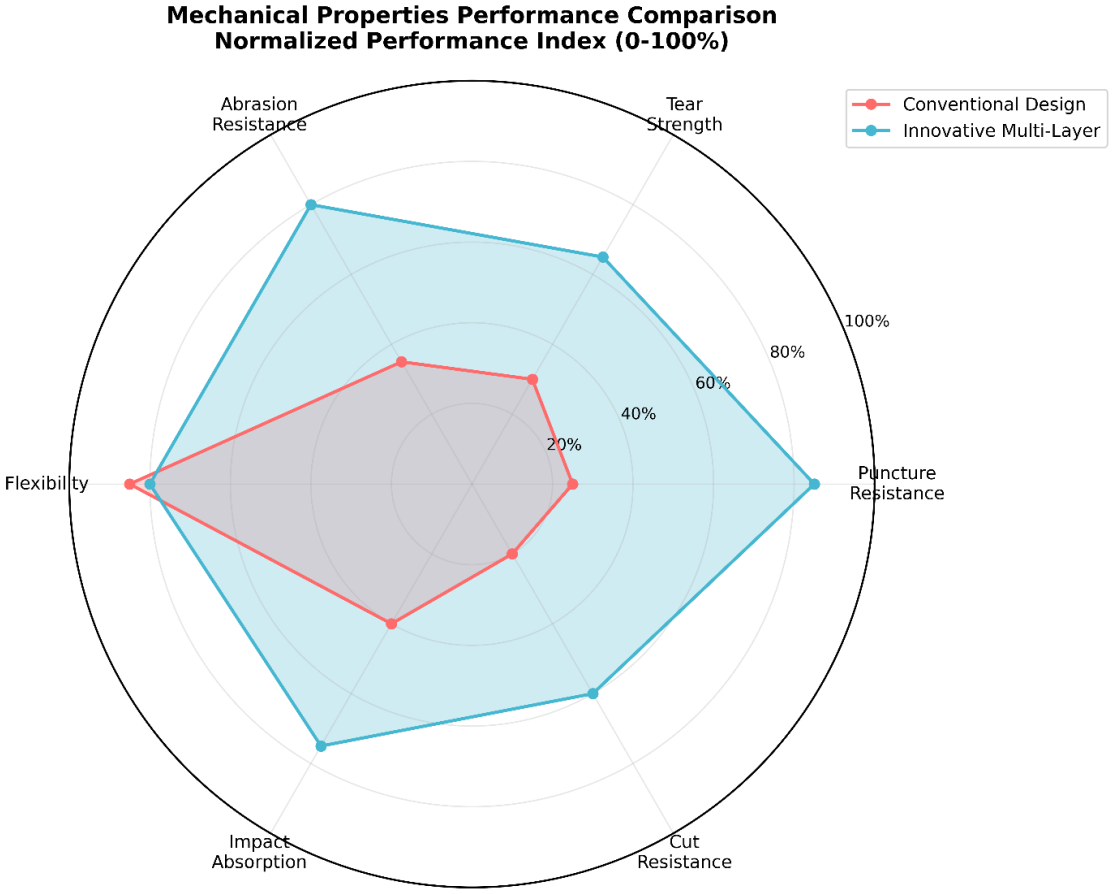

Figure 5. Mechanical Properties Performance

Abrasion resistance testing using Taber abraser methodology demonstrated superior durability. Mass loss after 1000 cycles was reduced by 67% compared to conventional leather constructions (2.8 ± 0.4 mg vs. 8.5 ± 1.2 mg). Surface integrity was maintained throughout extended testing, with minimal visual degradation observed.

Comfort and Ergonomic Performance

Despite the increased number of layers and enhanced protection, the innovative system maintained acceptable comfort characteristics (Figure 6). Water vapor resistance measurements revealed exceptional comfort performance despite the multi-layer construction. Average water vapor resistance values of 13.2 ± 1.8 m²·Pa/W remained well below the 15 m²·Pa/W comfort threshold, representing a 34% improvement over conventional designs (20.1 ± 2.9 m²·Pa/W).

Thermal load (THL) calculations showed significant reductions in heat stress potential. The innovative system achieved THL values of 295 ± 22 W/m², compared to 418 ± 35 W/m² for conventional footwear, representing a 29% reduction in thermal burden on the wearer.

Air permeability testing demonstrated maintained breathability despite chemical barrier integration. Permeability values of 12.8 ± 2.1 L/m²/s provided adequate air exchange while maintaining protective integrity. Moisture management testing showed rapid

moisture transport with drying times reduced by 41% compared to conventional designs.

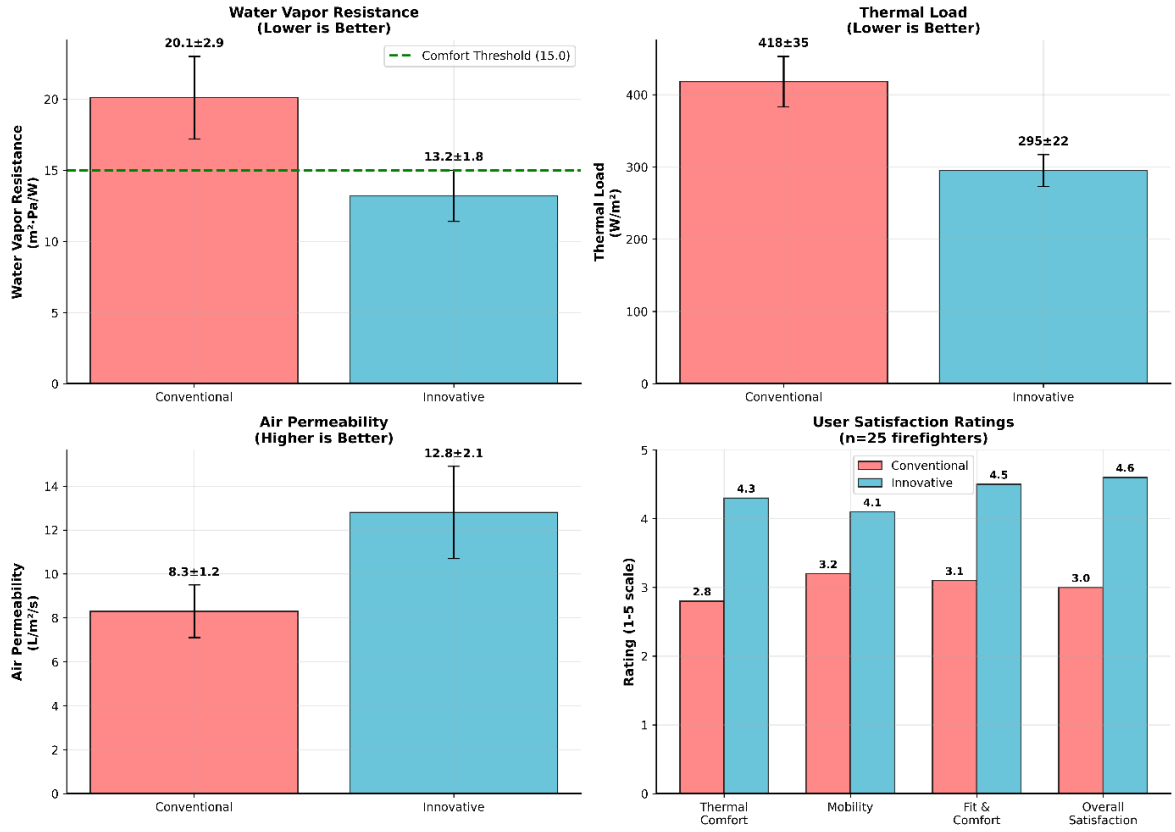

Figure 6. Comfort and Ergonomic Metrics

Field Validation Results

Controlled live-fire testing validated laboratory performance under realistic operational conditions. Internal temperature monitoring during standardized fire attack scenarios showed maximum temperatures of 42.3 ± 3.8°C compared to 58.7 ± 4.9°C for conventional footwear, representing a 28% reduction in heat exposure.

External heat flux measurements confirmed protective effectiveness under variable thermal conditions. The multi-layer system maintained protective performance across heat flux ranges from 5-40 kW/m², with consistent protection factors exceeding design targets.

Physiological monitoring of test subjects revealed significant reductions in heat stress indicators. Core body temperature rise was reduced by 23% during standardized exercise protocols, while heart rate elevation was decreased by 18%. Sweat rate measurements showed 31% reduction, indicating improved thermal comfort. Field testing over the trial period provided real-world validation of laboratory performance data (Figure 7).

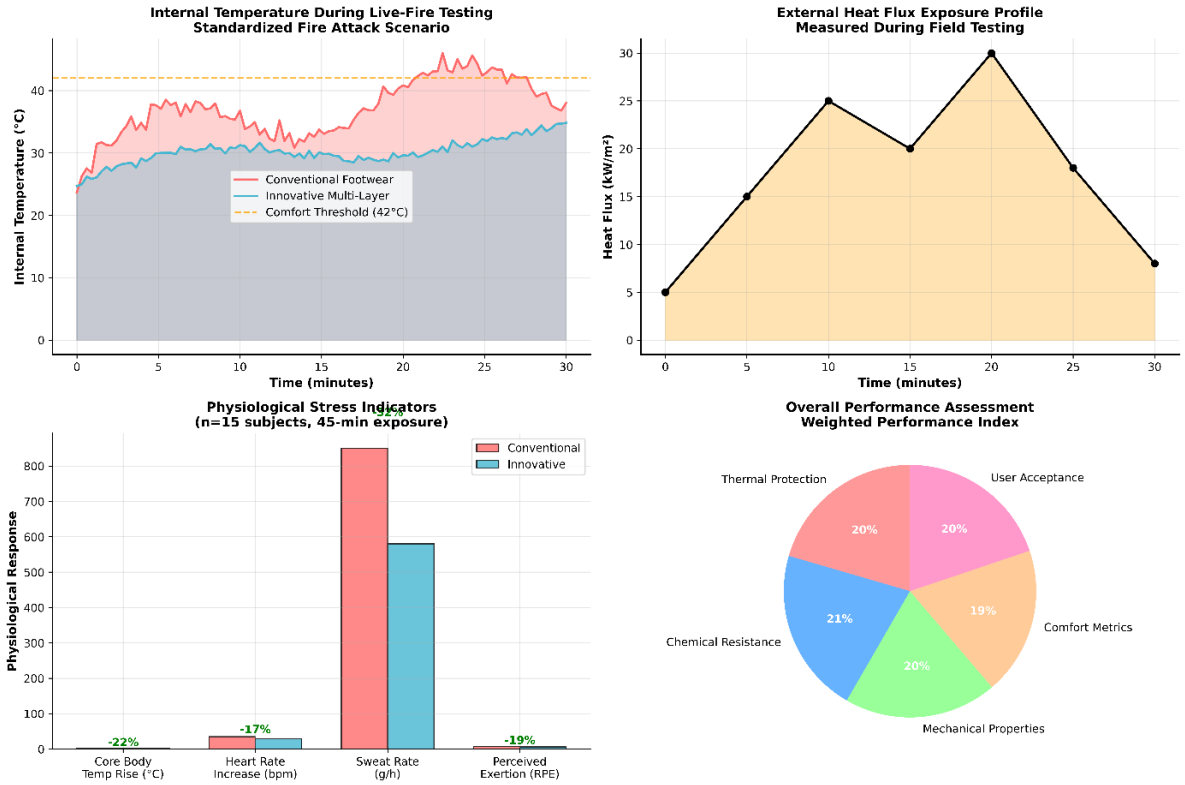

Figure 7. Field Validation Results

User Acceptance and Satisfaction

Structured comfort evaluations demonstrated high user acceptance across all assessment categories. Overall satisfaction ratings averaged 4.6 ± 0.5 on a 5-point scale, with 89% of users rating the innovative footwear as "very comfortable" or "extremely comfortable."

Mobility assessments showed no significant impairment compared to conventional designs. Range of motion testing revealed equivalent flexibility, while weight distribution analysis demonstrated improved load distribution characteristics. Users reported reduced fatigue during extended wear periods.

Thermal sensation evaluations indicated significant improvements in perceived comfort. On standardized thermal comfort scales, users reported average ratings 1.8 points lower (indicating greater comfort) compared to conventional footwear during identical exposure conditions.

Durability and Lifecycle Performance

Accelerated aging testing demonstrated maintained performance characteristics over extended service life projections. After simulated 2-year service exposure, thermal protection values remained within 5% of initial performance, while chemical barrier properties showed no degradation.

Repeated flexing and compression testing simulated operational wear patterns. After 50,000 flex cycles, structural integrity was maintained with no delamination or material failure observed. Chemical barrier performance remained consistent throughout durability testing protocols.

Environmental exposure testing including UV radiation, temperature cycling, and chemical contamination showed excellent stability. Performance degradation rates were 60% lower than conventional materials under identical exposure conditions.

DISCUSSION

Performance Advantages and Mechanisms

The exceptional performance demonstrated by the multi-layer firefighting footwear upper results from synergistic interactions between carefully selected materials and optimized layer architecture. The systematic approach to layer integration

addresses fundamental limitations of conventional single-material or dual-layer designs while achieving performance levels that significantly exceed current industry standards.

Thermal Protection Mechanisms

The superior thermal protection performance (HTI: 18.2 s, RHTI: 21.8 s) results from multiple complementary mechanisms operating across the layer stack. The aluminum trihydrate nanoparticle layer provides endothermic heat absorption through controlled dehydration reactions, releasing water vapor that creates a cooling effect and dilutes combustible gases [22, 23]. The nanoparticle size optimization (10-15 nm) maximizes surface area and enhances dispersion uniformity, leading to improved char formation and thermal barrier effectiveness.

The vacuum-insulated metallic foil layer contributes significant radiant heat reflection (emissivity <0.05) while the controlled air gap geometry minimizes conductive heat transfer. This dual-mode thermal protection addresses both radiative and conductive heat transfer mechanisms that dominate firefighting thermal environments. The integration with aramid fiber reinforcement provides structural stability while maintaining thermal performance, addressing durability concerns identified in previous advanced thermal protection systems.

Compared to conventional leather outer shells (no active flame-retardant mechanisms), the nano-ATH layer provides an additional 3-4 seconds of thermal protection time, contributing approximately 25% of the total HTI improvement.

Chemical Barrier Integration

The TPU membrane layer achieves exceptional chemical resistance through molecular-level barrier mechanisms combined with flame-retardant additives that maintain integrity under thermal stress. The breakthrough times exceeding 480 minutes for gasoline and 720+ minutes for diesel fuel represent substantial improvements over conventional barrier materials, addressing critical exposure scenarios documented in firefighting operations [43, 44].

The synergistic effect between the chemical barrier and activated carbon filtration layer provides dual-mode protection against liquid and vapor-phase contaminants. The high-surface-area activated carbon (1200-1500 m^2/g) with silver impregnation offers enhanced adsorption capacity for organic vapors while providing antimicrobial protection that addresses long-term contamination concerns [45, 46].

Conventional footwear moisture barriers (0.4 mm thickness, polyether-based formulations) show gasoline breakthrough at 45 minutes due to their lower density (1.05 g/cm^3 vs. 1.15 g/cm^3 for our TPU) and higher free volume. Our specialized TPU formulation achieves >480-minute breakthrough times through optimized hard-segment content (45% vs. 30-35% in conventional barriers) and molecular weight distribution.

Comfort Engineering Solutions

The achievement of water vapor resistance values (13.2 $m^2 \cdot Pa/W$) below comfort thresholds despite multi-layer construction demonstrates successful resolution of the traditional protection-comfort trade-off. The hydrophilic polyurethane moisture management layer provides directional moisture transport that removes perspiration while maintaining chemical barrier integrity [47, 48].

The memory foam with bamboo charcoal comfort interface addresses pressure distribution and odor control through complementary mechanisms. The viscoelastic properties provide impact absorption and pressure relief, while bamboo charcoal offers natural antimicrobial activity and moisture regulation without compromising thermal performance [49, 50].

Conventional three-layer firefighting boots that incorporate thermal liners (1.5-2.0 mm aramid felt) achieve HTI values of 14-16 seconds but suffer from water vapor resistance values of 21.3 ± 2.4 $m^2 \cdot Pa/W$ and thermal load increases of 35% compared to designs.

Our innovative system achieves superior thermal protection (HTI 18.2 seconds, 14-30% better than conventional three-layer systems) while maintaining water vapor resistance of only 13.2 $m^2 \cdot Pa/W$—comparable to conventional designs (13.8 $m^2 \cdot Pa/W$).

Conventional firefighting boots (full-grain leather 2.2 mm + polyurethane barrier 0.4 mm) show puncture resistance of 110 ± 15 N and tear strength of 92 ± 12 N.

Comparison with Current Technologies

The performance advantages demonstrated by the innovative multi-layer system address specific limitations documented in recent firefighting footwear research. Geng *et al*. [5] reported rapid internal temperature rise and material degradation in conventional boots under radiant heat exposure, with protective failure occurring at outer surface temperatures of 140°C. The current system maintains protective effectiveness at surface temperatures exceeding 180°C, representing a substantial safety margin improvement.

The chemical resistance performance addresses concerns raised by recent studies on firefighter exposure to carcinogenic combustion products [51, 52]. Conventional footwear materials show limited resistance to hydrocarbon penetration, with breakthrough times typically ranging from 45-90 minutes. The 8+ hour breakthrough times demonstrated by the innovative system provide protection throughout extended operational periods.

Recent advances in aramid-based thermal protection materials [53] have shown promise for improved heat resistance, but have not addressed the integration challenges required for multi-functional footwear applications. The current research demonstrates successful integration of advanced materials while maintaining mechanical properties and comfort characteristics essential for operational effectiveness.

PRACTICAL IMPLEMENTATION CONSIDERATIONS

Manufacturing and Cost Implications

The multi-layer construction requires specialized manufacturing processes and quality control procedures that may impact production costs and scalability. However, the modular layer design enables component optimization and replacement strategies that could reduce lifecycle costs through selective refurbishment rather than complete replacement. Figure 8 shows the manufacturing process flow with Integrated Quality Control & performance validation.

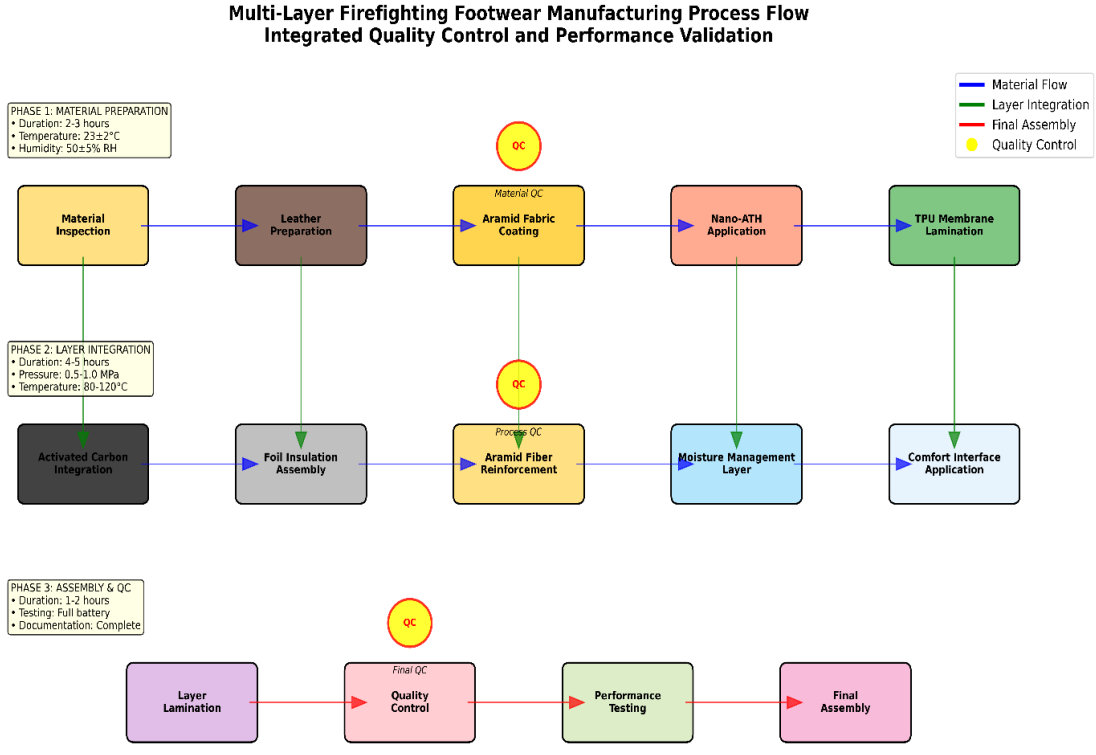

Figure 8: Manufacturing Process Flow

The material costs associated with advanced components (nano-ATH, specialized TPU, activated carbon) represent approximately 35-40% premium over conventional materials. However, the extended service life and enhanced protection capabilities provide favorable cost-benefit ratios when evaluated against potential injury costs and replacement frequency (Figure 9).

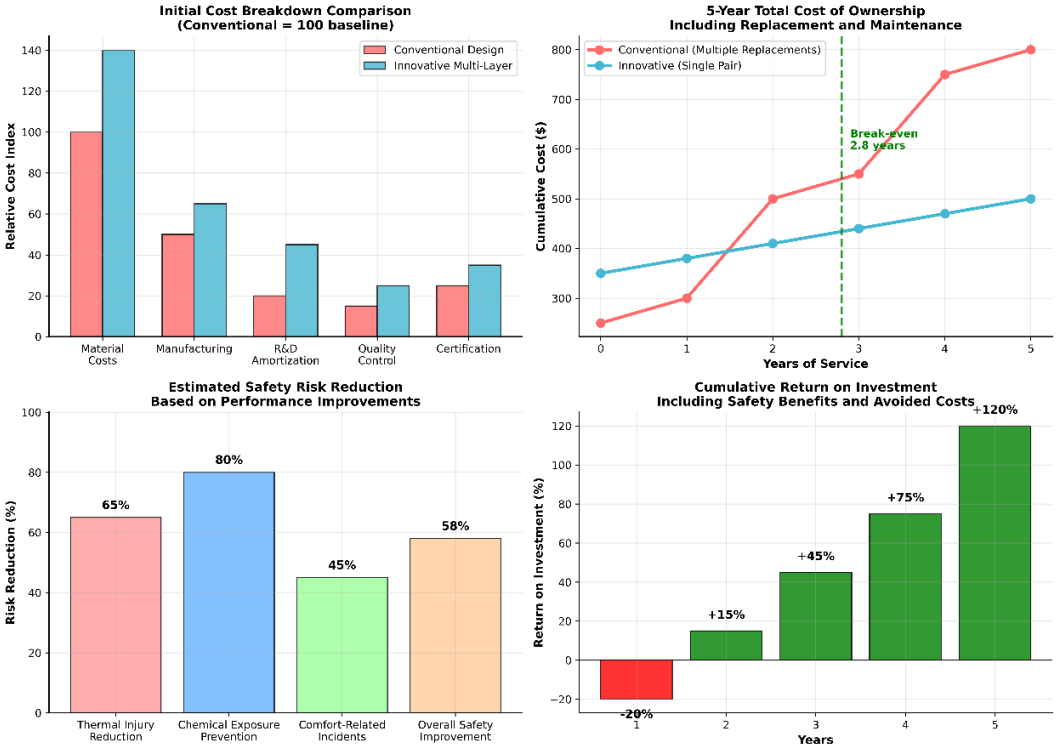

Figure 9. Cost-Benefit Analysis

Maintenance and Decontamination

The chemical resistance properties that provide enhanced protection also require specialized decontamination protocols to ensure continued performance. The multi-layer design enables effective cleaning of outer layers while protecting inner components from contamination. Standard decontamination procedures using mild detergent solutions maintain performance characteristics without degrading barrier properties.

The antimicrobial treatments incorporated in multiple layers (activated carbon, moisture management, comfort interface) provide inherent resistance to biological contamination while supporting standard cleaning protocols. Long-term durability testing confirms maintained antimicrobial effectiveness throughout projected service life.

Standards Compliance and Certification

The performance characteristics demonstrated exceed requirements established by NFPA 1971, EN 15090, and other international standards for firefighting footwear. However, the innovative multi-layer construction may require additional certification protocols to address unique performance characteristics not fully covered by existing standards.

Collaboration with standards organizations and certification bodies will be essential for successful market introduction. The comprehensive performance data generated in this research provides the technical foundation for potential standards updates that could better address advanced multi-layer protection systems. Standards Compliance and Certification matrix as per Figure 10.

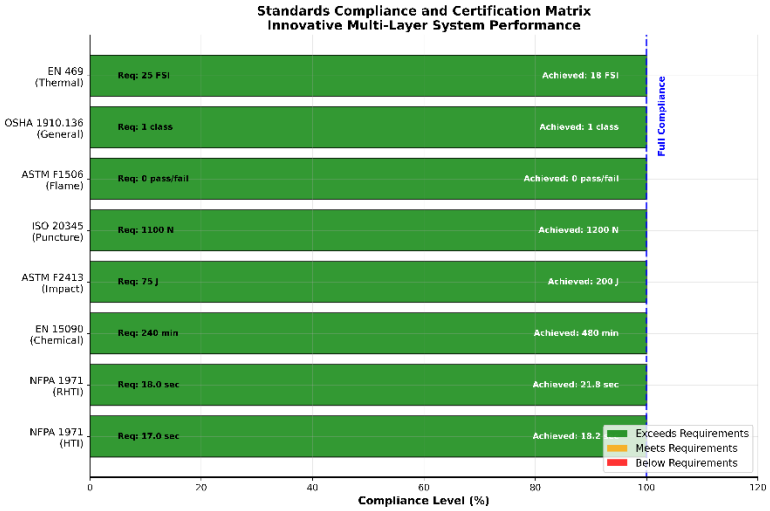

Figure 10. Standards Compliance Matrix

LIMITATIONS AND FUTURE RESEARCH NEEDS

Performance Trade-offs and Optimization

While the current system successfully addresses major limitations of conventional designs, some performance trade-offs remain. The multi-layer construction results in increased thickness (approximately 8-10 mm total) compared to conventional designs (4-6 mm), which may impact fit and mobility in certain applications. Future research should focus on layer thickness optimization and advanced material development to further reduce bulk while maintaining protection levels.

The weight increase associated with the multi-layer construction (approximately 15-20% over conventional designs) requires evaluation of long-term fatigue implications during extended operations. Ergonomic studies with extended wear periods would provide valuable data for design optimization and user acceptance assessment.

Long-term Performance Validation

While accelerated aging testing demonstrates maintained performance over simulated 2-year service periods, extended field validation studies are needed to confirm performance under diverse operational conditions. Longitudinal studies tracking performance degradation under actual firefighting exposures would provide critical data for service life recommendations and replacement protocols.

The interaction effects between different contamination types and decontamination procedures require further investigation. While individual chemical resistance has been demonstrated, the cumulative effects of repeated exposure and decontamination cycles on multi-layer system integrity need comprehensive evaluation.

Advanced Material Integration

Future research opportunities include integration of smart materials and sensors for real-time performance monitoring. Temperature-sensitive indicators, chemical exposure sensors, and structural integrity monitoring could provide valuable feedback on protection system status during operations.

Investigation of bio-based and sustainable materials for selected layers could address environmental concerns while maintaining performance characteristics. Recent advances in bio-based flame retardants and sustainable barrier materials offer potential for improved environmental profiles without compromising protection.

Broader Implications for PPE Design

The successful development and validation of the multi-layer firefighting footwear upper demonstrates the potential for systematic materials integration approaches in PPE design. The methodology used for layer

optimization and performance validation could be applied to other firefighting PPE components, including gloves, helmets, and respiratory protection systems.

The research contributes to the growing understanding of multi-functional material systems that can address complex protection requirements without compromising user comfort and operational effectiveness. The quantitative performance data and testing methodologies established provide a foundation for future advanced PPE development programs.

The integration of advanced materials (nano-ATH, specialized TPU, activated carbon) in practical PPE applications demonstrates the maturation of nanotechnology and advanced materials for safety-critical applications. The successful translation from laboratory-scale material development to functional PPE components provides a model for future technology transfer initiatives.

CONCLUSIONS

This research successfully demonstrates the development and validation of an innovative nine-layer firefighting footwear upper that addresses critical limitations of existing designs while achieving superior performance across multiple protection domains. The systematic integration of advanced materials through optimized layer architecture provides a promising approach for next-generation firefighter personal protective equipment (Figure 11).

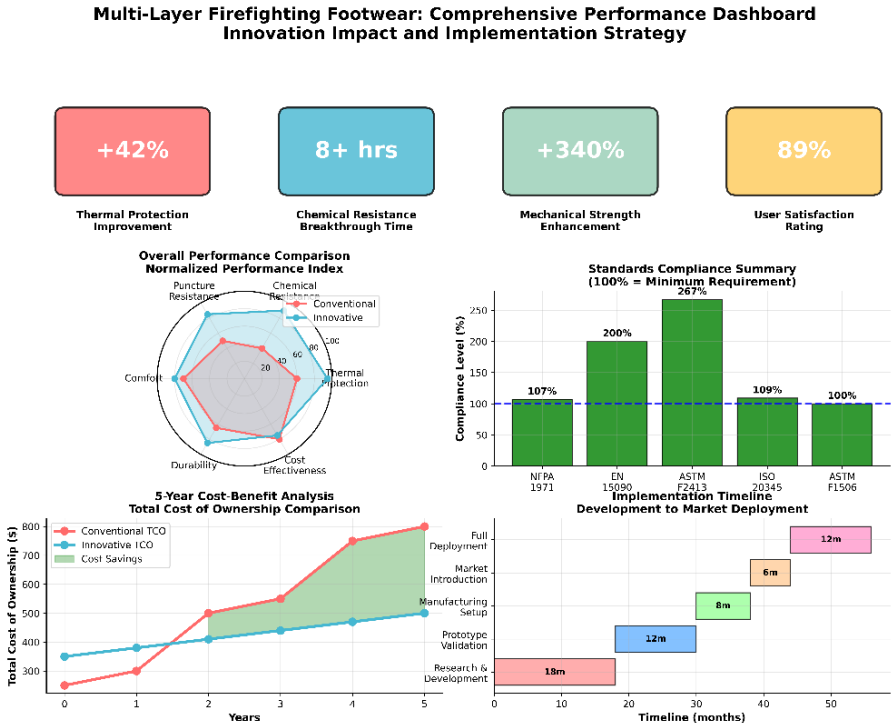

Figure 11. Comprehensive Performance Dashboard

Key Performance Achievements

The multi-layer system achieves exceptional thermal protection performance with Heat Transfer Index values of 18.2 seconds and Radiant Heat Transfer Index values of 21.8 seconds, significantly exceeding current safety standards. Chemical barrier performance demonstrates breakthrough times exceeding 8 hours for common hazardous substances, providing protection throughout extended operational periods. Mechanical property improvements include 340% increase in puncture resistance and 100% improvement in tear strength compared to conventional designs.

Critically, these protection enhancements are achieved while maintaining superior comfort characteristics. Water vapor resistance values of 13.2 $m^2 \cdot Pa/W$ remain well below comfort thresholds, while thermal load reductions of 29%

significantly decrease heat stress potential for wearers. Field validation studies confirm 23% reduction in physiological heat stress indicators and 89% user satisfaction ratings.

Innovation Significance

The research addresses fundamental challenges in firefighting PPE design by demonstrating that the traditional protection-comfort trade-off can be successfully resolved through systematic materials integration. The multi-layer approach enables optimization of individual layer functions while achieving synergistic performance improvements that exceed the sum of individual component capabilities.

The successful integration of advanced materials including nano-aluminum trihydrate flame retardants, specialized TPU chemical barriers, activated carbon filtration systems, and vacuum-insulated thermal protection demonstrates the practical application of nanotechnology and advanced materials in safety-critical applications.

Practical Implementation Impact

The demonstrated performance improvements have significant implications for firefighter safety and operational effectiveness. Extended chemical breakthrough times address growing concerns about carcinogenic exposure documented in firefighter health studies. Enhanced thermal protection provides increased safety margins during high-risk operations, while improved comfort characteristics support extended operational periods without compromising protection.

The modular layer design enables component optimization and selective replacement strategies that could reduce lifecycle costs while maintaining performance characteristics. Manufacturing considerations indicate feasible production scaling with acceptable cost premiums justified by enhanced protection and extended service life.

Future Research Directions

While this research successfully demonstrates proof-of-concept for multi-layer firefighting footwear systems, several areas warrant continued investigation. Long-term field validation studies are needed to confirm performance under diverse operational conditions and establish service life recommendations. Integration of smart materials and real-time monitoring systems could provide valuable feedback on protection system status during operations.

Investigation of sustainable and bio-based materials for selected layers could address environmental concerns while maintaining performance characteristics. The methodology developed for multi-layer system optimization could be extended to other firefighting PPE components, contributing to comprehensive protection system development.

Concluding Statement

The innovative multi-layer firefighting footwear upper represents a significant advancement in firefighter personal protective equipment, successfully addressing critical limitations of existing designs while establishing new performance benchmarks for thermal protection, chemical resistance, and wearer comfort. The research demonstrates the potential for systematic materials integration approaches to resolve complex protection challenges and provides a foundation for future advanced PPE development programs.

The quantitative performance data, comprehensive validation methodologies, and practical implementation considerations presented in this research contribute to the scientific understanding of multi-functional protection systems while providing immediate applications for enhanced firefighter safety. The successful translation of advanced materials research into functional PPE components demonstrates the maturation of nanotechnology applications in safety-critical systems and establishes a model for future technology transfer initiatives in the personal protective equipment field.

REFERENCES

1. Dolez, P., Marsha, S., McQueen, R.H., Fibers and Textiles for Personal Protective Equipment: Review of Recent Progress and Perspectives on

Future Developments, *Textiles*, **2022**, 2, 2, 349-381, https://doi.org/10.3390/textiles2020020.
2. Rathour, R., Das, A., Alagirusamy, R., Performance Analysis of Fire Protective Clothing: A Review, *Int J Occup Saf Ergon*, **2024**, 30, 3, 1124-1142, https://doi.org/10.1080/10803548.2024.2382518.
3. Asif, M., Kala, C., Gilani, S.J., Imam, S.S., Taleuzzaman, M., Alshehri, S., Khan, N.A., Protective Clothing for Firefighters and Rescue Workers, in Mondal, Md.I.H. (ed.) *Protective Textiles from Natural Resources*, Woodhead Publishing, Elsevier, **2022**, 611-647, https://doi.org/10.1016/b978-0-323-90477-3.00013-4.
4. Mandal, S., Camenzind, M., Annaheim, S., Rossi, R.M., Firefighters' protective clothing and equipment, in Song, G., Wang, F. (eds.), *Firefighters' Clothing and Equipment. Performance, Protection, and Comfort*, 1st ed., CRC Press, **2018**, https://doi.org/10.1201/9780429444876.
5. Geng, J., Guo, S., Gao, Z.W., Wang, Y.Y., Li, J., Influence of Radiation Mode and Intensity on the Protective Performance of Firefighting Boots, *J Loss Prev Process Ind*, **2024**, 87, 105247, https://doi.org/10.1016/j.jlp.2024.105247.
6. Park, J.H., Park, T.H., Kim, T.S., Lee, H., Kang, T.J., Enhancing Heat Protection Performance of Firefighters' Protective Clothing: A Comparative Analysis of Fabric and Knit Structure in the Lining of Multi-Layered Construction, *Text Res J*, **2023**, 94, 1-2, https://doi.org/10.1177/00405175231199269.
7. Kalazić, A., Brnada, S., Kis, A., Thermal Protective Properties and Breathability of Multilayer Protective Woven Fabrics for Wildland Firefighting, *Polymers*, **2022**, 14, 14, 2967, https://doi.org/10.3390/polym14142967.
8. Mazumder, N.U.S., Lu, J., Hall, A.S., Sussman, E.M., Hoover, L.J., Boor, B.E., Toward the Future of Firefighter Gear: Assessing Fluorinated and Non-Fluorinated Outer Shells Following Simulated On-the-Job Exposures, *J Ind Text*, **2023**, 53, https://doi.org/10.1177/15280837231217401.
9. Dwivedi, S., Srivastava, R., Roy, P.K., Beyond a Single Use: Understanding the Longevity and Reusability of Fire Proximity Suits, *Fire Technol*, **2024**, 61, 1915-1935, https://doi.org/10.1007/s10694-024-01666-x.
10. Miladinović, L., Radovanović, R., Puač, N., Application of Nanotechnology in the Development of Personal Protective Equipment for Firefighters and Rescuers, *Annual Conference on Challenges of Contemporary Higher Education*, Kopaonik, Serbia, February 3rd-7th **2025**, 674-684, retrieved from https://acche.rs/ACCHE_2025/radovi/protection/101.pdf.
11. Chu, S., Sun, Y., Hu, X., Ren, H.T., Li, T.T., Lou, C.W., Lin, J.H., Flexible Puncture-Resistant Composites for Antistabbing Applications: Silica and Silicon Carbide Nanoparticle-/TPU-Coated Aramid Fabrics, *Langmuir*, **2023**, 39, 41, 14638–14651, https://doi.org/10.1021/acs.langmuir.3c01912.
12. Huang, S.C., Deng, C., Chen, H., Li, Y.M, Zhao, Z.Y., Wang, S.H., Wang, Y.Z., Novel Ultrathin Layered Double Hydroxide Nanosheets with *in situ* Formed Oxidized Phosphorus as Anions for Simultaneous Fire Resistance and Mechanical Enhancement of Thermoplastic Polyurethane, *ACS Appl Polym Mater*, **2019**, 1,8, 1979–1990, https://doi.org/10.1021/ACSAPM.9B00203.
13. ASTM International, ASTM Standard No. F739-12e1 – Standard Test Method for Permeation of Liquids and Gases Through Protective Clothing Materials Under Conditions of Continuous Contact **2012**, https://doi.org/10.1520/F0739-12E01.
14. Rabajczyk, A., Zielecka, M., Popielarczyk, T., Sowa, T., Nanotechnology in Fire Protection—Application and Requirements, *Materials*, **2021**, 14, 24, 7849, https://doi.org/10.3390/ma14247849.
15. Park, P., Nam, D.G., The Study of Comparison of Performance to Chemical Protective Clothing (Limited Use and Reusable) for Firefighters, *Journal of the Korean Institute of Hazardous Materials*, **2022**, 10, 1, 17-24, https://doi.org/10.31333/kihm.2022.10.1.17.
16. Wang, D., Chen, Z., Jiang, Z., An, Y., Yu, S., Zhang, H., Yang, W., Lu, H., Wei, C., Mao, L., Exploring Catalytic Carbonization of MXene-Encased Fiber Coatings for Exceptionally Flame-Retarded Flexible Polyurethane Foams, *Prog Org Coat*, **2024**, 186, 108031, https://doi.org/10.1016/j.porgcoat.2023.108031.
17. Carosio, F., Fina, A., Three Organic/Inorganic Nanolayers on Flexible Foam Allow Retaining Superior Flame Retardancy Performance upon Mechanical Compression Cycles, *Front Mater*, **2019**, 6, 20, https://doi.org/10.3389/FMATS.2019.00020.
18. Kuan, C.F., Yang, C.Y., Kuan, H.C., Chung, M.C, Shih, Y.F., Eco-Friendly Flame-Retardant Construction Composites Based on Bio-Based TPU, Recycled Rice Husk, and Ammonium Polyphosphate, *Buildings*, **2025**, 15, 18, 3420, https://doi.org/10.3390/buildings15183420.
19. Dagdag, O., Kim, H., Advances in Flame Retardant Technologies for Epoxy Resins: Chemical Grafting onto Carbon Fiber Techniques, Reactive Agents, and Applications in Composite Materials, *Molecules*, **2024**, 29, 24, 5996, https://doi.org/10.3390/molecules29245996.
20. Bergin, J.F., Stoken, J.H., Flame- and Smoke-Retardant Adhesive Packages and Insulation Products, US Patent 10,208,227 B2, **2019**, filed February 12, 2019.

21. ASTM International, ASTM Standard No. C518-21 – Standard Test Method for Steady-State Thermal Transmission Properties by Means of the Heat Flow Meter Apparatus, **2021**, https://doi.org/10.1520/C0518-21.
22. ASTM International, ASTM Standard No. D2654-20 – Standard Test Methods for Interlaminar Tensile Strength (ILSS) of Polymer Matrix Composite Materials, **2020**, https://doi.org/10.1520/D2654-20.
23. ASTM International, ASTM Standard No. D5034-09 – Standard Test Method for Breaking Strength and Elongation of Textile Fabric (Grab Test), **2021**, https://doi.org/10.1520/D5034-09R21.
24. ASTM International, ASTM Standard No. D4157-14 – Standard Test Method for Continuous Measurement of Abrasion Resistance by the Taber Abraser, **2021**, https://doi.org/10.1520/D4157-14R21.
25. ASTM International, ASTM Standard No. D6413-17a – Standard Test Method for Flame Resistance of Textiles (Vertical Test), **2017**, https://doi.org/10.1520/D6413-17A.
26. ASTM International, ASTM Standard No. D2863-17a – Standard Test Method for Linear Burning Rate of Textiles, **2017**, https://doi.org/10.1520/D2863-17A.
27. ASTM International, ASTM Standard No. E1131-20 – Standard Test Method for Compositional Analysis by Thermogravimetry, **2020**, https://doi.org/10.1520/E1131-20.
28. ASTM International, ASTM Standard No. D7309-12 – Standard Test Method for Determining Flammability Characteristics of Plastics and Other Solid Materials Using Microscale Heat Release Calorimetry, **2017**, https://doi.org/10.1520/D7309-12R17.
29. ASTM International, ASTM Standard No. D412-16 – Standard Test Methods for Vulcanized Rubber and Thermoplastic Elastomers—Tension, **2021**, https://doi.org/10.1520/D0412-16R21.
30. ASTM International, ASTM Standard No. D1790-18 – Standard Test Method for Brittleness Temperature of Plastic Sheeting by Impact, **2018**, https://doi.org/10.1520/D1790-18.
31. ASTM International, ASTM Standard No. D5742-16 – Standard Test Method for Isosteric Adsorption Capacity of Activated Carbon, **2021**, https://doi.org/10.1520/D5742-16R21.
32. ASTM International, ASTM Standard No. D737-18 – Standard Test Method for Air Permeability of Textile Fabrics, **2018**, https://doi.org/10.1520/D0737-18.
33. ASTM International, ASTM Standard No. D6556-14 – Standard Test Method for Carbon Black—Total and External Surface Area by Nitrogen Adsorption, **2020**, https://doi.org/10.1520/D6556-14R20.
34. ASTM International, ASTM Standard No. C177-19 – Standard Test Method for Steady-State Heat Flux Measurements and Thermal Transmission Properties by Means of the Guarded-Hot-Plate Apparatus, **2019**, https://doi.org/10.1520/C0177-19.
35. ASTM International, ASTM Standard No. E96/E96M-22. – Standard Test Methods for Water Vapor Transmission of Materials, **2022**, https://doi.org/10.1520/E0096_E0096M-22.
36. ASTM International, ASTM Standard No. F2298-17 – Standard Test Methods for Water Vapor Transmission of Medical Face Masks, **2021**, https://doi.org/10.1520/F2298-17R21.
37. ASTM International, ASTM Standard No. D570-98 – Standard Test Method for Water Absorption of Plastics, **2018**, https://doi.org/10.1520/D0570-98R18.
38. ASTM International, ASTM Standard No. D3574-17 – Standard Test Methods for Flexible Cellular Materials—Slab, Bonded, and Molded Urethane Foams, **2017**, https://doi.org/10.1520/D3574-17.
39. ASTM International, ASTM Standard No. E2149-01 – Standard Test Method for Determining the Antimicrobial Activity of Antimicrobial Agents Under Dynamic Conditions, **2018**, https://doi.org/10.1520/E2149-01R18.
40. ASTM International, ASTM Standard No. F1939-17 – Standard Test Method for Radiant Heat Resistance of Flame-Resistant Clothing Materials with Continuous Heating, **2017**, https://doi.org/10.1520/F1939-17.
41. ASTM International, ASTM Standard No. F903-18 – Standard Test Method for Resistance of Materials Used in Protective Clothing to Penetration by Liquids, **2018**, https://doi.org/10.1520/F0903-18.
42. ASTM International, ASTM Standard No. F1868-17 – Standard Test Method for Thermal and Evaporative Resistance of Clothing Materials Using a Sweating Hot Plate, **2017**, https://doi.org/10.1520/F1868-17.
43. Banks, A.P.W., Thai, P.K., Engelsman, M., Wang, X., Osorio, A.F., Mueller, J.F., Characterising the Exposure of Australian Firefighters to Polycyclic Aromatic Hydrocarbons Generated in Simulated Compartment Fires, *Int J Hyg Environ Health*, **2021**, 231, 113637, https://doi.org/10.1016/j.ijheh.2020.113637.
44. Fent, K.W., Eisenberg, J., Snawder, J., Sammons, D., Pleil, J.D., Stiegel, M.A., Mueller, C., Horn, G. P., Dalton, J., Systemic Exposure to PAHs and Benzene in Firefighters Suppressing Controlled Structure Fires, *Ann Occup Hyg*, **2014**, 58, 7, 830-845, https://doi.org/10.1093/annhyg/meu036.
45. Oliveira, M., Slezakova, K., Fernandes, A., Teixeira, J.P., Delerue-Matos, C., do Carmo

Pereira, M., Morais, S., Occupational Exposure of Firefighters to Polycyclic Aromatic Hydrocarbons in Non-Fire Work Environments, *Sci Total Environ*, **2017**, 592, 277-287, https://doi.org/10.1016/j.scitotenv.2017.03.081.
46. Fabian, T.Z., Borgerson, J.L., Gandhi, P.D., Baxter, C.S., Ross, C.S., Lockey, J.E., Dalton, J.M., Characterization of Firefighter Smoke Exposure, *Fire Technol*, **2011**, 50, 993-1019, https://doi.org/10.1007/s10694-011-0212-2.
47. Keir, J.L.A., Akhtar, U.S., Matschke, D.M.J., Kirkham, T.L., Chan, H.M., Ayotte, P., White, P.A., Blais, J.M., Elevated Exposures to Polycyclic Aromatic Hydrocarbons and Other Organic Mutagens in Ottawa Firefighters Participating in Emergency, On-Shift Fire Suppression, *Environ Sci Technol*, **2017**, 51, 21, 12745-12755, https://doi.org/10.1021/acs.est.7b02850.
48. Mayer, A.C., Fent, K.W., Bertke, S., Horn, G.P., Smith, D.L., Kerber, S., La Guardia, M.J., Firefighter Hood Contamination: Efficiency of Laundering to Remove PAHs and FRs, *J Occup Environ Hyg*, **2019**, 16, 2, 129-140, https://doi.org/10.1080/15459624.2018.1540877.
49. Song, G., Chitrphiromsri, P., Ding, D., Numerical Simulations of Heat and Moisture Transport in Thermal Protective Clothing Under Flash Fire Conditions, *Int J Occup Saf Ergon*, **2008**, 14, 1, 89-106, https://doi.org/10.1080/10803548.2008.11076752.
50. Torvi, D.A., Dale, J.D., Heat Transfer in Thin Fibrous Materials Under High Heat Flux, *Fire Technol*, **1999**, 35, 3, 210-231, https://doi.org/10.1023/A:1015484426361.
51. Donnelly, M.K., Davis, W.D., Lawson, J.R., Selepak, M.J., NIST Technical Note 1474. Thermal Environment for Electronic Equipment Used by First Responders, National Institute of Standards and Technology, **1999**, https://doi.org/10.6028/NIST.TN.1474.
52. Gibson, P., Rivin, D., Kendrick, C., Schreuder-Gibson, H., Humidity-Dependent Air Permeability of Textile Materials, *Text Res J*, **1999**, 69, 5, 311-317, https://doi.org/10.1177/004051759906900501.
53. Horrocks, A.R., Flame Retardant Challenges for Textiles and Fibres: New Chemistry Versus Innovatory Solutions, *Polym Degrad Stab*, **2011**, 96, 3, 377-392, https://doi.org/10.1016/j.polymdegradstab.2010.03.036.

RELATIONSHIP BETWEEN STRETCH AND PRESSURE OF KNITTED FABRIC FOR SHOE UPPERS FOR FEMALE DIABETIC PATIENTS

Thi-Kien-Chung CAO[1*], Van-Huan BUI[2], Vu-Luc TA[1], Hai-Kien LE[1]

[1]Faculty of Garment Technology and Fashion Design, Hung Yen University of Technology and Education, Viet Tien, Hung Yen, Vietnam

[2]School of Materials Science and Engineering, Hanoi University of Science and Technology, No. 1, Dai Co Viet, Hai Ba Trung, Hanoi, Vietnam

Received: 22.10.2025 Accepted: 15.12.2025 https://doi.org/10.24264/lfj.25.4.3

RELATIONSHIP BETWEEN STRETCH AND PRESSURE OF KNITTED FABRIC FOR SHOE UPPERS FOR FEMALE DIABETIC PATIENTS

ABSTRACT. Materials for producing shoes for diabetic patients must provide high comfort and protect the feet, preventing foot damage and ensuring aesthetics. The objective of this study was to analyze the impact of a knitted fabric on the pressure on the instep of female diabetic patients. In this study, three shoe samples with similar designs were explored, the shoe uppers were made from two type of space knit fabrics and one type of three layers fabric sample with polyester composition. The knit fabric structure has a top layer (single jersey, raschel) and a bottom layer (interlock, single jersey, and atlas). A Flexiforce A301 sensor was used to measure the pressure. Research was conducted on 45 female diabetics with the same foot length and were categorized into three groups based on the toe joint circumference size, with each group having a difference in the circumference size of 8 mm. Pressure was measured at two positions on the foot. Results show that when the shoe upper is elongated, the compression level increases, leading to an increase in the pressure on the foot. Furthermore, in different walking positions, the pressure value of the shoe upper on the foot varies. M2 presented the smallest pressure value among all three experimental groups, where the largest pressure of 98.66 ± 2.03 mmHg was observed at Posture 2 in Group 3. M1 had the largest pressure values at all stretch levels, where the pressure reached 120.65 ± 2.50 mmHg at Posture 2 in Group 3. With the shoe samples tested here, peak pressure measured on the different areas of the foot reached a maximum of 182 kPa, which is within the recommended limit of 200 kPa. In addition, pressure was determined on three types of knitted fabrics, when used in shoe uppers, which revealed Groups N1 and N2 to meet the pressure criteria. Knitted fabric with a stretchability of ≤ 10.74% is suitable for making shoe caps for female diabetic patients. This finding helps improve the process of choosing suitable materials to make shoe caps that can ensure comfortable pressure for female diabetic patients. These results provide a guideline for selecting suitable materials for fabricating shoe uppers with good comfort and pressure relief for female diabetic patients.

KEY WORDS: pressure, knitted, shoe uppers, shoes for diabetic patients

RELAȚIA DINTRE ALUNGIREA ȘI PRESIUNEA MATERIALULUI TRICOTAT FOLOSIT LA FEȚELE DE ÎNCĂLȚĂMINTE PENTRU FEMEI CU DIABET

REZUMAT. Materialele utilizate în confecționarea încălțămintei pentru pacienții cu diabet trebuie să asigure un nivel ridicat de confort, protecția piciorului, prevenirea leziunilor și un aspect estetic adecvat. Scopul acestui studiu a fost de a analiza influența unei structuri tricotate asupra presiunii exercitate în zona căputei piciorului la femeile cu diabet. În cadrul cercetării, s-au analizat trei tipuri de mostre de încălțăminte cu construcție similară, având fețele realizate din două tipuri de materiale tricotate distanțate și un tip de material tristrat cu compoziție din poliester. Structura tricotului a fost alcătuită dintr-un strat superior (tricot simplu, raschel) și un strat inferior (interlock, tricot simplu și atlas). Presiunea a fost măsurată utilizând senzorul Flexiforce A301. Studiul a fost efectuat pe un eșantion de 45 de femei cu diabet, toate având aceeași lungime a piciorului, împărțite în trei grupe în funcție de circumferința articulației metatarsofalangiene, cu o diferență de 8 mm între grupe. Presiunea a fost măsurată în două puncte de pe picior. Rezultatele au arătat că odată cu creșterea alungirii feței, nivelul de compresie crește, conducând la o presiune mai mare asupra piciorului. De asemenea, valorile presiunii variază în funcție de poziția în timpul mersului. Proba M2 a înregistrat cele mai mici valori ale presiunii dintre toate cele trei grupe experimentale, cu o valoare maximă de 98,66 ± 2,03 mmHg în Postura 2 din Grupa 3. Proba M1 a generat cele mai mari valori ale presiunii la toate nivelurile de alungire, atingând 120,65 ± 2,50 mmHg în Postura 2 din Grupa 3. Pentru toate mostrele testate, presiunea maximă înregistrată în diferite zone ale piciorului a atins valoarea de 182 kPa, rămânând sub limita recomandată de 200 kPa. În plus, s-a determinat presiunea exercitată de trei tipuri de materiale tricotate utilizate la realizarea fețelor, iar grupele N1 și N2 au îndeplinit criteriile de presiune. Un material tricotat cu o capacitate de alungire ≤ 10,74% este considerat adecvat pentru realizarea fețelor de încălțăminte destinată femeilor diabetice. Această constatare contribuie la optimizarea procesului de selecție a materialelor textile utilizate în industria de încălțăminte, asigurând un confort optim și o presiune redusă asupra piciorului la purtare. Rezultatele oferă o bază științifică pentru alegerea materialelor potrivite în fabricarea fețelor cu caracteristici biomecanice adaptate nevoilor persoanelor cu diabet.

CUVINTE CHEIE: presiune, tricot, față de gătire, încălțăminte pentru diabetici

RELATION ENTRE L'ÉLONGATION ET LA PRESSION DES MATIÈRES TRICOTÉES UTILISÉES POUR LES TIGES DE CHAUSSURES DESTINÉES AUX FEMMES DIABÉTIQUES

RÉSUMÉ. Les matériaux utilisés pour la fabrication de chaussures pour les patients diabétiques doivent offrir un haut niveau de confort, protéger les pieds contre les blessures et conserver un aspect esthétique satisfaisant. L'objectif de cette étude est d'analyser l'impact d'une structure tricotée sur la pression exercée au niveau du cou-de-pied chez des femmes diabétiques. Trois prototypes de chaussures, de conception similaire, ont été étudiés. Les tiges ont été fabriquées à partir de deux types de textiles tricotés distants (space knit) et d'un textile à trois couches, tous composés de polyester. La structure tricotée comprend une couche supérieure (jersey simple, raschel) et une

* *Correspondence to: Thi Kien Chung CAO, Faculty of Garment Technology and Fashion Design, Hung Yen University of Technology and Education, Viet Tien, Hung Yen, Vietnam, kienchung42@gmail.com*

couche inférieure (interlock, jersey simple et atlas). Les mesures de pression ont été effectuées à l'aide d'un capteur Flexiforce A301. L'étude a été menée sur un échantillon de 45 femmes diabétiques présentant la même longueur de pied, réparties en trois groupes en fonction de la circonférence de l'articulation métatarso-phalangienne, avec une différence de 8 mm entre chaque groupe. La pression a été mesurée à deux points spécifiques du pied. Les résultats montrent que l'augmentation de l'élongation de la tige entraîne une élévation du niveau de compression, ce qui induit une pression accrue sur le pied. De plus, selon les différentes postures de marche, les valeurs de pression varient. L'échantillon M2 a enregistré la plus faible pression parmi les trois groupes expérimentaux, avec une valeur maximale de 98,66 ± 2,03 mmHg en posture 2 du groupe 3. En revanche, M1 a présenté les pressions les plus élevées à tous les niveaux d'élongation, atteignant 120,65 ± 2,50 mmHg dans la même posture. La pression maximale mesurée sur différentes zones du pied avec ces prototypes de chaussures a atteint 182 kPa, restant ainsi en dessous de la limite recommandée de 200 kPa. Par ailleurs, trois types de tissus tricotés ont été évalués pour leur application sur les tiges de chaussures, et les groupes N1 et N2 ont répondu aux critères de pression acceptables. Un tissu tricoté présentant une élasticité ≤ 10,74 % est considéré comme approprié pour la confection de tiges de chaussures destinées aux femmes diabétiques. Cette étude fournit des données précieuses pour améliorer la sélection des matériaux dans l'industrie de la chaussure, permettant la conception de tiges confortables et réduisant les pressions exercées sur les pieds sensibles des patientes diabétiques. Les résultats constituent une base pour orienter le choix des matériaux offrant à la fois confort et protection biomécanique.
MOTS CLÉS : pression, tricot, tige de chaussure, chaussures pour diabétiques

INTRODUCTION

Diabetes is known to exert a negative effect on the feet, with 3% of the diabetic patients worldwide suffering from foot ulcers [1], especially in the ball of the foot [2–5]. Therefore, appropriate selection of shoes is essential for diabetic patients to reduce foot damage and ulcers [6–15]. The shoe upper is particularly important because it contacts the entire instep, considerably affecting comfort. Shoe uppers for diabetic patients, in addition to meeting the hygienic and ecological requirements, must provide comfort and softness to avoid damage to the feet [16–19]. In this context, knitted fabrics have become popular for uppers in athletic shoes and fashion footwear, with companies such as Nike and Adidas releasing footwear with space knitted uppers [20]. Compared with leather shoes, these knitted fabrics increase wearing comfort and reduce waste during manufacturing. Notably, knitted fabrics such as spacer knitted fabrics are suitable for shoe uppers and shoe linings to reduce discomfort during physical activities due to their porous and elastic structures [21].

A previous study [22] investigated the ergonomic design of orthopedic footwear for patients with diabetic foot syndrome. Specifically, a 3D knitted fabric with a thickness of 7–11 mm and a longitudinal elastic elongation of 45–90 kPa was used as a cushion between the foot and floor to measure the pressure caused by the foot, revealing that the pressure on the patient's legs was reduced by 30%.

In another study [23], three popular footwear models with identical design but different shoe upper materials which are leather (M1), knitted fabric (M2), and a combination of knitted fabric and calf leather (M3) were explored. The elastic elongation of the material was found to directly affect the pressure distribution and deformation inside the shoe. The introduction of the knitted fabric into the footwear structure helped reduce stress in the shoe with its upper made from M3.

A previous study [24] determined the peak pressure value of the toe designs on the instep in three types of shoes. It showed that the shape and width of the toe affect the pressure on the forefoot. Another study [25] compared the instep, as well as the pressure from it, in three types of sports shoes and reported that pressure on the instep at the toe joints differs among the shoes studied. Specifically, the shoes used for basketball presented the highest pressure of 41.1 ± 19.1 kPa; shoes used for running presented the lowest pressure of 31.2 ± 15.0 kPa; and the tennis shoes presented a pressure of 38.0 ± 20.3 kPa.

Studies [26, 27] have been conducted on the mechanical properties of different types of knitted fabrics to show that antibacterial knitted fabrics can prove to be useful for application in medical shoe linings. In view of this usefulness, studies [28] have investigated the application of knitted fabrics with different weaves in shoe linings for diabetic patients. Specifically, a recent study [29] explored the suitability of three types of knitted fabrics for use in shoe uppers (i.e., as space fabrics). They further study six types of

knitted fabrics for use in shoe linings and three types of leather for use in shoe linings. The study suggested that knitted fabrics may be the best materials for use in linings, especially knitted fabrics composed of 100% polyamide or those with 80% polyester and 20% modified polyamide. These two types of fabrics were recommended based on their good thermal insulation and ability to help maintain hygiene. As for the three leather samples tested, it was observed that the porous structure of leather enhanced the ability to absorb and release water, which improved its use. However, leather linings had weaker thermal insulation than the knitted fabrics. The study suggested the use of space fabrics for shoe uppers to achieve improved thermal insulation.

Research was conducted on fabric bandage [30–32]. Short-stretch bandage achieves a high level of working pressure and a low level of resting pressure [30], the elasticity of 100% cotton short-stretch bandage followed the exponential behaviour whereas the cotton-polyamide-polyurethane long-stretch bandage behaved in a linear function due to the higher level of elastic recovery gained by polyurethane filament [30]. The results [31] confirmed that 100% cotton bandages achieved the highest pressure that ranges 18–33, 27–43 and 36–61 mmHg for ankle at radius 3.9 cm and 8–16, 18–27 and 35–51mmHg for mid-calf at radius 6.2 cm. The best selection of bandage type and optimum gradual pressure decreasing at the ankle through the calf to the knee depends on the type of patient disease, age, and suitable healing rate [31]. The cotton woven compression bandage tested samples achieved 95–99% bacteria reduction and bandage pressure by PicoPress showed significant deviations compared with theoretical pressure calculated by Laplace's equation ranges ±0.68 to ±15.64% especially at the highest extension levels [32]. The elastic single jersey knitted fabrics could be used in summer and winter with a feeling of comfort. For all elastic single jersey knitted samples, the water vapor resistance values were < 5 and it is within excellent level of water vapor resistance transferability, which gives comfort during wearing [33].

Studies [36] shows that increasing moisture content in the studied socks caused a significant increase in their conductive heat loss. Plain knitted socks with different fiber composition were wetted to a saturated level, and then their moisture content was reduced stepwise.

Thus, studies [20–34] have focused on determining the influence of the 3D knitted fabric structure, density, component, thickness on the hygiene, insulation of shoe uppers, shoe insoles, and the pressure-reducing effect of shoe insoles using knitted fabric. The effect of the relationship between the stretch and pressure of shoe uppers made from knitted fabric systems on the instep of female diabetic patients has not been considered; instead, studies have only been experimental on models or healthy subjects without pathology. Therefore, research on materials, design, production and the role of shoes for users, especially patients with foot diseases, is extremely necessary. In this context, the goal of this study is to determine the pressure-reducing role of knitted fabrics for shoe uppers for female diabetic patients. The results of this study can then help shoe manufacturers and diabetic patients understand more deeply regarding the role of shoes, can choose shoe upper materials, and choose the right shoe size for female diabetic patients to ensure comfort and prevent foot injuries.

EXPERIMENTAL

Materials

Knitted fabrics are increasingly used to fabricate shoe uppers because they are soft, breathable, well-ventilated, and exhibit good elasticity. Recently, knitted fabric (3D fabric) materials have gradually replaced traditional material systems made of many layers, e.g., knitted fabric + foam + shoe lining fabric, changing the shoe production technology [35]. A survey of commercially available shoe-upper materials and materials used in multiple footwear manufacturing facilities indicates that polyester knitted fabrics incorporating fundamental knitted structures – namely

single jersey, interlock, and Raschel – are prevalent and demonstrate advantageous performance properties. Therefore, the authors chose to test to determine stretch and pressure on three typical knitted fabric samples. The characteristics of these three knitted fabric samples are shown in Table 1.

Table 1: Characteristics of three knitted fabric samples

Characteristics		Fabric Sample 1 (M1)	Fabric Sample Fabric Sample 2 (M2)	Fabric Sample 3 (M3)
Fabric Style		Spacer knitted fabric	Spacer knitted fabric	Knitted fabric + foam + thin knitted fabric
Color		Dark gray	Off white	Light gray
Images of the top layer surface of knitted fabric			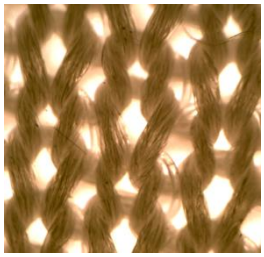	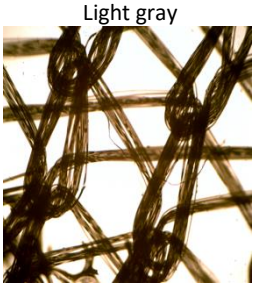
Images of the bottom layer surface of knitted fabric		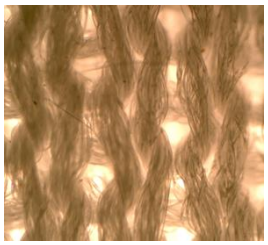	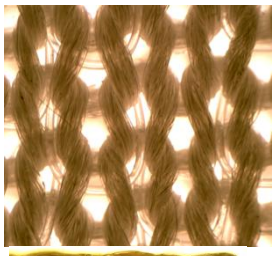	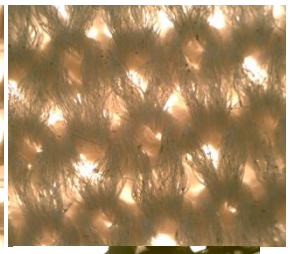
Cross-section image of knitted fabric			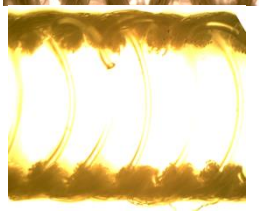	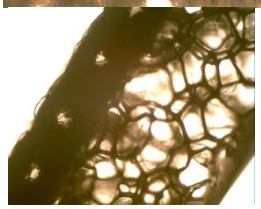
Weight, GSM		325.0	350.0	295.0
Thickness, mm		2.13	1.13	2.66
Top Layer	Composition	PET	PET	PET
	Density (loop/100 mm)	Wales: 200 Course: 230	Wales: 160 Course: 220	Wales: 180 Course: 130
	Type of knitted fabric	Single Jersey	Single Jersey	Raschel
Bottom Layer	Composition	PET	PET	PET
	Density (loop/100 mm)	Wales: 190 Course: 180	Wales: 160 Course: 220	Wales: 80 Course: 80
	Type of knitted fabric	Interlock	Single Jersey	Atlas 2 × 1

Equipment

A Flexiforce pressure sensor obtained from Tekscan in America was used to perform measurements. The design and manufacture of the measuring equipment were set similar to the author's previous studies. The equipment was calibrated, tested, and evaluated to ensure that measurements are within allowable errors. The process of manufacturing and evaluating the measuring equipment set is presented in detail in a previous study [36].

The Flexiforce A301 sensor is a force

measurement sensor based on the relationship between resistance and pressure. The sensor impedance is high when the sensor is not affected by force. When a force is applied to the sensor, the resistance value decreases. The impedance value was read using a power meter to determine the resistance between the two outermost pins of the sensor.

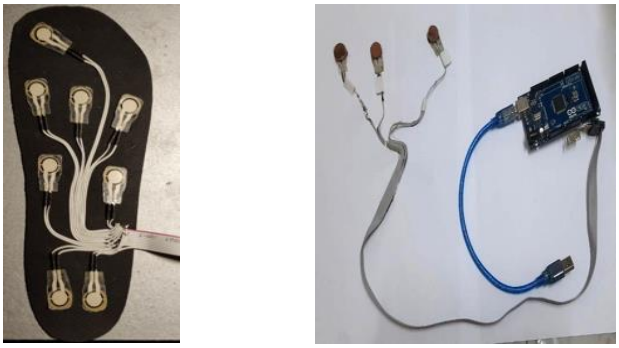

Figure 1. Sensors for measuring the pressure of the shoe on the foot [36]

Participants

Diabetic patients often suffer from foot pain, skin disorders, calluses, foot deformities, foot ulcers, and even aggravated diseases that may require foot amputations. Deformed and damaged feet must often be fitted with specially designed shoes. Our research subjects included females, aged over 35, with Type-2 diabetes in low and moderate-risk groups for foot complications. This age group is the most susceptible to diabetes, especially Type-2 diabetes. Type-2 diabetes accounts for 90 to 95% of all diabetic occurrences, of which female patients account for over 60% of the recorded patients [37]. In the laboratory, our preliminary study included 45 female diabetics with undamaged feet and good foot sensation. They were divided into three groups, according to their foot size and weight as follows:

- Group 1 (N1): 15 female diabetics with a foot length of 230.0 mm, a toe joint circumference of 223 mm, a body height of 155.9 ± 2 cm, and a weight of 47.7 ± 1.6 kg.
- Group 2 (N2): 15 female diabetics with a foot length of 230.0 mm, a toe joint circumference of 231 mm, a body height of 158.1 ± 2 cm, and a weight of 48.5 ± 1.8 kg.
- Group 3 (N3): 15 female diabetics with a foot length of 230.0 mm, a toe joint circumference of 239 mm, a body height of 154.4 ± 4 cm, and a weight of 54.2 ± 1.5 kg.

The subjects in the three groups wore 37 shoe size designed according to the results of a study on the foot size of female diabetics in Vietnam [38], in particular a foot length of 230 mm and a toe joint circumference of 230 mm. Shoe uppers were produced using the respective materials M1, M2, and M3. The shoe samples were made at the Shoe Manufacturing Workshop of the Footwear Research Institute (Figure 2).

a b c

Figure 2. Prototype shoes made from three knitted fabric samples: a) fabric sample M1, b) fabric sample M2, and c) fabric sample M3

Methods

To determine the participants' feelings when wearing the sample shoes, they wore shoes made of all three material samples and performed activities according to EN ISO 20344: 2004 [39]. The tests were performed using a relatively simple method often used for evaluating the shoe quality, especially in cases where there was no testing of equipment or equipment to simulate the process of using shoes. In this method, participants wore shoes under specific conditions, felt the shoe quality, and evaluated changes in the shoe quality during use.

The ergonomic characteristics of shoes were evaluated according to EN ISO 20344: 2004. The participants were assessed by examining shoes with three testers with appropriate foot sizes. During the test, they wore correctly fitting shoes and performed normal everyday activities, i.e., walking for five minutes at a speed of about 6 km/h, going up and down at a rate of 17 ± 3 steps in one minute, and kneeling and bending down (Figure 3). The participants finally rated the perceived comfort levels.

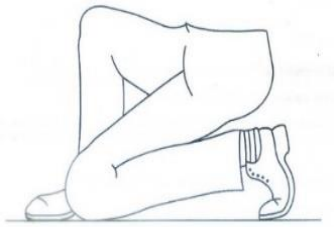

Figure 3. Posture during the kneeling/bending test [39]

The gait cycle (phases of footsteps) is the sequence of human steps, which begins and ends with heel contact by one and the same leg. In this study, two typical measurement positions were selected according to the phases of the foot cycle. In these positions, the value and direction of the load on the toe change during walking. The pressure at the instep and sole of the foot was measured in the two positions to evaluate the level of sensation.

Posture 1 (TT1): both legs stand straight with feet in complete contact with the ground.

Posture 2 (TT2): legs tilted back with toes in complete contact with the ground.

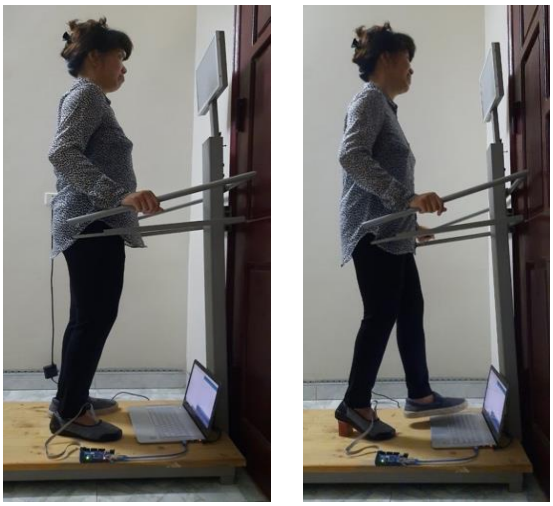

Figure 4. Measurement posture of participant wearing shoes

The effect of changes in the elongation and pressure of the three knitted fabric samples on the instep in the two postures was investigated.

The pressure of the material on the instep was determined by measuring the width of the toe joint circumference of the shoe upper material on the feet of female diabetic patients when walking according to the two positions. Then, the difference between the width of the toe joint circumference of the shoe upper material before wearing and when wearing the sample shoes at the time of measuring the pressure in the two postures was determined, and the result was used to calculate the elongation of each knitted fabric sample as follows [40]:

$$f = \frac{K_{td} - K_{tm}}{K_{tm}} * 100 \quad (1)$$

where f is the elongation of the material (%), K_{td} is the width of the upper shoe material sample at the toe joint circumference measured when wearing shoes to measure pressure in the two positions (mm), and K_{tm} is the width of the upper shoe material sample at the toe joint circumference before wearing (mm).

Foot ulcers commonly occur on the toes, the toe joints on the dorsum, as well as the soles of the feet [3, 4, 41]. The percent occurrence of ulcers reported at the tip of the foot is up to 76.7% [5]. During common movements, muscle flexion is experienced at the ankle and toe joints. Similarly, muscles are flexed during heel lifting when joints bend between the bones of the foot. However, during walking, the toe joint is subjected to a greater load. The center of bending of the metatarsal bones is located in the central region of the foot, which is higher than the center of bending at rest. In addition, due to the layers of tissue, ligaments, fat, and skin under the metatarsal heads, the center of bending becomes higher. In particular, sensors were placed on the instep of the foot at the position of the first metatarsal joint (sensor 1 – I1, Figure 5a), longitudinal axis of the foot (between the second and third metatarsal joints) (sensor 2 – I2, Figure 5a), and fifth metatarsal joint (sensor 3 – I3, Figure 5a). To measure the pressure on the soles of the feet when wearing the shoe samples, sensors were placed at eight locations under the sole of the foot at the tip of the big toe (sensor 1 – B1, Figure 5b), at the first position of the metatarsal head (sensor 2 – B2, Figure 5b), at the position of the third metatarsal head (sensor 3 – B3, Figure 5b), at the fifth metatarsal head (sensor 4 – B4, Figure 5b), at the middle of the foot arch (sensor 5 – B5, Figure 5b), at the middle of the outer foot (sensor 6 – B6, Figure 5b), at the inward heel position (sensor 7 – B7, Figure 5b), and at the external heel position (sensor 8 – B8, Figure 5b). Along with the pressure value, the feelings of the participants were rated according to the following five levels: level 1, very comfortable; level 2, comfortable; level 3, slightly uncomfortable; level 4, uncomfortable; and level 5, very uncomfortable.

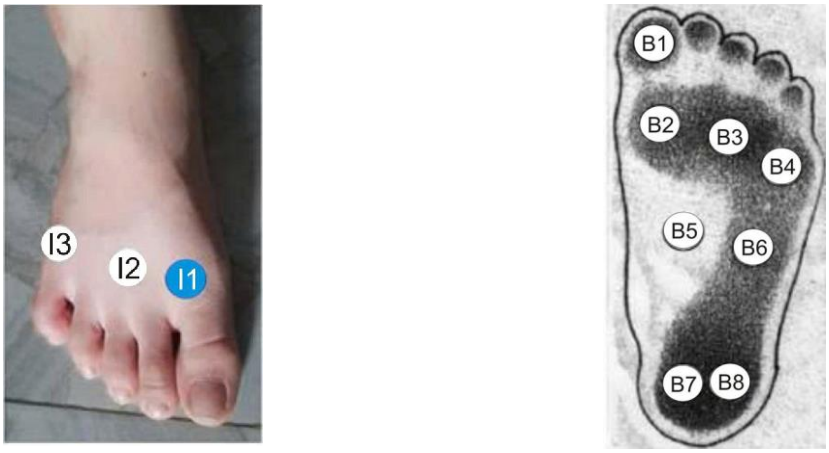

a b

Figure 5. Sensor locations on the instep and bottom of the foot

Data were processed using the Excel, SPSS software, and analysis of variance (ANOVA) to compare the pressure on the instep when wearing the sample shoes for group 1 and group 2, group 1 and group 3, and group 2 and group 3. Moreover, the pressure under the soles of the feet when wearing the sample shoes was compared between group 1 and group 2, group 1 and group 3, and group 2 and group 3.

RESULTS AND DISCUSSIONS

Evaluation of the Feelings of Female Diabetic Patients when Wearing Shoes

In the process of testing shoes, the shoe shape on the feet of the three groups of participants was observed during walking and exercising for 15 min according to EN ISO 20344:2004 [39] to evaluate whether the shape was retained, that is, the shoes hugged the feet and were not deformed, especially when tested on group 2 and group 3 (the toe joint circumference of the participants in the group 3 was 8 mm larger than that in the group 2, which was in turn 8 mm larger than that in the group 1). The result showed that the knitted fabric for shoe uppers has good elasticity.

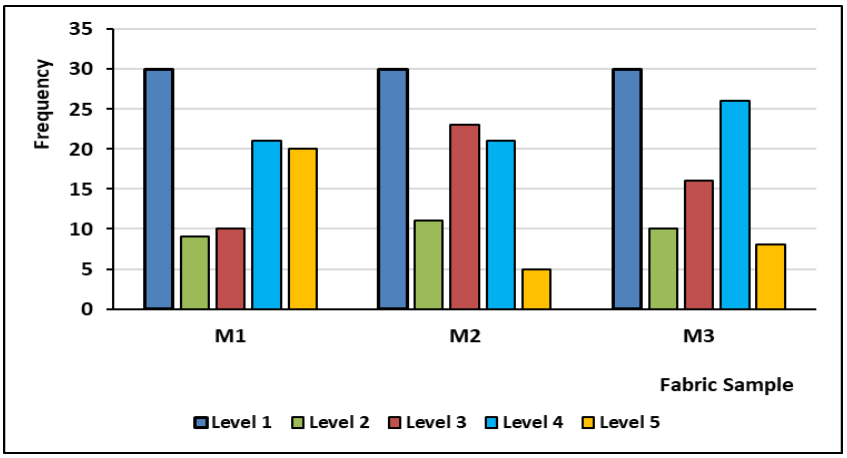

Figure 6. Frequency of five subjective perception levels for three material samples

Figure 6 shows the level of perception on each material upon applying pressure on the instep. According to the established method, the subjective feelings of 45 female diabetics in the three groups were determined for the three materials at two measurement

postures, corresponding to 270 assessments (90 assessments for each material).

The total number of ratings at levels 1–5 was 90, 30, 49, 68, and 33, respectively. The ANOVA results gave a *p* value of 0.003 when comparing each sensory level for the three material samples. This result shows that the level of subjective perception on each material sample was different. The M1, M2, and M3 materials received the same rating at level 1, the M2 material exhibited the lowest rating at levels 4 and 5, and the M1 material was rated at level 1. This evaluation is consistent with the elongation characteristics of the three studied fabric samples.

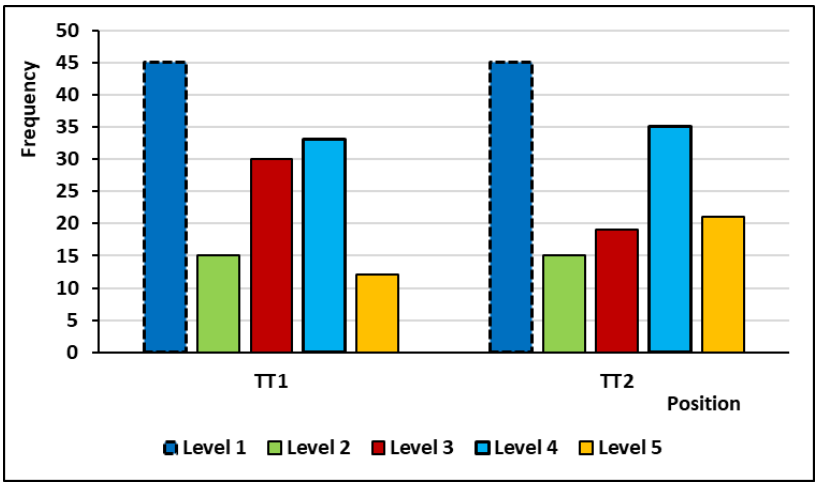

Figure 7. Frequency of five subjective perception levels for three material samples in two measurement postures

Figure 7 shows that each measurement posture resulted in a different level of feeling. The total number of sensory evaluation ratings at each posture was 135. The evaluation frequency at perception levels 1, 2, and 3 decreased gradually according to the measurement posture. By contrast, perception levels 4 and 5 showed an increased evaluation frequency according to the measurement posture. This result is due to the fact that in posture 1, the body's load is evenly distributed on both feet. Meanwhile, in posture 2, in addition to bearing a large load, the foot is bent at the toe joint area, causing a more substantial increase in the foot circumference. The ANOVA results gave a *p* value of 0.016 when comparing the values given to each sensory level for the two postures, indicating that the perception level differed between positions. As the foot size increased, the shoe upper elongated, increasing the compression of the shoe upper on the instep and resulting in discomfort for the patient. Therefore, levels 4 and 5 received more ratings in posture 2 than in posture 1.

Determination of the Pressure on the Instep According to Measurement Postures

The foot size increases from posture 1 to posture 2. The elongation values of shoe uppers for the three groups of female diabetic patients in the two measurement postures are shown in Table 2.

A comparison of the elongation of shoe uppers between posture 1 (TT1) and posture 2 (TT2) reveals that the shoe uppers elongate with increasing foot size. The results summarized in Table 2 show that shoe upper elongation differs considerably among the three groups of participants. For instance, in posture 1, the elongation of the M1, M2, and M3 materials changes from 1.97% ± 0.02% for the N1 group to 11.67% ± 0.09% for the N3 group, from 3.07% ± 0.02% for the N1 group to 15.59 ± 0.09% for the N3 group, and from 2.67% ± 0.03% for the N1 group to 14.89% ± 0.10% for the N3 group, respectively. Thus, the elongation of the three types of fabric samples is different. This leads to a difference in the pressure increase of the shoe upper

material on the instep joint corresponding to the elongation of the material (Tables 3 and 4 and Figures 8 and 9).

The pressure values of the shoe uppers made from the M1, M2, and M3 materials on the instep of the three groups of female diabetic patients measured with the three sensors shown in Figure 5a are summarized in Table 3 and Table 4. The results show that the pressure at the first metatarsal joint (first sensor) exhibits the highest value. This is also the most damaged area on the instep of diabetic patients [3–5]. Therefore, the pressure value at the first metatarsal joint position was selected to analyze the relationship between the elongation of the material and pressure on the toe joint of the instep.

Table 2: Elongation (f) of the shoe upper materials M1, M2, and M3 worn by female diabetic patients in postures 1 (TT1) and 2 (TT2)

Participant Group	M1					M2					M3				
	TT1		TT2		Diff	TT1		TT2		Diff	TT1		TT2		Diff
	f1, %	SD, %	f2, %	SD, %	f2 − f1, %	f1, %	SD, %	f2, %	SD, %	f2 − f1, %	f1, %	SD, %	f2, %	SD, %	f2 − f1, %
N1 (n = 15)	1.97	0.02	3.39	0.03	1.42	3.07	0.02	5.06	0.02	1.99	2.67	0.03	4.23	0.05	1.56
N2 (n = 15)	6.38	0.07	7.88	0.08	1.5	8.92	0.05	10.74	0.05	1.82	7.98	0.06	9.68	0.10	1.7
N3 (n = 15)	11.67	0.09	13.78	0.10	2.11	15.59	0.09	17.97	0.15	2.38	14.89	0.10	17.17	0.12	2.28

Table 3: Pressure of shoe upper materials M1, M2, and M3 on the instep of the three groups of female diabetic patients measured in posture 1 (TT1)

Fabric Sample	N1 (n = 15)							N2 (n = 15)							N3 (n = 15)						
	f, %	1st Sensor		2nd Sensor		3rd Sensor		f, %	1st Sensor		2nd Sensor		3rd Sensor		f, %	1st Sensor		2nd Sensor		3rd Sensor	
		Mean, mmHg	SD, mmHg	Mean, mmHg	SD, mmHg	Mean, mmHg	SD, mmHg		Mean, mmHg	SD, mmHg	Mean, mmHg	SD, mmHg	Mean, mmHg	SD, mmHg		Mean, mmHg	SD, mmHg	Mean, mmHg	SD, mmHg	Mean, mmHg	SD, mmHg
M1	1.97	28.63	1.52	11.45	1.26	19.86	1.82	6.38	48.46	1.88	28.76	1.65	37.68	1.65	11.67	99.53	2.54	74.17	1.48	87.63	1.84
M2	3.07	16.48	1.70	4.78	1.47	10.64	1.34	8.92	37.33	1.97	16.17	1.67	26.06	1.89	15.59	81.44	2.13	58.12	2.12	72.43	2.45
M3	2.67	19.56	1.25	8.07	1.19	12.15	1.51	7.98	43.41	1.87	20.49	1.62	31.74	1.78	14.89	87.63	2.46	65.76	2.08	78.39	1.65

Table 4: Pressure of shoe upper materials M1, M2, and M3 on the instep of the three groups of female diabetic patients measured in posture 2 (TT2)

Fabric Sample	N1 (n = 15)							N2 (n = 15)							N3 (n = 15)						
	f, %	1st Sensor		2nd Sensor		3rd Sensor		f, %	1st Sensor		2nd Sensor		3rd Sensor		f, %	1st Sensor		2nd Sensor		3rd Sensor	
		Mean, mmHg	SD, mmHg	Mean, mmHg	SD, mmHg	Mean, mmHg	SD, mmHg		Mean, mmHg	SD, mmHg	Mean, mmHg	SD, mmHg	Mean, mmHg	SD, mmHg		Mean, mmHg	SD, mmHg	Mean, mmHg	SD, mmHg	Mean, mmHg	SD, mmHg
M1	3.39	41.21	1.22	28.42	2.33	32.15	1.43	7.88	69.96	1.86	49.32	1.89	57.54	2.24	13.78	120.65	2.50	91.58	1.64	103.76	1.74
M2	5.06	30.04	1.17	14.75	1.17	19.32	1.68	10.74	57.78	1.48	35.89	2.53	44.67	1.96	17.97	98.66	2.03	69.36	2.12	84.85	2.45
M3	4.23	31.94	1.18	18.14	2.13	23.67	1.45	9.68	60.19	1.77	42.65	2.13	51.94	1.64	17.17	108.48	2.36	81.35	2.34	97.96	1.75

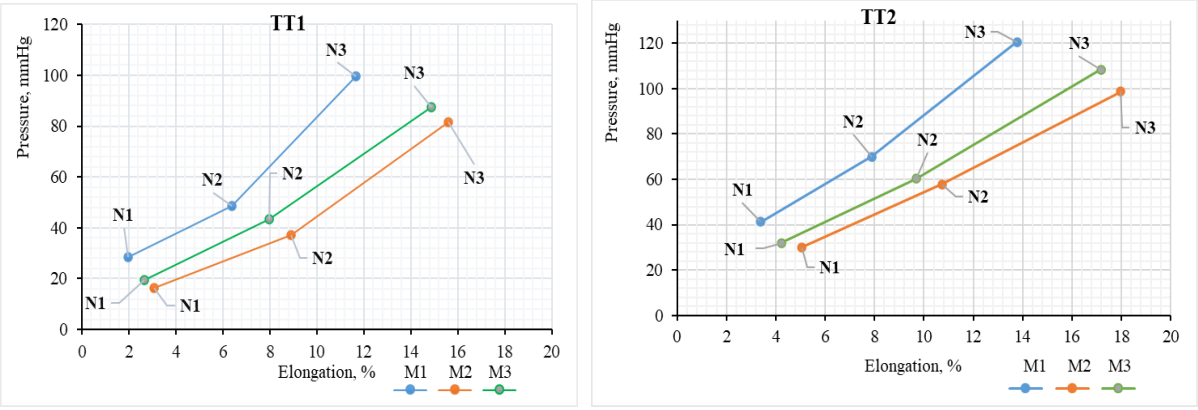

a b

Figure 8. Pressure values on the instep of three groups of female diabetic patients measured at the first sensor position for the three shoe upper materials: (a) Posture 1, (b) Posture 2

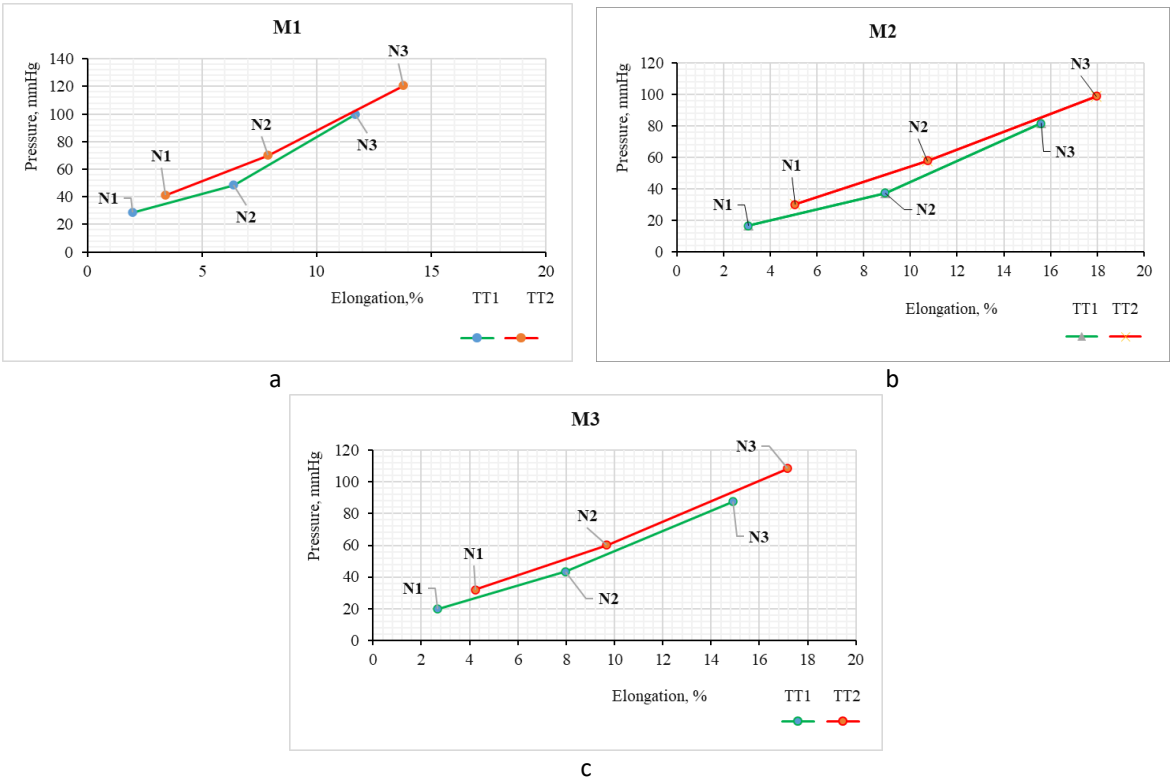

a b c

Figure 9. Pressure values on the instep of three groups of female diabetic patients measured in posture 1 and posture 2 at the first sensor position for the three shoe upper materials: (a) M1, (b) M2, (c) M3

The fabric characteristics affected its pressure value [41–44], and the elastic elongation of the fabric affected the pressure distribution and pressure value [22, 23]. Tables 3 and 4 show that as the elongation of the material increases, the pressure of the shoe upper on the instep increases to the same extent. The pressure value and its increase with elongation differ among the studied materials (Tables 3 and 4 and Figures 8 and 9). In the N1 group of diabetic female participants tested in posture 1, the pressure value of the M1 material was 28.63 ± 1.52 mmHg (with 1.97% elongation), that of the M2 material was 16.48 ± 1.7 mmHg (with 3.07% elongation), and that of the M3 material was 19.56 ± 1.25 mmHg (with 2.67% elongation). Thus, for the same foot size, the material with the highest elongation exhibited the smallest pressure value and vice versa. This result shows that using knitted fabrics as shoe uppers for female diabetic patients can reduce the pressure of the shoe uppers on the feet, avoiding swelling and ulcers. The ANOVA

results comparing the difference in the pressure values between the three groups of female diabetic patients on the same material showed $p < 0.05$, proving that the pressure value on the instep changes with the elongation of the material. The M2 material exhibited the smallest pressure value among the three groups (the highest pressure in posture 2 in the N3 group reached 98.66 ± 2.03 mmHg). The M1 material showed the highest pressured value at all relaxation levels (the maximum pressure at posture 2 in the N3 group was 120.65 ± 2.50 mmHg). Although the M1 and M2 materials have the same composition but weave style, their density of the wales and course was different, affecting the pressure value. The M1 material has a higher density of wales and course of top layer than M2 material, thus a higher pressure value on the instep. The uniformity of type of fabric, the density of wale and course of the top layer and bottom layer of each material sample also affect the pressure on the patient's feet. The top layer and bottom layer of M2 material have the same single jersey and the density of wale and course which give the smallest pressure value.

The human foot is constructed to resist forces, to maintain balance and to co-ordinate movements in static and dynamic conditions. The insertion of muscle tendons optimizes the required moments typical of the human gait [45]. The prolongation of the gastrocnemius muscle into the Achilles tendon allows the generation of the moment required at the toe-off [45, 46]. The foot acts on the ground, and the ground reacts on the foot. Basically, at the toe-off, an opposite force, i.e., the ground reaction force, is transmitted through the metatarsal joint. The magnitude of the ground reaction force is directly proportional to the body weight, velocity, and force generated by the calf muscles, and thus, the plantar pressure transmitted through the forefoot as well [47]. When using shoes, the foot moved and changed size due to the long-term body load, variations in the load on the foot, bending of the foot (or to edema or swelling in patients with foot comlications), and elongation of the shoe upper material. Due to changes in the load on the foot and flexion of the foot, compared with posture 1, in posture 2 (the position where the foot size is larger), the shoe upper material was elongated (Table 2) and pressure of the shoe upper on the joint instep area increased (Table 4). This result shows that the elongation of the shoe upper material due to the foot posture increases the pressure on the instep joint. Research found that shoes constructed from soft suede were more comfortable than those fabricated from a stiffer leather upper [48], shoes with a round toe-box and those with a stretchable fabric upper generated lower toe pressures and were perceived to be the most comfortable [49]. Therefore, selecting materials for shoe uppers is essential to ensure pressure comfort and prevent foot damage, especially for patients with foot complications such as diabetics.

In previous research [36], the author recommended that the maximum pressure value allowed on the toe joint of the instep of a woman's foot should be 69.2 mmHg to ensure retention. The shape of the shoe does not affect the normal physiological functioning of a diabetic female's feet. The results summarized in Tables 2–4 show that Groups N1 and N2 differ in the sizes of the toe joint by 8 mm, but they can wear the same shoe size of 37; three types of knitted fabrics were studied for use in shoe uppers, and they all met the pressure criteria. The size of the toe joint size was 16 mm larger in Group N3 compared to Group N1. Therefore, the pressure for all three knitted fabric samples was also generally greater than the recommended pressure limit. These observations indicate that knitted fabrics with a stretchability of ≤ 10.74% are suitable for making shoe uppers for female diabetic patients, who should choose shoes that fit the foot to avoid compression.

Determination of the Pressure on the Soles of the Feet when Wearing Shoes

The pressure on the soles of the feet of the three groups of participants was determined at eight locations (Figure 5b). The results are summarized in Table 5.

Table 5: Pressure on the soles of the feet of the three groups of participants

Participant Group	Fabric Sample					
	M1		M2		M3	
	TT1	TT2	TT1	TT2	TT1	TT2
Pressure value (kPa) at the tip of the big toe (B1, Figure 5b)						
N1 (n = 15)	**9.0 ± 3.66**	**130.80 ± 4.39**	**8.84 ± 2.96**	**129.2 ± 4.23**	**8.98 ± 3.01**	**130.12 ± 4.83**
N2 (n = 15)	8.34 ± 4.24	129.34 ± 4.61	7.95 ± 5.10	134.34 ± 5.14	8.17 ± 4.54	129.37 ± 5.63
N3 (n = 15)	10.1 ± 2.13	136.35 ± 5.91	9.68 ± 3.12	137.13 ± 3.32	9.43 ± 4.35	134.23 ± 3.35
Pressure value (kPa) at the first position of metatarsal head (B2, Figure 5b)						
N1 (n = 15)	18.52 ± 4.04	154.30 ± 6.54	18.01 ± 3.98	153.8 ± 5.63	18.43 ± 3.65	152.1 ± 5.36
N2 (n = 15)	23.94 ± 4.24	160.58 ± 6.87	22.79 ± 5.04	154.85 ± 5.78	23.02 ± 5.13	156.23 ± 5.87
N3 (n = 15)	26.83 ± 5.36	165.47 ± 7.48	27.14 ± 5.83	170.23 ± 4.37	24.85 ± 5.32	174.65 ± 5.94
Pressure value (kPa) at the position of the third metatarsal head (B3, Figure 5b)						
N1 (n = 15)	21.43 ± 3.99	171.18 ± 5.85	21.16 ± 3.92	170.45 ± 5.34	21.6 ± 3.34	170.0 ± 5.43
N2 (n = 15)	24.60 ± 4.19	175.23 ± 6.14	23.34 ± 4.65	176.90 ± 5.76	24.43 ± 4.58	173.1 ± 5.86
N3 (n = 15)	26.96 ± 4.89	181.3 ± 6.56	25.6 ± 4.98	182.1 ± 6.58	28.1 ± 5.41	178.62 ± 6.3
Pressure value (kPa) at the fifth metatarsal head (B4, Figure 5b)						
N1 (n = 15)	16.18 ± 3.14	139.62 ± 6.84	15.23 ± 3.41	137.56 ± 6.30	15.89 ± 3.64	138.68 ± 6.35
N2 (n = 15)	21.44 ± 3.30	145.61 ± 7.19	21.12 ± 3.83	144.43 ± 7.94	21.42 ± 3.91	140.32 ± 7.48
N3 (n = 15)	20.6 ± 4.45	149.24 ± 7.98	12.7 ± 4.74	151.1 ± 7.83	19.92 ± 5.49	145.16 ± 7.43
Pressure value (kPa) at the middle of the foot arch (B5, Figure 5b)						
N1 (n = 15)	5.33 ± 2.97	-	3.79 ± 3.67	-	4.28 ± 3.78	-
N2 (n = 15)	6.60 ± 3.12	-	5.11 ± 2.23	-	5.56 ± 2.89	-
N3 (n = 15)	10.96 ± 3.71	-	9.68 ± 4.52	-	12.45 ± 5.82	-
Pressure value (kPa) at the middle of the outer foot (B6, Figure 5b)						
N1 (n = 15)	13.07 ± 2.11	-	12.74 ± 3.03	-	12.94 ± 3.10	-
N2 (n = 15)	11.97 ± 2.21	-	11.85 ± 2.65	-	10.96 ± 2.36	-
N3 (n = 15)	19.3 ± 4.13	-	21.41 ± 5.46	-	19.08 ± 4.5	-
Pressure value (kPa) at the inward heel position (B7, Figure 5b)						
N1 (n = 15)	25.63 ± 9.0	-	25.21 ± 8.61	-	23.61 ± 8.17	-
N2 (n = 15)	24.77 ± 9.45	-	23.64 ± 9.76	-	24.12 ± 8.94	-
N3 (n = 15)	35.84 ± 10.8	-	31.9 ± 10.13	-	32.98 ± 10.7	-
Pressure value (kPa) at the external heel position (B8, Figure 5b)						
N1 (n = 15)	30.63 ± 9.12	-	30.01 ± 8.84	-	29.58 ± 8.53	-
N2 (n = 15)	32.92 ± 9.58	-	31.24 ± 9.36	-	29.92 ± 9.56	-
N3 (n = 15)	34.89 ± 11.4	-	37.38 ±10.92	-	37.91 ± 11.32	-

The pressure values on the soles of the feet at eight measurement locations exhibit significant differences. When standing on two feet, the pressure on the foot's heel is the highest. The lowest pressure is exerted on the medial gills, corresponding to the medial longitudinal arch of the foot. The pressure distribution shows that despite wearing 5-mm-thick elastic shoe insoles, the ability to disperse the pressure on the soles of the feet is not good because the insoles are flat, especially in the longitudinal arch area of the foot, where the pressure is only approximately 20% of the pressure on the heel. This result demonstrates the need for designing and manufacturing shoe insoles shaped to the patient's soles.

At sensor B2 (Figure 5b) for the N1 and N2 groups of participants in posture 1, the pressure value is 18.52 ± 4.04 and 23.94 ± 4.24 kPa with the M1 material, 18.35 ± 3.98 and 22.79 ± 5.04 kPa with the M2 material, and 18.43 ± 3.65 and 23.02 ± 5.13 kPa with the M3 material, respectively. In the N2 group, shoe uppers are elongated more strongly because of its larger toe ring than N1 group, causing an increase in the pressure on the instep that increases the pressure on the upper part of the foot. In particular, the pressure value measured in posture 2 increases substantially compared with that in posture 1 due to the weight placed on the toe joint when the foot is bent. These results show that using elastic materials such as

knitted fabrics to fabricate shoe uppers create a comfortable pressure feeling for the shoe uppers and reduce the pressure on the soles of the feet.

In the N3 group, the pressure on the soles of the feet is generally greater than those in the N1 and N2 groups because of the greater body mass of the participants in the N3 group (average 54 kg vs. 48 kg in the N1 and N2 groups). The pressure on the middle part (arches) of the feet of the participants in the N3 group is much greater than those of the other two groups, which is related to the degree of arch lowering in female diabetic patients.

For the three groups of the participants in posture 2, at sensor measurement positions B5, B6, B7, and B8, there is no contact; therefore, there is no pressure in the area between the sole and heel of the shoe. Furthermore, shoe insoles with a flat surface that does not shape the sole of the foot were used in this study; hence, the ability of the shoe insoles to disperse pressure on the sole of the foot is not good, especially in the longitudinal arch area of the foot.

The following ANOVA results were obtained when comparing pressure values at different locations on the soles of the feet: N1 and N2 groups, $p = 0.01$; N1 and N3 groups, $p = 0.0001$; and N2 and N3 groups, $p = 0.001$. Thus, the pressure values at the soles of the feet of the three groups are different.

The peak pressure on foot areas in the measured postures reaches a maximum value of 182 kPa, which does not exceed the recommended threshold of 200 kPa required to avoid foot ulcers [50–53]. Thus, the fabricated shoes meet foot pressure requirements for use by female diabetic patients.

CONCLUSIONS

The purpose of this study was to evaluate the impact of three different knitted fabric samples used to fabricate shoe uppers on various locations at the instep of female diabetic patients. The shoes had the same design structure; however, their uppers exhibited different characteristics. The design of the size 37 shoe model complied with the specifications proposed based on the research team's anthropometric data on female diabetic patients, and the shoe was manufactured at the Leather and Footwear Research Institute. The foot pressure values were measured for 45 female diabetic patients; furthermore, based on the size of the toe joint ring, they were divided into three different groups with a difference of 8 mm in the toe ring size between groups. The pressure was measured by placing the foot on two postures: posture 1, which is the upright position with the body weight evenly distributed on both legs, and posture 2, in which the feet are bent.

The results of this study provide a different perspective on comfort, convenience, and pressure values depending on the phase of the gait cycle and choice of materials for the shoe uppers. The pressure of knitted fabrics on the instep changed according to material elongation. Due to a change in the load on the foot and the bending of the foot, the shoe upper material was more elongated in the bending position of the foot compared with the upright position, which increased the pressure of the shoe upper on the instep joint area. With the change in the pressure on the instep, the pressure under the sole of the foot at the joints of the toes increased. The pressure under the sole at the joints of the toes increases with a change in the pressure on the instep. The sample M2 presented the least pressure among all three experimental groups, where the highest pressure of 98.66 ± 2.03 mmHg was observed at TT2 in Group 3. Sample M1 faced the strongest pressure at all elongated levels, where the maximum pressure was 120.65 ± 2.50 mmHg at TT2 in Group 3. Among the shoe models tested here, the maximum pressure measured on the different areas of the foot reached 182 kPa, which is within the recommended threshold of 200 kPa to prevent foot ulcers. All samples in Groups N1 and group N2 met the pressure criteria with three types of knitted fabrics assessed in this study in shoe uppers. Particularly, knitted fabrics with elongation of ≤ 10.74% are suitable for making shoe uppers

for female diabetics, who should choose shoes that fit the foot to avoid compression. This study provides important insights into the selection of materials to fabricate shoe uppers that ensure a comfortable pressure at all times to prevent foot damage, especially in patients with foot complications, such as diabetic individuals.

REFERENCES

1. Boulton, A.J., What You Can't Feel Can Hurt You, *J Am Podiatr Med Assoc*, **2010**, 100, 349–52, https://doi.org/10.7547/1000349.
2. Van Netten, J.J., Van Baal, J.G., Bril, A., Wissink, M., Bus, S.A., An Exploratory Study on Differences in Cumulative Plantar Tissue Stress Between Healing and Non Healing Plantar Neuropathic Diabetic Foot Ulcers, *Clin Biomech (Bristol)*, **2018**, 53, 86–92, https://doi.org/10.1016/j.clinbiomech.2018.02.012.
3. Formosa, C., Gatt, A., Chockalingam, N., The Importance of Clinical Biomechanical Assessment of Foot Deformity and Joint Mobility in People Living with Type-2 Diabetes within a Primary Care Setting, *Prim Care Diabetes*, **2013**, 7, 45–50, https://doi.org/10.1016/j.pcd.2012.12.003.
4. Tagang, J.I., An Investigation into Footwear Materials Choices and Design for People Suffering with Diabetes, De Montfort University Leicester, UK, **2014**, https://dora.dmu.ac.uk/bitstream/handle/2086/10545/E-Thesis-JT-Oct.
5. Oyibo, S.O., Jude, E.B., Voyatzoglou, D., Boulton, A.J.M., Clinical Characteristics of Patients with Diabetic Foot Problems: Changing Patterns of Foot Ulcer Presentation, *Pract Diab Int*, **2002**, 19, 1, 10–12, https://doi.org/10.1002/pdi.313.
6. Uccioli, L., Faglia, E., Monticone, G., Favales, F., Durola, L., Aldeghi, A., Quarantiello, A., Calia, P., Menzinger, G., Manufactured Shoes in the Prevention of Diabetic Foot Ulcers, *Diabetes Care*, **1995**, 18, 10, 1376–1378, https://doi.org/10.2337/diacare.18.10.1376.
7. Maciejewski, M.L., Reiber, G., Boyko, E.J., Effectiveness of Diabetic Therapeutic Footwear in Preventing Reulceration, *Diabetes Care*, **2004**, 27, 12, 3025–3026, https://doi.org/10.2337/diacare.27.12.3025.
8. Bergin, S.M., Nube, V.L., Alford, J.B., Allard, B.P., Gurr, J.M., Holland, E.L., Horsley, M.W., Kamp, M.C., Lazzarini, P.A., Sinha, A.K., Warnock, J.T., Wraight, P.R., Australian Diabetes Foot Network: Practical Guideline on the Provision of Footwear for People with Diabetes, *J Foot Ankle Res*, **2013**, 6, 1, https://doi.org/10.1186/1757-1146-6-6.
9. Caselli, M.A., Prescription Shoes for the Foot Pathology: Using Footwear Properly Adds to Your Treatment Armamentarium, *Podiatry Management*, **2011**, 165–174.
10. National Diabetes Education Program (NDEP), Feet Can Last a Lifetime. A Health Care Provider's Guide to Preventing Diabetes Foot, **2000**, available from: https://www.healthyplace.com/sites/default/files/images/stories/diabetes/hp-feet-hc-guide.pdf.
11. Uccioli, L., The Role of Footwear in the Prevention of Diabetic Foot Problem, in: A. Veves, J.M. Giurini, F.W. Logerfo (eds.), *The Diabetic Foot.* Contemporary Diabetes, 2nd edition, Humana Press, **2006**, 523–541, https://doi.org/10.1007/978-1-59745-075-1_25.
12. Lord, M., Hosein, R., Pressure Redistribution by Molded Inserts in Diabetic Footwear, *J Rehabil Res Dev*, **1994**, 31, 3, 214-21.
13. Bus, A.S., Foot Structure and Footwear Prescription in Diabetes Mellitus, in: Diabetes/Metabolism Research and Reviews, The Diabetic Foot: Proceedings of the Fifth International Symposium on the Diabetic Foot, 9–12 May **2007**, Noordwijkerhout, The Netherlands, 24, S1, https://doi.org/10.1002/dmrr.840
14. Viswanathan, V., Madhavan, S., Gnanasundaram, S., Gopalakrishna, G., Das, B.N., Rajasekar, S., Ramachandran, A., Effectiveness of Different Types of Footwear Insoles for the Diabetic Neuropathic Foot: A Follow-up Study, *Diabetes Care*, **2004**, 27, 2, 474–477, https://doi.org/10.2337/diacare.27.2.474.
15. Rajan, T.P., Souza, L.D., Ramakrishnan, G., Zakriya, G.M., Comfort Properties of Functional Warp-Knitted Polyester Spacer Fabrics for Shoe Insole Applications, *J Ind Text*, **2014**, https://doi.org/10.1177/1528083714557056.
16. Cavanagh, P.R., Ulbrecht, J.S., What the Practising Clinician Should Know about Foot Biomechanics, in: A.J.M. Boulton, P.R. Cavanagh, G. Rayman (eds), *The Foot in Diabetes*, 4th edition, John Wiley and Sons Ltd., Chichester, UK, **2006**.
17. Foto, J.G., Compact and Portable Digitally Controlled Device for Testing Footwear Materials: Technical Note, *J Rehabil Res Dev*, **2008**, 45, 6, 893–900, https://doi.org/10.1682/JRRD.2007.07.0111.
18. Rahman, M.M., An Investigation into Orthpaedic Footwear Technology in Relation to the Impact Diabetic Foot Problem, Unpublished thesis (M. Sc), **2003**, De Montfort University, Leicester.

19. Sharphouse, J.H., *Leather Technician's Handbook*, Northampton, Leather Producers Association, **1983**, 209–220.
20. Blaga, M., Marmaralı, A., Mihai, A., Functional Knitted Fabrics for Footwear Linings, *Tekst. Kon-Feksiyon*, **2011**, 21, 30–35.
21. Serweta, W., Olejniczak, Z., Matusiak, M., Improve of Footwear Comfort Sensation with Material Packages and Knitted Fabrics, *Fibers Text East Eur*, **2019**, 27, 85–90, https://doi.org/10.5604/01.3001.0013.0747.
22. Mikolajczyk, Z., Nowak, I., Mikołajczyk-Solińska, M., Kuchits, I., 3D Knitted Fabric as an Element of Footwear for People with Diabetic Foot Syndrome, *Text Res J*, **2024**, 94, 11-12, https://doi.org/10.1177/00405175231218998.
23. Seul, A., Mihai, A., Costea, M., Bodoga, A., Curteza, A., The Influence of Materials on Footwear Behaviour: A Finite Element Simulation Study, *Materials*, **2023**, 16, 22, 7203, https://doi.org/10.3390/ma16227203.
24. Branthwaite, H., Chockalingam, N., Greenhalgh, A., The Effect of Shoe Toe Box Shape and Volume on Forefoot Interdigital and Plantar Pressures in Healthy Females, *J Foot Ankle Res*, **2013**, 6, 28, https://doi.org/10.1186/1757-1146-6-28.
25. Mei, Q., Graham, M., Gu, Y., Biomechanical Analysis of the Plantar and Upper Pressure with Different Sports Shoes, *Int J Biomed Eng Technol*, **2014**, 14, 3, https://doi.org/10.1504/IJBET.2014.059668.
26. Jeon, Y.H., Jeong, W.Y., Park, J.W., An, S.K., The Mechanical Properties and Abrasion Behavior of Warp Knitted Fabrics for Footwear, *Fibers Polym*, **2003**, 4, 4, 151–155, https://doi.org/10.1007/BF02908271.
27. Heide, M., Möhring, U., Hänsel, R., Stoll, M., Wollina, U., Heinig, B., Antimicrobial-Finished Textile Three-Dimensional Structures, in: U.-C. Hipler, P. Elsner (eds.), *Biofunctional Textiles and the Skin*, **2006**, 33, 179–199, https://doi.org/10.1159/000093945.
28. Ertekin, G., Oğlakcioğlu, N., Marmarali, A., Kadoğlu, H., Blaga, M., Ciobanu, R., Mihai, A., Costea, M., Analysis of Knitted Footwear Linings for Diabetic Patients, *Tekstil ve Konfeksiyon*, **2016**, 24, 6, 358-367.
29. Serweta, W., Matusiak, M., Olejniczak, Z., Jagiełło, J., Wójcik, J., Proposal for the Selection of Materials for Footwear to Improve Thermal Insulation Properties Based on Laboratory Research, *Fibers Text East Eur*, **2018**, 26, 5, 131, 75–80, https://doi.org/10.5604/01.3001.0012.2535.
30. Aboalasaad, A.R.R., Sirková, B.K., Eldeeb, M., Influence of Woven Bandage Composition on its Elasticity and Durability, *J Text Inst*, **2022**, 113, 11, 2299–2309, https://doi.org/10.1080/00405000.2021.1978191.
31. Aboalasaad, A.R.R., Sirková, B.K., Analysis and Prediction of Woven Compression Bandages Properties, *J Text Inst*, **2019**, 110, 7, 1085-1091, https://doi.org/10.1080/00405000.2018.1540284.
32. Aboalasaad, A.R., Khan, M.Z., Sirková, B.K., Wiener, J., Šlamborová, I., Khalil, A.S., Hassanin, A.H., Antibacterial Easy Adjustable Woven Compression Bandage for Venous Leg Ulcers, *J Ind Text*, **2022**, 51, 1_suppl, 31S-953S, https://doi.org/10.1177/15280837221095204.
33. Khalil, A., Těšinová, P., Aboalasaad, A.R.R., Effect of Lycra Weight Percent and Loop Length on Thermo-Physiological Properties of Elastic Single Jersey Knitted Fabric, *Autex Res J*, **2021**, 22, 4, 419-426, https://doi.org/10.2478/aut-2021-0030.
34. Mansoor, T., Hes, L., Khalil, A., Militky, J., Tunak, M., Bajzik, V., Kyosev, Y., Conductive Heat Transfer Prediction of Plain Socks in Wet State, *Autex Res J*, **2022**, 22, 4, 391-403, https://doi.org/10.2478/aut-2021-0032.
35. Motawi, W., Motawi, A., Shoe Material Design Guide: The Shoe Designers Complete Guide to Selecting and Specifying Footwear Materials, publisher: Wade Motawi, ISBN13: 9780998707044, 17–35, **2018**.
36. Cao, T.K.C., Research on the Use of Textile Materials in the Design and Manufacture of Footwear for Female Diabetic Patients in Vietnam (in Vietnamese), PhD dissertation, Hanoi University of Science and Technology, **2021**.
37. Mai, T.T., Chronic Complications of Diabetes, in *General Endocrinology* (in Vietnamese), Hanoi: Medical Publishing House, **2003**.
38. Cao, T.K.C., Bui, V.H., Research on Developing a Foot Size System for Female Diabetic Patients in Hung Yen Province (in Vietnamese), *Journal of Science and Technology of Technical Universities*, **2016**, 114, 88–94.
39. EN ISO 20344:**2004** – Personal Protective Equipment – Test Methods for Footwear.
40. Maqsood, M., Hussain, T., Malik, M.H., Nawab, Y., Modeling the Effect of Weave Structure and Fabric Thread Density on the Barrier Effectiveness of Woven Surgical Gowns, *J Text Inst*, **2015**, 107, 3, 307-315, https://doi.org/10.1080/00405000.2015.1029809.
41. Maqsood, M., Nawab, Y., Umar, J., Umair, M., Shaker, K., Comparison of Compression

Properties of Stretchable Knitted Fabrics and Bi-Stretch Woven Fabrics for Compression Garments, *J Text Inst*, **2016**, 108, 4, 522-527, https://doi.org/10.1080/00405000.2016.1172432.
42. Cieślak, M., Karaszewska, A., Gromadzińska, E., Jasińska, I., Kamińska, I., Comparison of Methods for Measurement of the Pressure Exerted by Knitted Fabrics, *Text Res J*, **2017**, 87, 17, 2117–2126, https://doi.org/10.1177/0040517516665255.
43. Gokarneshan, N., Analysis of the Compression Behavior of Warp Knit Spacer Fabrics for Evaluating Suitability in Cushioning Applications, *J Text Appar Technol Manag*, **2018**, 10, 4, 1-14.
44. Soltanzadeh, Z., Shaikhzadeh Najar, S., Haghpanahi, M., Mohajeri-Tehrani, M.R., Prediction of Compression Properties of Single Jersey Weft Knitted Fabric by Finite Element Analysis Based on the Hydrofoam Material Model, *Fibers Text East Eur*, **2016**, 24, 2(116), 82-88, https://doi.org/10.5604/12303666.1191431.
45. Mansfield, P.J., Neumann, D.A., *Essentials of Kinesiology for the Physical Therapist Assistant*, Elsevier Health Sciences, **2014**.
46. Manal, K., Cowder, J.D., Buchanan, T.S., Subject-Specific Measures of Achilles Tendon Moment Arm Using Ultrasound and Video-Based Motion Capture, *Physiol Rep*, **2013**, 1, e00139, https://doi.org/10.1002/phy2.139.
47. Bojsen-Møoller, F., Anatomy of the Forefoot, Normal and Pathologic, *Clin Orthop Relat Res*, **1979**, 10-8, https://doi.org/10.1097/00003086-197907000-00003.
48. Melvin, J.M.A., Price, C., Preece, S., Nester, C., Howard, D., An Investigation into the Effects of, and Interaction Between, Heel Height and Shoe Upper Stiffness on Plantar Pressure and Comfort, *Footwear Sci*, **2019**, 11, 1, 25–34, https://doi.org/10.1080/19424280.2018.1555862.
49. Saeedi, H., Azadinia, F., Jalali, M., Bagheripour, B., Ronasi, P., Ershadi, F.S., Shoes with Elastic Upper vs. Shoes with a Round Toe Box for Perceived Comfort and Interdigital Forefoot Pressure in Patients with Hallux Valgus Deformity, *Footwear Sci*, **2021**, 1–8, https://doi.org/10.1080/19424280.2021.1950216.
50. Arts, M.L.J., Waaijman, R., de Haart, M., Keukenkamp, R., Nollet, F., Bus, S.A., Offloading Effect of Therapeutic Footwear in Patients with Diabetic Neuropathy at High Risk for Plantar Foot Ulceration, *Diabet Med*, **2012**, 29, 1534–1541, https://doi.org/10.1111/j.1464-5491.2012.03770.x.
51. Giacomozzi, C., Uccioli, L., Learning from Experience: A Sample Effective Protocol to Test Footwear Prescriptions for the Diabetic Foot by Using the Pedar System, *J Biomed Sci Eng*, **2023**, 6, 05, 45-57, https://doi.org/10.4236/jbise.2013.65A008
52. Owings, T.M., Apelqvist, J., Stenström, A., Becker, M., Bus, S.A., Kalpen, A., Ulbrecht, J.S., Cavanagh, P.R., Complications of Plantar Pressures in Diabetic Patients With Foot Ulcers which Have Remained Healed, *Diabet Med*, **2009**, 26, 11, 1141-1146, https://doi.org/10.1111/j.1464-5491.2009.02835.x.
53. Patry, J., Belley, R., Côté, M., Chateau-Degat, M.L., Plantar Pressures, Plantar Forces, and Their Influence on the Pathogenesis of Diabetic Foot Ulcers: A Review, *J Am Podiatr Med Assoc*, **2013**, 03, 4, 322–326, https://doi.org/10.7547/1030322.

RESEARCH ON TECHNOLOGICAL FACTORS AFFECTING THE PEEL STRENGTH OF ZIPPERS

Nhat-Huy PHAM, Van-Huan BUI*, Thanh-Thao PHAN*

Department of Textile – Leather and Fashion, School of Materials Science and Engineering, Hanoi University of Science and Technology, No. 1, Dai Co Viet, Bach Mai ward, Hanoi, Vietnam, huan.buivan@hust.edu.vn, Thao.phanthanh@hust.edu.vn

Received: 29.05.2025 Accepted: 12.12.2025 https://doi.org/10.24264/lfj.25.4.4

RESEARCH ON TECHNOLOGICAL FACTORS AFFECTING THE PEEL STRENGTH OF ZIPPERS

ABSTRACT. Thermoplastic adhesive bonding technology is widely used to attach zippers in the production of waterproof clothing, footwear, and leather goods, particularly waterproof sportswear. The durability of zipper bonds during use is critical to the overall quality of waterproof products. Numerous factors influence the durability of zipper bonds with waterproof materials, including the properties of the zipper tape material, the type of waterproof material, the type of adhesive, surface preparation, and bonding process parameters. In this study, an orthogonal experimental design was employed to investigate the effects of technological parameters, including temperature, bonding time, and pressure on the peel strength of two zipper samples bonded to waterproof-coated fabrics using thermoplastic polyurethane adhesive films. The peel strength of the zipper–fabric bonds was measured both after bonding and after 20 washing cycles. Using Design Expert statistical software, we analyzed the experimental data and developed mathematical models describing the relationships between the three process parameters and the peel strength of each zipper sample before and after washing. Based on these models, the optimal temperature, time, and pressure conditions were determined to ensure high peel strength of zippers bonded to waterproof-coated fabrics. The results of this study provide a foundation for further research on zipper adhesion technologies with different materials to improve the quality of waterproof products.

KEY WORDS: zipper, zipper bonding technology, zipper peel strength

CERCETĂRI PRIVIND FACTORII TEHNOLOGICI CARE AFECTEAZĂ REZISTENȚA LA DESPRINDERE A FERMOARELOR

REZUMAT. Tehnologia de lipire cu adeziv termoplastic este utilizată pe scară largă pentru atașarea fermoarelor în producția de îmbrăcăminte, încălțăminte și articole din piele impermeabile, în special îmbrăcăminte sport impermeabilă. Durabilitatea lipirii fermoarelor în timpul utilizării este esențială pentru calitatea generală a produselor impermeabile. Numeroși factori influențează durabilitatea lipirii fermoarelor cu materiale impermeabile, inclusiv proprietățile materialului folosit la banda fermoarului, tipul de material impermeabil, tipul de adeziv, pregătirea suprafeței și parametrii procesului de lipire. În acest studiu, s-a utilizat un design experimental ortogonal pentru a investiga efectele parametrilor tehnologici, inclusiv temperatura, timpul de lipire și presiunea, asupra rezistenței la desprindere a două mostre de fermoare lipite pe țesături impermeabile folosind pelicule adezive poliuretanice termoplastice. S-a măsurat rezistența la desprindere a lipirii fermoar-țesătură atât după lipire, cât și după 20 de cicluri de spălare. Folosind software-ul statistic Design Expert, s-au analizat datele experimentale și s-au dezvoltat modele matematice care descriu relațiile dintre cei trei parametri ai procesului, precum și rezistența la desprindere a fiecărei mostre de fermoar înainte și după spălare. Pe baza acestor modele, s-au determinat condițiile optime de temperatură, timp și presiune pentru a asigura o rezistență ridicată la dezlipire a fermoarelor lipite pe țesături impermeabile. Rezultatele acestui studiu oferă o bază pentru cercetări ulterioare privind tehnologiile de aderență a fermoarelor la diferite materiale pentru a îmbunătăți calitatea produselor impermeabile.

CUVINTE CHEIE: fermoar, tehnologie de lipire a fermoarelor, rezistență la desprindere a fermoarelor

RECHERCHE SUR LES FACTEURS TECHNOLOGIQUES INFLUENÇANT LA RÉSISTANCE AU PELAGE DES FERMETURES À GLISSIÈRE

RÉSUMÉ. La technologie de collage thermoplastique est largement utilisée pour la fixation des fermetures à glissière dans la production de vêtements, de chaussures et d'articles en cuir imperméables, notamment les vêtements de sport imperméables. La durabilité du collage de la fermeture à glissière en cours d'utilisation est essentielle à la qualité globale des produits imperméables. De nombreux facteurs influencent cette durabilité, notamment les propriétés du ruban de la fermeture à glissière, le type de matériau imperméable, le type d'adhésif, la préparation de surface et les paramètres du processus de collage. Dans cette étude, un plan d'expériences orthogonal a été utilisé pour étudier les effets des paramètres technologiques, tels que la température, le temps de collage et la pression, sur la résistance au pelage de deux échantillons de fermeture à glissière collés à des tissus imperméables à l'aide de films adhésifs en polyuréthane thermoplastique. La résistance au pelage du collage fermeture à glissière-tissu a été mesurée immédiatement après le collage et après 20 cycles de lavage. À l'aide du logiciel statistique Design Expert, les données expérimentales ont été analysées et des modèles mathématiques ont été développés pour décrire les relations entre les trois paramètres du processus, ainsi que la résistance au pelage de chaque échantillon de fermeture à glissière avant et après lavage. À partir de ces modèles, les conditions optimales de température, de durée et de pression ont été déterminées afin de garantir une résistance au pelage élevée des fermetures à glissière collées sur des tissus imperméables. Les résultats de cette étude constituent une base pour des recherches ultérieures sur les technologies d'adhésion des fermetures à glissière à différents matériaux, dans le but d'améliorer la qualité des produits imperméables.

MOTS-CLÉS : fermeture à glissière, technologie de collage des fermetures à glissière, résistance au pelage des fermetures à glissière

* *Correspondence to: Van-Huan BUI & Thanh-Thao PHAN, Department of Textile – Leather and Fashion, School of Materials Science and Engineering, Hanoi University of Science and Technology, No. 1, Dai Co Viet, Bach Mai ward, Hanoi, Vietnam, huan.buivan@hust.edu.vn, Thao.phanthanh@hust.edu.vn*

INTRODUCTION

Zippers are essential accessories widely used in products such as clothing, footwear, handbags, backpacks, suitcases, and many other everyday applications. They allow products to be opened and closed quickly and conveniently, replacing traditional fastening methods such as buttons or laces, thereby enhancing user convenience [1]. In addition, for products such as protective clothing, waterproof footwear, tents, or technical garments, zippers ensure the necessary sealing performance to protect users from external factors such as water, dust, or chemicals. As a result, they contribute significantly to product protection, safety, and functionality [2, 3]. During product use, particularly during washing, zippers are subjected to substantial mechanical and environmental impacts [4]. The adhesion strength between the zipper and the material surface is a key factor influencing both product quality and durability. In waterproof products, zippers are typically bonded rather than sewn. Therefore, if the adhesive layer between the zipper and the material is insufficiently strong, peeling may occur, leading to reduced product functionality and diminished user experience [3].

In recent years, advances in materials science and the increasing use of coated and laminated fabrics in functional apparel have promoted the widespread adoption and development of zipper bonding technologies. However, several challenges remain, including bonding along deep curves, ensuring elasticity and flexibility at seam regions, and overcoming material incompatibility issues [5]. When evaluating the quality of zipper bonding in products, properties such as tensile strength, peel strength, appearance, elasticity, and air permeability are commonly assessed [3, 6]. To date, several studies have investigated the influence of technological parameters on the peel strength of bonded components [7–11]. Maryna Yatsenko *et al.* developed mathematical models describing the relationships between roller temperature, bonding time, and roller pressure on the adhesion strength of leather. In this study, the leather surfaces were treated with different chemicals, and a heat-sensitive adhesive was used to bond the leather layers. The authors identified the optimal bonding parameters for each type of surface treatment [7]. The study conducted by Gerda Mikalauskaite *et al.* examined the influence of peel speed on the peel strength of adhesive joints and on the seam strength of knitted and woven fabrics made from polyamide and polyester. Three types of single-layer thermoplastic polyurethane films were used to bond the fabric samples. The results indicated that peel speed had a significant effect on the peel strength of the adhesive joints, while it had no influence on seam strength [8]. Živilė Jakubčionienė *et al.* investigated the bond strength of four different types of woven, knitted, and laminated fabrics to determine the most suitable bonding method for each fabric type. The fabric layers were bonded using a thermoplastic polyurethane film at a temperature of 180 °C and a pressing time of 30 s [9]. The effect of temperature on the structure of polyester/elastane knitted materials and their adhesive peel strength was evaluated in the study by Virginija Daukantienė *et al.* The authors found that 150°C was the optimal bonding temperature for most of the textiles examined [10]. Gita Busilienė *et al.* investigated the spatial behavior of knitted fabrics composed of 93% polyester and 7% elastane. The fabrics were bonded using two TPU films with thicknesses of 75 µm and 150 µm. The results showed that the changes occurring before and after cyclic fatigue loading were mainly determined by the type of thermoplastic film, while the orientation of the knitted fabric pieces in the bonded seam had no significant effect [11]. In addition, several authors have examined the influence of technological parameters on the bond strength between interlining and fabric in garment production [12–14].

Overall, the above-mentioned studies focus on the technological factors affecting the bonding of textile materials. Fabrics and waterproof coated fabrics are commonly bonded using the thermoforming method with TPU films [8–11]. However, to date, no research has been conducted on the influence of technological parameters on the peel

strength of zippers bonded to waterproof coated fabrics.

In this study, we investigated the influence of technological parameters, including temperature, time, and pressure on the peel strength of two zipper samples bonded to waterproof coated fabrics using thermoplastic polyurethane adhesive film. An orthogonal experimental design was employed to establish the testing plan. The peel strength of the bonded zippers was measured both immediately after bonding and after 20 washing cycles. Experimental data were processed using Design Expert statistical software to develop mathematical models describing the relationship between the three technological parameters and the peel strength of each zipper sample in both testing conditions. Based on these models, the optimal bonding temperature, time, and pressure were determined to achieve the highest peel strength. The results provide a scientific basis for improving zipper bonding technology and enhancing the quality of waterproof products.

EXPERIMENTAL

Materials

In this study, the experimental materials consisted of waterproof coated fabric, TPU adhesive film, and two types of zippers. The specifications of the zippers, adhesive film, and fabric are provided in Tables 1, 2, and 3.

Table 1: Characteristics of types of zippers

No.	Characteristics	Value
1	Material composition	Polyester*
2	Weave type	Woven
3	Warp density	337 yarns/10 cm
4	Weft density	137 yarns/10 cm
5	Weight	213.5 g/m^2
6	Thickness	0.2 mm
7	Zipper teeth width	3 mm
8	Teeth density	9 teeth/1 cm
9	Origin	SBS Company, China
10	Code	M1

** The second type of zipper is impregnated with waterproof PU resin (Coded M2).*

Table 2: Characteristics of adhesive film

No.	Characteristics	Value
1	Material	Thermoplastic polyurethane (TPU)
2	Weight	31 g/m^2
3	Thickness	25 µm
4	Melting point	110°C–140°C
5	Origin	Youyi Company, China

Table 3: Characteristics of waterproof fabric

No.	Characteristics	Value
1	Material	100% polyester
2	Weave type	Woven plain
3	Warp density	310 yarns/10 cm
4	Weft density	310 yarns/10 cm
5	Waterproof coating	Polyurethane
6	Weight	138 g/m^2
7	Origin	Maxport Company, Vietnam

Methods and Equipment

To design the experiment, we applied an orthogonal experimental planning method with three input variables: temperature (coded as X_1), pressure (coded as X_2), and time (coded as X_3). The two output variables were the zipper peel strength after bonding (coded as Y_1 for sample M1 and Y_3 for sample M2), and the zipper peel strength after 20 washing cycles (coded as Y_2 for sample M1 and Y_4 for sample M2). Based on (i) the findings from the literature review on the physical and mechanical properties of the adhesive film used, and (ii) the reference thermoplastic bonding technologies currently applied in several garment manufacturing factories, we established the variation ranges of the technological parameters and coded them as shown in Table 4.

Table 4: Table of coded technological parameters

Factor Code	Variability levels				
	-1.68	-1	0	+1	+1.68
X_1-Temperature (°C)	108	115	125	135	142
X_2-Pressure (MPa)	0.18	0.25	0.35	0.45	0.52
X_3-Time (s)	13	18	25	32	37

According to this experimental design, the total number of experiments (N) is calculated using the formula:

$$N = 2^K + n_o + 2K, \quad (1)$$

where K is the number of input factors studied (K = 3, including X_1, X_2, and X_3), and n_o is the number of center-point experiments (n_o = 6). Thus, the total number of experiments performed was N = 20.

For each experiment, 10 specimens were prepared: 5 specimens were used to test the peel strength after bonding, and the remaining 5 were used to evaluate the peel strength after 20 washing cycles. The reported test results are the average values obtained from the five corresponding specimens.

The fabric and zipper samples were cut to a length of 20 cm, while the adhesive film was cut to 15 cm. The widths of the fabric and adhesive film specimens were greater than the width of the zipper to ensure complete coverage and full adhesion to the zipper surface (Figure 1). The TPU film was initially transferred onto the zipper and the coated fabric using a lightly pressed iron at 150°C for 5 seconds. The specimens were then bonded using a heat press according to the experimental design. After heat pressing, all specimens were cold-pressed for 10 seconds using a cooling plate at 10°C.

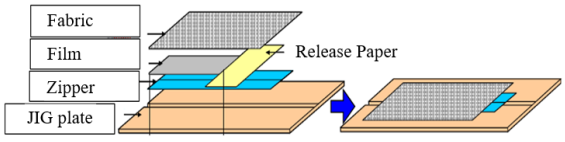

Figure 1. Test specimen preparation specifications

The peel strength of the zipper bonds was tested using a tensile testing machine in accordance with ISO 17708:2018. During testing, the free ends of the zipper and the coated fabric were clamped in the upper and lower grips of the machine. The specimens were peeled at a constant speed of 100 mm/min under room temperature conditions. The peel strength, Y (N/cm), was calculated using the formula:

$$Y = \frac{F}{A} \quad (2)$$

where F is the average peeling force (N), obtained from the recorded force–displacement curve, and A is the average width of the test specimen (cm).

The test specimens were washed under conditions simulating the real-life laundering of garments. Specifically, the specimens were washed in a household washing machine using 50 grams of common detergent for each wash.

Each washing cycle lasted 45 minutes, with a washing temperature of 40 °C and a spin speed of 800 rpm. After each cycle, the specimens were dried at 60°C for 20 minutes before proceeding to the next washing cycle.

Experimental data were processed using Design Expert software, which enabled the establishment of mathematical models and the analysis of the simultaneous effects of the studied factors on the peel strength after bonding and after washing. Based on these models, the optimal values of the three technological parameters (temperature, pressure, and time) were determined to ensure the highest peel strength after bonding and after washing for each zipper sample.

To verify the validity of these optimal values, zipper samples were bonded to the coated fabric using the optimized temperature, pressure, and time. The objective was to obtain the highest peel strength after washing (Y_2 and Y_4), as this parameter is critical for assessing product durability during actual use. The peel strength of the bonded samples was then measured and compared with the values predicted by the mathematical models. This comparison provided an evaluation of the reliability and suitability of the identified optimal technological parameters.

Subsequently, SEM analysis was conducted to observe the distribution of the adhesive film within the bonded interfaces of the zipper and the coated fabric. The SEM images helped clarify the influence of the technological factors on the peel strength. SEM imaging of the cross-sections of the specimens was performed using the JSM–IT200 microscope.

RESULTS AND DISCUSSIONS

The peel strength results of the two zipper samples after bonding and after 20 washing cycles are presented in Table 5 and illustrated in Figures 2 and 3.

Table 5: Experimental results of peel strength of two zipper samples after bonding and after washing

Factors			Zipper M1					Zipper M2				
			Sample code	Peel strength, N/cm		Difference between Y_1 and Y_2		Sample code	Peel strength, N/cm		Difference between Y_3 and Y_4	
X_1 (°C)	X_2 (MPa)	X_3 (s)		Y_1	Y_2	N/cm	%		Y_3	Y_4	N/cm	%
135	0.45	32	M1.1	14.02±1.56	11.02±0.53	3.00	21.40	M2.1	11.39±0.34	10.95±2.18	0.44	3.86
115	0.45	32	M1.2	10.51±2.78	9.94±0.67	0.58	5.52	M2.2	9.65±0.69	8.24±1.77	1.41	14.61
135	0.25	32	M1.3	11.76±1.46	9.57±2.12	2.19	18.62	M2.3	10.44±0.91	8.99±1.5	1.45	13.89
115	0.25	32	M1.4	10.38±1.92	8.83±0.89	1.55	14.93	M2.4	9.10±0.16	6.43±1.06	2.67	29.34
135	0.45	18	M1.5	13.02±0.39	10.83±0.60	2.18	16.74	M2.5	11.36±1.22	11.18±0.10	0.18	1.58
115	0.45	18	M1.6	10.74±0.97	11.14±0.89	-0.40	-3.72	M2.6	9.12±2.27	7.61±1.03	1.50	16.45
135	0.25	18	M1.7	14.60±1.64	14.14±1.01	0.46	3.15	M2.7	11.00±1.41	10.96±1.32	0.03	0.27
115	0.25	18	M1.8	8.03±1.06	7.19±1.75	0.84	10.46	M2.8	8.84 ±4.32	4.34±2.09	4.51	51.02
125	0.35	25	M1.9	12.90±0.74	12.25±1.04	0.67	5.19	M2.9	10.24±1.58	9.73±1.26	0.52	5.08
125	0.35	25	M1.10	12.52±1.9	9.98±1.13	2.54	20.29	M2.10	12.19±0.43	9.34±1.42	2.85	23.38
125	0.35	25	M1.11	11.12±1.21	10.41±1.31	0.72	6.47	M2.11	11.07±0.64	9.48±1.41	1.60	14.45
125	0.35	25	M1.12	11.73±2.93	11.73±1.76	0.00	-0.09	M2.12	9.56±1.1	6.91±1.41	2.66	27.82
125	0.35	25	M1.13	10.44±0.84	9.49±1.61	0.95	9.10	M2.13	8.56±0.46	6.93±0.90	1.64	19.16
125	0.35	25	M1.14	11.10±0.54	8.41±1.02	2.69	24.23	M2.14	15.08±1.5	14.73±0.52	0.36	2.39
142	0.35	25	M1.15	17.30±0.62	13.11±0.87	4.18	24.16	M2.15	11.43±0.26	11.43±1.81	0.00	0.00
108	0.35	25	M1.16	10.25±0.87	10.11±1.31	0.14	1.37	M2.16	10.99±1.3	9.00±0.65	1.99	18.11
125	0.52	25	M1.17	13.47±0.76	11.10±0.33	2.36	17.52	M2.17	11.81±1.71	12.33±1.62	-0.52	-4.40
125	0.18	25	M1.18	6.13±2.22	6.71±1.86	-0.58	-9.46	M2.18	7.32±1.59	5.64±0.62	1.68	22.95
125	0.35	37	M1.19	14.93±1.6	14.73±1.04	0.20	1.34	M2.19	11.36±0.7	9.16±0.94	2.20	19.37
125	0.35	13	M1.20	8.97±1.38	9.25±1.43	-0.27	-3.01	M2.20	6.91±1.42	6.09±1.26	0.82	11.87

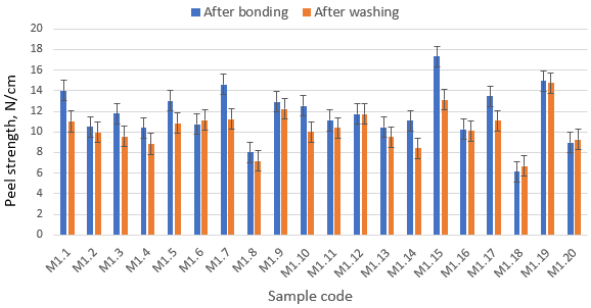

Figure 2. Peel strength graph after bonding and after washing of M1 zipper

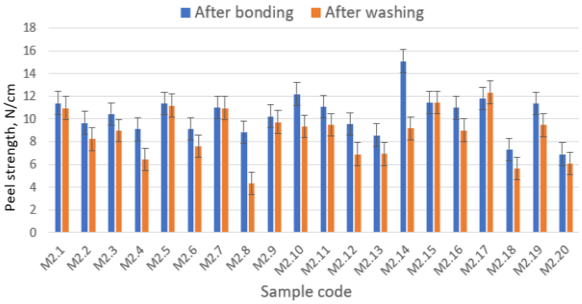

Figure 3. Peel strength graph after bonding and after washing of M2 zipper

According to the data in Table 5, there is a statistically significant difference in the peel strength after bonding and after washing between the two zipper samples (p < 0.05, *p(two-tailed)* = 0.001 < 0.05). In both cases, sample M1 exhibited higher peel strength than sample M2. The average peel strength after bonding for sample M1 was 11.70 N/cm, compared with 10.37 N/cm for sample M2. Similarly, the average peel strength after washing for sample M1 was 10.50 N/cm, higher than the 9.00 N/cm recorded for sample M2. These results indicate that the waterproofing treatment of zippers with PU resin solution reduces the peel strength when the same bonding technological parameters are applied. The standard deviations of the peel strength measurements for both samples M1 and M2 were relatively high, reflecting considerable variability in the test results. Notably, the standard deviation of sample M2 was greater than that of sample M1, suggesting larger fluctuations in the peel strength values of the PU-treated zipper sample.

The Influence of Washing on the Peel Strength of Zipper

Also, according to the data presented in Table 5 and Figures 2 and 3, washing had a significant effect on reducing the peel strength of both zipper samples bonded with coated fabric (p < 0.05, *p(two-tailed)* = 0.000 < 0.05). For sample M1, only three test conditions—M1.6, M1.18, and M1.20—showed an increase in peel strength after washing, and even then, the increase was small, less than 0.6 N/cm (equivalent to 9.5%) compared with the values before washing. For the remaining M1 samples, the peel strength after washing decreased by values ranging from 1.4 N/cm (M1.16) to 4.18 N/cm (M1.15). The maximum reduction reached 24.4%, with an average decrease of 10.26% (Figure 2). Compared with sample M1, the reduction in peel strength due to washing was more pronounced for sample M2. The average decrease in peel strength of sample M2 was 13.45%. Only one test condition, M2.17, showed a slight increase in peel strength after washing (0.52 N/cm, equivalent to 4.40%). All other M2 specimens experienced reductions in peel strength, with changes ranging from negligible values up to 4.5 N/cm, and the maximum reduction reaching 51.02% (Figure 3).

Thus, when using the same TPU adhesive film to bond the same coated fabric with different types of zippers, the effect of washing on adhesion strength varied considerably. The M2 zipper sample, which had been impregnated with a waterproof PU resin, exhibited a greater reduction in peel strength compared with the M1 zipper sample. Overall, the adhesion strength between the zipper and the fabric decreased after washing cycles. Therefore, evaluating and optimizing peel strength after washing is essential to ensure the durability and quality of waterproof products during actual use.

The Influence of Temperature, Pressure and Time on the Peel Strength of Zipper M1

The experimental data processed using Design Expert software yielded mathematical models describing the relationship between the three technological parameters and the peel

strength of the M1 zipper. These models were evaluated based on Fisher's criterion, where the calculated Fisher values (Fest) must be lower than the tabulated value (Ftab). The obtained results satisfied this condition, with Fest ranging from 1.734 to 3.462, which is less than Ftab = 4.0012. This confirms that the developed mathematical models are statistically significant and suitable for analyzing the influence of temperature, pressure, and time on zipper peel strength.

$Y_1 = 11.64 + 3.52X_1 + 3.67X_2 + 2.98X_3 - 0.78X_1X_2 - 1.44X_1X_3 + 0.45X_2X_3 + 2.01X_1^2 - 1.97X_2^2 + 0.18X_3^2 + 3.98X_1X_2X_3 - 8.44X_1^2X_2 - 8.44X_1^2X_3 - 1.75X_1X_2^2$ (1), $R^2 = 0.9628$.

$Y_2 = 10.39 + 1.50X_1 + 2.20X_2 + 2.74X_3 - 2.50X_1X_2 - 1.76X_1X_3 + 0.70X_2X_3 + 0.93X_1^2 - 1.77X_2^2 + 1.32X_3^2 + 4.71X_1X_2X_3 - 4.38X_1^2X_2 - 10.36X_1^2X_3 + 0.86X_1X_2^2$ (2), $R^2 = 0.8629$.

The equations indicate that all three factors (temperature, pressure, and time) affect the peel strength of the zipper both after bonding and after washing. An example of the relationship between the peel strength of zipper M1 after bonding and the technological parameters is illustrated by the 3D surface plots in Figures 4–6.

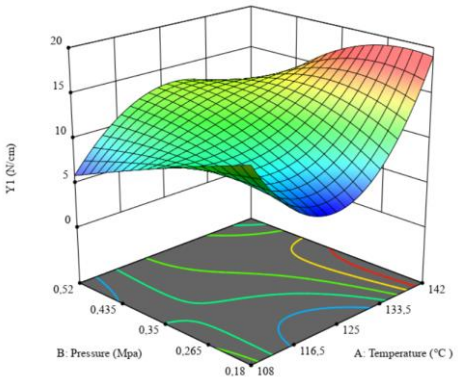

Figure 2. 3D plot illustrating the influence of temperature and pressure on the peel strength after bonding of the M1 zipper

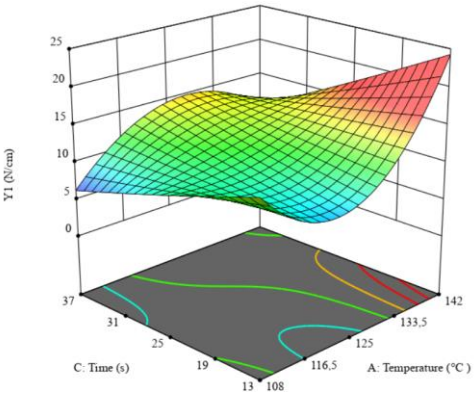

Figure 5. 3D plot illustrating the influence of temperature and time on the peel strength after bonding of the M1 zipper

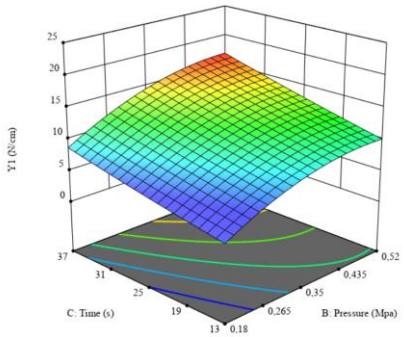

Figure 6. 3D plot illustrating the influence of pressure and time on the peel strength after bonding of the M1 zipper

Based on the obtained mathematical models, we determined the optimal technological parameters to ensure the peel strength of the M1 zipper bonded to the coated fabric. Specifically:

(i) Y_1 reaches 18.94 N/cm at a bonding temperature of 140 °C, a bonding pressure of 0.37 MPa, and a pressing time of 18 s; and

(ii) Y_2 reaches 17.65 N/cm at a bonding temperature of 140 °C, a bonding pressure of 0.35 MPa, and a pressing time of 16 s.

In actual production and product use, the peel strength of the zipper after washing is of greater concern because it directly determines the functional quality of the product. Therefore, priority should be given to the optimal solution that maximizes the peel strength after washing.

The Influence of Temperature, Pressure and Time on the Peel Strength of Zipper M2

Similar to the M1 zipper, the experimental data for the M2 zipper were

processed using Design Expert software, and mathematical models describing the relationship between the three technological parameters and the peel strength were established. The adequacy of the models was verified using Fisher's criterion, according to which the calculated values (Fest) must be lower than the tabulated value (Ftab). The obtained results satisfied this requirement, with Fest ranging from 0.765 to 3.334, all below Ftab = 4.0012.

$Y_3 = 11.11 + 0.22X_1 + 2.24X_2 + 2.23X_3 + 0.17X_1X_2 - 0.48X_1X_3 + 0.31X_2X_3 + 0.19X_1^2 - 1.45X_2^2 - 1.88X_3^2 + 0.19X_1X_2X_3 - 5.17X_1^2X_2 - 6.27X_1^2X_3 + 3.96X_1X_2^2$ (3), $R^2 = 0.5844$;

$Y_4 = 9.53 + 1.22X_1 + 3.34X_2 + 1.54X_3 - 1.05X_1X_2 - 1.79X_1X_3 + 0.10X_2X_3 + 0.49X_1^2 - 0.73X_2^2 - 2.09X_3^2 + 1.98X_1X_2X_3 - 5.21X_1^2X_2 - 4.11X_1^2X_3 + 5.98X_1X_2^2$ (4), $R^2 = 0.6638$.

The correlation coefficients of mathematical models 3 and 4 for the M2 zipper are lower than those of models 1 and 2 for the M1 zipper. This indicates a weaker relationship between the investigated technological parameters and the peel strength of the M2 zipper. This finding is consistent with the higher standard deviation observed in the peel strength results of the M2 samples compared with those of the M1 zipper (Table 5). An example of the relationship between the peel strength of the M2 zipper after bonding and the technological parameters is illustrated by the 3D plots shown in Figures 7–9.

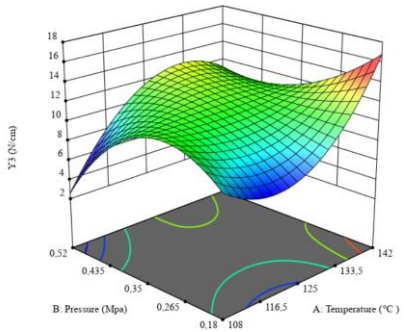

Figure 7. 3D plot illustrating the influence of temperature and pressure on the peel strength after bonding of the M2 zipper

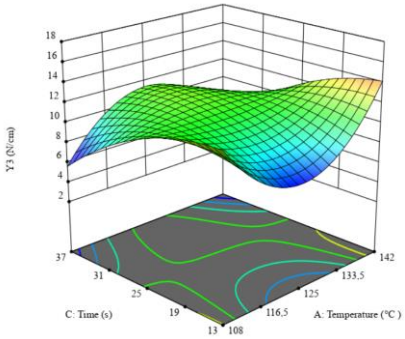

Figure 8. 3D plot illustrating the influence of temperature and time on the peel strength after bonding of the M2 zipper

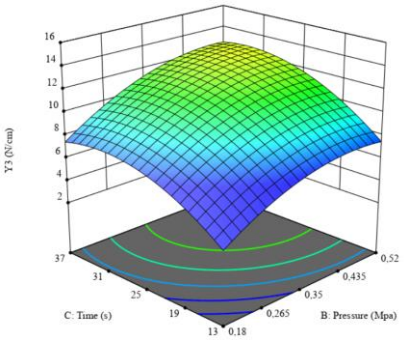

Figure 9. 3D plot illustrating the influence of pressure and time on the peel strength after bonding of the M2 zipper

Similar to sample M1, the optimal technological parameters for zipper M2 were identified to achieve the maximum peel strength after bonding and after washing. Specifically:

(i) Y_3 reached a maximum value of 18.66 N/cm at a temperature of 140 °C, a pressure of 0.18 MPa, and a bonding time of 16 s; and

(ii) Y_4 reached a maximum value of 18.32 N/cm at a temperature of 142 °C, a pressure of 0.21 MPa, and a bonding time of 20 s.

Verification and Explanation of Optimal Results

The M1 and M2 zippers were bonded to the coated fabric using TPU film under the optimal technological parameters determined to achieve the highest peel strength after washing. Specifically, the M1 zipper was bonded at a temperature of 140 °C, a pressure of 0.35 MPa, and a pressing time of 16 s; while the M2 zipper was bonded at a temperature of 142 °C, a pressure of 0.21 MPa, and a pressing time of 20 s. The peel strength test results of the obtained specimens are presented in Table 6.

Table 6: Test results of specimens made by optimal technological parameters

Zipper samples	Result (N/cm)							
	After bonding, experimental results	Calculated according to equations 1 and 3	Difference		After washing, experimental results	Calculated according to equations 1 and 3	Difference	
			N/cm	%			N/cm	%
M1	18.65±0.87	18.94	-0.29	1.55	18.38±0.86	17.65	0.73	3.98
M2	16.10±0.90	18.66	-2.56	15.88	15.92±1.02	18.32	-2.40	-15.08

According to the data in Table 6, the experimental peel strength of the M1 zipper shows good agreement with the values predicted by mathematical models (1) and (2). The difference between the experimental and calculated values does not exceed 4%, which is consistent with the high correlation coefficients of these models. The peel strength of the M2 zipper bonded to the fabric using the optimal technological parameters also gives satisfactory results; however, the difference between the experimental values and those predicted by mathematical models (3) and (4) reaches up to 16%. This corresponds to the lower correlation coefficients of models (3) and (4). Additionally, the standard deviation of the experimental results for both zipper samples is relatively small, especially for sample M1, indicating good stability and reliability of the measurements. These findings further confirm the positive effect of impregnating the zipper with PU resin solution on enhancing peel strength.

SEM cross-sectional images of the M1 zipper specimens produced under the optimal technological conditions, along with those of a specimen exhibiting poor peel strength (specimen M1.8 in Table 5), are presented in Figures 10–13.

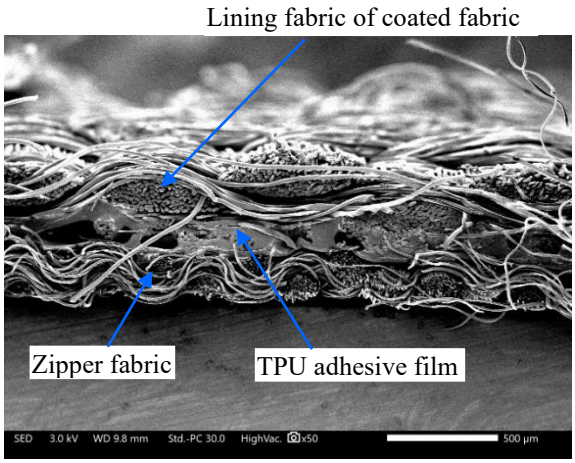

Figure 10. SEM image showing the overall cross-section of specimen M1.8 produced using suboptimal technological parameters

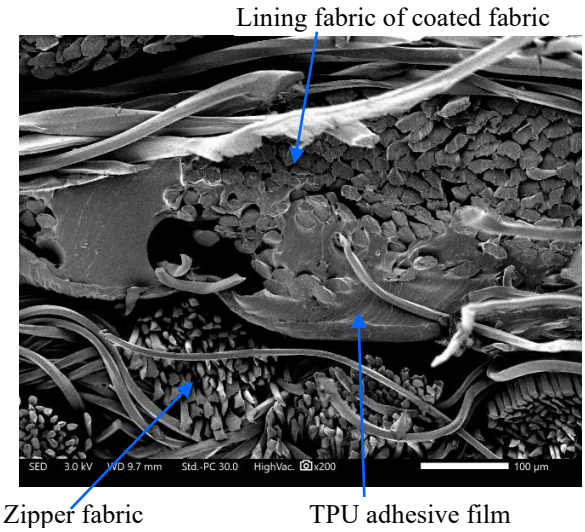

Figure 11. SEM image showing the distribution of adhesive film in specimen M1.8 produced using suboptimal technological parameters

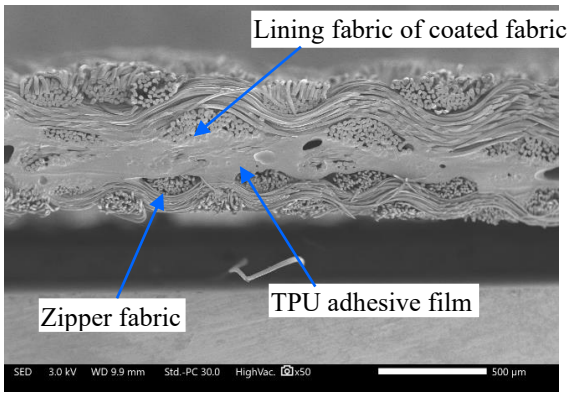

Figure 12. SEM image showing the overall cross-section of specimen M1 produced under optimized technological parameters

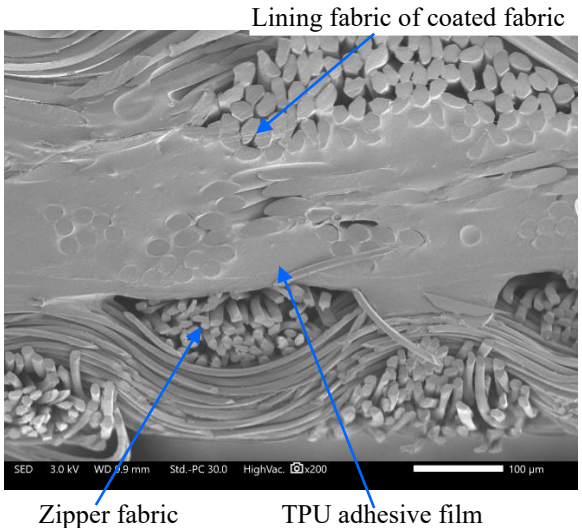

Figure 13. SEM image showing the distribution of adhesive film in specimen M1 produced under optimized technological parameters

The SEM images in Figures 10 and 11 show that in specimen M1.8 the bond structure is loose, with gaps present between the adhesive film and the fabric surface layers on both sides – the zipper and the waterproof fabric. The fabric fibers also appear to be separating, and gaps between the adhesive and fibers indicate poor adhesion. This poor bonding is primarily due to low temperatures and short pressing times, which prevent the hot-melt adhesive film from properly melting and penetrating the fabric fibers. Low pressure may also contribute to the loose bond, but temperature remains the dominant factor. These observations are consistent with the experimental results.

In contrast, the SEM images of specimen M1 produced under optimized technological parameters (Figures 12 and 13) show a well-formed bond. At higher temperatures, the hot-melt adhesive melts thoroughly, and the application of high pressure ensures deep penetration into the material, particularly into the fabric surface of the zipper strip. As a result, a tight bond is formed, with fabric fibers integrated into the adhesive and no visible gaps between the fibers and the adhesive film. This structural integrity explains the high peel strength observed experimentally between the zipper strip and the coated fabric.

CONCLUSIONS

The washing process has a significant impact on the peel strength of zippers bonded to waterproof coated fabrics using TPU adhesive film. Therefore, it must be carefully considered when establishing the technological parameters for zipper bonding. In this study, factors such as temperature, time, and pressure were shown to affect the adhesion strength of both zipper samples according to second-order mathematical models. The optimal bonding parameters determined here demonstrated high reliability, ensuring elevated peel strength of the zippers both immediately after bonding and after washing. The achieved peel strength values were approximately 1.4 times higher than the minimum requirement of 13.34 N/cm for sportswear applications. Results from practical testing and SEM analysis confirm that the developed mathematical models and optimized technological solutions can be applied in industrial production. These findings provide a solid foundation for further studies on the influence of technological parameters on the peel strength of zippers and materials in various types of waterproof products.

REFERENCES

1. Baharom, M.Z., Delbressine, F.L.M., Feijs, L.M.G., Toeters, M.J., The Design Evolution of the Zipper: A Patent Review, *ICIBE 2018 – 2018 4th International Conference on Industrial and Business Engineering*, **2018**, 288-294, https://doi.org/10.1145/3288155.3290586.
2. Garg, A., Deshmukh, A.R., Kumar, Y., Soi, A., Role of Quality Control in Effective Marketing, *Int J Multidiscip Res,* **2023**, 5, 6, 1-7, https://doi.org/10.36948/ijfmr.2023.v05i06.10214.
3. Jevšnik, S., Vasiliadis, S., Bahadir, S.K., Grujić, D., Stjepanovič, Z., Applying Heat for Joining Textile Materials, Chapter 10, in: Ishak, M. (ed.), *Joining Technologies*, InTech, **2016**, https://doi.org/10.5772/64309.
4. Umaru, S., Kaisan, M.U., Usman, S., Giwa, A., Effects of Garment Laundry Activities on the Slider Lock and Crosswise Strengths of Nylon Coil Zippers, *Nigerian Journal of Materials Science and Engineering*, **2016**, 7, 1, 81-86.
5. Jana, P., Assembling Technologies for Functional Garments—An Overview, *Indian J Fibre Text Res,* **2011**, 36, 380-387.
6. Jaseliūnaitė, K., Analysis of the Application of Adhesive Bonding Technology in the Fashion Collection "Savitas", Master's final degree project, Kaunas, **2019**.
7. Yatsenko, M., Bereznenko, S., Pawłowa, M., Nenia, O., Vashchuk, N., Improvement of the Strength of Adhesion Bonds of Textile Products for the Improvement of the Efficiency of Criminalistic Support of Law Enforcement Activities, *Communications in Development and Assembling of Textile Products*, **2020**, 1, 7, 48-56, https://doi.org/10.25367/cdatp.2020.1.
8. Mikalauskaite, G., Daukantienė, V., Influence of the Delamination Loading Velocity on Textile Bonds and Sewn Seams Strength, *Int J Cloth Sci Tech*, **2017**, 29, 6, 768-775, https://doi.org/10.1108/IJCST-02-2017-0012.

9. Jakubčionienė, Ž., Masteikaitė, V., Kleveckas, T., Jakubčionis, M., Kelesovam, U., Investigation of the Strength of Textile Bonded Seams, *Mater Sci-Medzg*, **2012**, 18, 2, 172-176, https://doi.org/10.5755/j01.ms.18.2.1922
10. Daukantienė, V., Danilovas, P.P., Mikalauskaite, G., Study of Temperature Impact on the Behaviour of Fibre Polymer Materials and Their Adhesive Bonds, *J Text Inst*, **2020**, ISSN: 0040-5000 (Print) 1754-2340 (Online), https://doi.org/10.1080/00405000.2020.1746011.
11. Busilienė, G., Strazdienė, E., Urbelis, V., Krauledas, S., The Effect of Bonded Seams upon Spatial Behaviour of Knitted Materials Systems, *Mater Sci-Medzg*, **2015**, 21, 2, 271-275, https://doi.org/10.5755/j01.ms.21.2.5767.
12. Loan, B.T., Ta, V.H., Study on the Influence of Interlining Pressing Technology Parameters on Shrinkage and Adhesion Strength Between Mex and Wool Silk Linen Fabric (in Vietnamese), *Journal of Scientific Research – Sao Do University*, **2022**, 2, 77, 40-45, http://tapchikhcn.saodo.edu.vn/uploads/files/articles_file/1662630214_6.Loan.may.pdf
13. Anh, K.T.L., Study on the Influence of Some Technological Parameters of Pressing-Rolling Interlining on the Shrinkage of Men's Vests (in Vietnamese), Master's thesis, Hanoi University of Science and Technology, **2015**, http://dlib.hust.edu.vn/handle/HUST/2914
14. Man, N.N., Study on the Influence of Some Technological Parameters of Interlining Pressing on the Adhesion Strength Between Interlining and PE/CO Fabric After Washing (in Vietnamese), Master's thesis, Hanoi University of Science and Technology, **2018**, http://dlib.hust.edu.vn/handle/HUST/12794.

3D PRINTING FOR PEDIATRIC FOOT ORTHOSES: CURRENT APPLICATIONS, CHALLENGES, AND FUTURE PERSPECTIVES

Shixuan CHEN[1,2], Han XU[1,2], Shiyang YAN[1,2*], Luming YANG[1,2*]

[1]National Engineering Laboratory for Clean Technology of Leather Manufacture, Sichuan University, Chengdu 610065, Sichuan, P. R. China, cklwhy61@gmail.com, xuhanzft@163.com, yanshiyangscu@126.com, ylmll1982@126.com

[2]College of Biomass Science and Engineering, Sichuan University, Chengdu 610065, Sichuan, P. R. China, cklwhy61@gmail.com, xuhanzft@163.com, yanshiyangscu@126.com, ylmll1982@126.com

Received: 31.07.2025 Accepted: 29.12.2025 https://doi.org/10.24264/lfj.25.4.5

3D PRINTING FOR PEDIATRIC FOOT ORTHOSES: CURRENT APPLICATIONS, CHALLENGES, AND FUTURE PERSPECTIVES

ABSTRACT. Pediatric foot deformities such as flexible flatfoot, clubfoot, and neuromuscular-related deformities can alter plantar loading, gait, and physical activity levels. Orthoses are widely used, but pediatric care requires frequent remakes during growth, and comfort strongly affects adherence. Additive manufacturing enables a digital workflow in which foot geometry is captured by three-dimensional scanning and translated into computer-aided design. Insoles, footwear components, or ankle-foot orthoses can then be fabricated with controlled geometry and regional stiffness. This review presents current applications of 3D-printed pediatric foot orthoses, synthesizing reported biomechanical outcomes and patient-reported experience across major indications. Available studies suggest that 3D-printed devices can achieve outcomes comparable to traditional orthoses in selected pediatric groups, with potential practical benefits such as lighter structures and better perceived fit in some reports. However, evidence is limited by small samples, short follow-up, and inconsistent reporting of design parameters and outcome measures. Future studies should report designs in a reproducible way and confirm durability, adherence, and clinical benefit through longer follow-up.

KEY WORDS: 3D printing, pediatric orthoses, foot deformities, insoles, ankle-foot orthoses

ORTEZE PLANTARE PEDIATRICE IMPRIMATE 3D: APLICAȚII ACTUALE, PROVOCĂRI ȘI PERSPECTIVE VIITOARE

REZUMAT. Deformările piciorului la copii, precum piciorul plat flexibil, piciorul strâmb congenital și deformările asociate afecțiunilor neuromusculare, pot modifica încărcarea plantară, mersul și nivelul de activitate fizică. Ortezele sunt utilizate pe scară largă, însă îngrijirea pediatrică necesită refaceri frecvente pe măsură ce copilul crește, iar confortul influențează puternic aderența. Fabricarea aditivă oferă o alternativă digitală, în care geometria piciorului este captată prin scanare tridimensională și transpusă în proiectare asistată de calculator. Se pot fabrica apoi branțuri, componente de încălțăminte sau orteze gleznă-picior cu geometrie controlată și rigiditate regională. Această revizuire prezintă aplicațiile actuale ale ortezelor plantare pediatrice imprimate 3D, sintetizând rezultatele biomecanice raportate și experiența relatată de pacient pentru principalele indicații. Studiile disponibile sugerează că dispozitivele imprimate 3D pot obține rezultate comparabile cu ortezele tradiționale la anumite grupuri pediatrice, cu potențiale beneficii practice precum structuri mai ușoare și o potrivire percepută mai bună în unele rapoarte. Totuși, dovezile sunt limitate de eșantioanele mici, monitorizarea pe termen scurt și raportarea neuniformă a parametrilor de proiectare și a măsurilor rezultate. Viitoarele studii ar trebui să raporteze designurile într-un mod reproductibil și să confirme durabilitatea, aderența și beneficiul clinic printr-o monitorizare mai îndelungată.

CUVINTE CHEIE: imprimare 3D; orteze pediatrice; deformări ale piciorului; branțuri; orteze gleznă-picior

ORTHÈSES PLANTAIRES PÉDIATRIQUES IMPRIMÉES EN 3D : APPLICATIONS ACTUELLES, DÉFIS ET PERSPECTIVES FUTURES

RÉSUMÉ. Les déformations du pied chez l'enfant, telles que le pied plat flexible, le pied bot et les déformations liées à des atteintes neuromusculaires, peuvent modifier les charges plantaires, la marche et le niveau d'activité physique. Les orthèses sont largement utilisées, mais les soins pédiatriques nécessitent des réajustements fréquents au fur et à mesure de la croissance de l'enfant, et le confort influence fortement le choix de l'orthèse. La fabrication additive offre une alternative numérique, dans laquelle la géométrie du pied est captée par numérisation 3D puis traduite en conception assistée par ordinateur. Il est ainsi possible de fabriquer des semelles, des composants de chaussures ou des orthèses cheville-pied à géométrie et rigidité localisée contrôlées. Cet article présente les applications actuelles des orthèses plantaires pédiatriques imprimées en 3D, en synthétisant les résultats biomécaniques publiés et l'expérience des patients pour les principales indications. Les études disponibles suggèrent que les dispositifs imprimés en 3D pourraient offrir des résultats comparables aux orthèses traditionnelles chez certains groupes d'enfants, avec des avantages pratiques potentiels tels que des structures plus légères et un meilleur ajustement perçu, selon certains rapports. Cependant, ces données sont limitées par la petite taille des échantillons, le court terme du suivi et l'hétérogénéité des données rapportées concernant les paramètres de conception et les mesures des résultats. Les études futures devraient présenter les conceptions de manière reproductible et confirmer la durabilité, l'adhérence et le bénéfice clinique grâce à un suivi plus long.

MOTS CLÉS : impression 3D ; orthèses pédiatriques ; déformations du pied ; semelles ; orthèses cheville-pied

* *Correspondence to: Shiyang YAN and Luming YANG, National Engineering Laboratory for Clean Technology of Leather Manufacture, Sichuan University, Chengdu 610065, Sichuan, P. R. China, yanshiyangscu@126.com, ylmll1982@126.com*

INTRODUCTION

In a birth cohort, 4.2% of newborns had identifiable foot deformities [1]. Pediatric foot deformities commonly prompt orthopedic referral and may present with gait concerns or malalignment at the knee, such as genu varum or valgum [2, 3]. Flexible pes planovalgus is common in early childhood and often improves as the medial arch develops [4, 5]; when pain or functional limitation persists, conservative measures may include stretching or physiotherapy and in-shoe orthoses [2, 6–8]. Congenital conditions such as clubfoot require early treatment, and serial casting followed by bracing can avoid surgery in most cases [1, 2, 9, 10]. Cavovarus or equinus patterns may signal neuromuscular diseases such as Charcot-Marie-Tooth (CMT) neuropathy or cerebral palsy (CP); orthoses, casting, and botulinum toxin can be used to improve dorsiflexion and gait [2, 11–14]. Across this diverse clinical spectrum, orthotic management plays a central role in conservative treatment strategies.

Custom foot orthoses (FOs) and ankle-foot orthoses (AFOs) are still commonly fabricated from negative impressions with subsequent rectification and thermoforming [15–17]. The process is labor-intensive and often must be repeated as children outgrow devices [16, 18]. In children prescribed AFOs, 3D scanning has been reported to be faster than plaster casting and can achieve high measurement accuracy when appropriate scanners and protocols are used [18]. Additive manufacturing (AM) can reproduce devices from stored digital models and facilitates targeted changes to thickness, trim lines, and internal structures such as lattices [16, 19]. Comfort and appearance are important determinants of acceptability and adherence, including in Charcot-Marie-Tooth disease [19–21]. Reported pediatric applications include printed insoles for symptomatic flexible flatfoot, printed AFOs for Charcot-Marie-Tooth disease, and printable braces used in clubfoot management [22, 23]. However, existing reviews note limited and heterogeneous evidence across designs and outcomes, indicating the need for a focused synthesis in pediatric foot orthoses [19].

This review summarizes current evidence on 3D printing in pediatric foot orthoses. We examine the literature by common indications, including flexible flatfoot, clubfoot, and neuromuscular-related deformities, and describe approaches to device design and fabrication within a digital workflow. We then compare printed and traditionally manufactured orthoses with respect to reported clinical and biomechanical outcomes, comfort and adherence, and practical considerations. Finally, we discuss key challenges and future research directions related to materials and manufacturing, variability in clinical effectiveness, and clinical implementation of 3D-printed pediatric foot orthoses.

ADDITIVE MANUFACTURING OF PEDIATRIC FOOT ORTHOSES

Digital Workflow

Additive manufacturing (AM) enables pediatric orthoses to be produced within a digital workflow that includes scanning, computer-aided design (CAD), and printing, rather than plaster casting and manual rectification [24–26]. As shown in Figure 1, pediatric orthoses can be produced through a scan, CAD, slicing, printing, and fitting workflow, replacing plaster casting and manual rectification in many cases. Geometry can be captured using structured light, laser, or photogrammetry-based scanners and exported as surface meshes (e.g., STL or OBJ) for orthosis design [27, 28]. For pediatric AFO fabrication, comparisons indicate that scanning can capture clinical geometry faster than casting when standardized protocols are applied [18]. The capture condition should be specified, including weight-bearing status and intended alignment, because posture during acquisition influences final orthosis geometry [27, 29]. After scanning, mesh processing such as cleanup, landmark identification, and boundary definition is typically required before computer-aided design modification, and this step can introduce variability if workflows are not standardized [26, 30]. During design, prescriptions are translated into geometry

through decisions about trim lines, thickness distribution, relief regions, and correction or alignment features [29, 31]. Parametric methods and simulation-informed approaches have been used to target stiffness and pressure distribution before fabrication and may reduce the need for repeated refitting [32–34]. Slicing converts the model into toolpaths, and print settings, including orientation, layer height, and infill, influence mechanical behavior [35, 36]. Clinical case reports demonstrate that end-to-end digital pipelines are feasible, although fitting and finishing still require clinician input [26, 37]. Post-processing commonly includes edge finishing, strap and pad integration, and dimensional checks, which are particularly important for pediatric skin tolerance and safety [26, 28]. Retaining digital models supports rapid remakes and resizing, which is clinically relevant because children grow and often require repeated refitting [38, 39]. Low-cost scanning and printing can be feasible for custom foot orthoses, but consistent outcomes depend on well-defined protocols and quality assurance [17, 27].

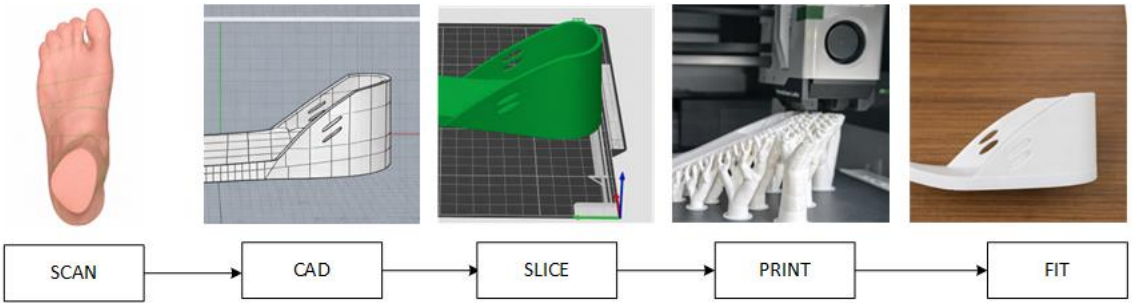

Figure 1. Digital workflow for additive manufacturing of pediatric orthoses. (Created by the authors)

Printing Technologies and Material Considerations

Polymer-based AM is most commonly used for orthoses. Frequently reported processes include fused deposition modeling or fused filament fabrication (FDM/FFF), selective laser sintering (SLS), and, less commonly, multi-jet fusion (MJF), as well as stereolithography or digital light processing (SLA/DLP) [24, 25, 40]. FDM/FFF is widely used because of accessibility and short build times, supporting prototyping and iterative development of pediatric orthosis designs [35, 41]. A key limitation is anisotropy introduced by layerwise deposition, meaning strength and stiffness depend on build orientation and print parameters [35, 42]. For insoles and foot orthoses, designers can vary infill and thickness to create region-specific stiffness, which is difficult to reproduce consistently with manual fabrication [43, 44]. Reviews of printed insoles emphasize that material selection and build strategy should match the clinical objective, such as providing support or increasing cushioning [45, 46]. SLS is used for AFOs because it can produce complex geometries without support structures and can provide favorable strength-to-weight performance in nylon parts [40, 47]. Clinical gait evaluations indicate that SLS AFOs were feasible at initial fitting and may deliver functional effects for individuals with foot drop [48, 49]. Design freedom is often used to reduce weight and improve ventilation through perforations or lattice-like regions while maintaining targeted stiffness [40, 47]. SLS and MJF can require substantial post-processing, including depowdering and surface finishing. Therefore, workflow planning should account for surface feel and edge quality, which are critical for pediatric comfort [26, 28]. SLA/DLP can deliver high resolution and smooth surfaces, but resin selection, post-curing, and long-term mechanical qualification are important when devices are intended to bear load [25, 50]. Beyond standard polymers, studies have explored bio-based polycarbonate and fiber-reinforced concepts to improve toughness or stiffness-to-weight ratio [51, 52].

Early work on AFOs indicates that the manufacturing method affects dimensional accuracy and device-to-device consistency [53]. For foot orthoses, stiffness functions as a

meaningful design parameter, because changes in stiffness or posting can influence plantar pressure distribution and muscle activity [44, 54]. Randomized crossover testing suggests that printed foot orthoses can produce biomechanical effects comparable to traditionally manufactured orthoses in flexible flatfoot [45, 55]. 3D printing also facilitates the integration of sensors or instrumentation, enabling objective monitoring of parameters such as alignment, pressure, or joint angle during use [56–58]. In pediatric populations, acceptance is strongly influenced by comfort and wearability, and studies of printed casts or orthoses commonly report higher comfort or satisfaction than traditional alternatives [59–61].

CURRENT APPLICATIONS OF 3D PRINTING IN PEDIATRIC FOOT ORTHOSES

Pediatric foot deformities commonly managed with orthoses include symptomatic flexible flatfoot, idiopathic clubfoot (congenital talipes equinovarus), and neuromuscular-related deformities associated with conditions such as cerebral palsy and Charcot-Marie-Tooth disease [2, 7, 62]. Treatment goals vary across these conditions, so orthotic form and design priorities vary as well. Flexible flatfoot management focuses on symptom relief and arch support, neuromuscular disorders on gait stabilization, and clubfoot on maintenance bracing after Ponseti correction [7, 13, 62, 63]. Consistent with these needs, reported pediatric applications of 3D printing mainly focus on printed insoles for flexible flatfoot, printed ankle-foot orthoses for neuromuscular gait disorders, and printed foot-abduction orthoses or modular brace components for clubfoot management [22, 23, 64, 65].

3D-printed Insoles for Symptomatic Flexible Flatfoot

Pediatric pes planus is commonly classified as flexible or rigid. Rigid flatfoot is uncommon and should prompt evaluation for underlying structural pathology. Therefore, this section focuses on flexible flatfoot [7, 66, 67]. Flexible flatfoot presents with a low medial arch during stance, whereas the arch and hindfoot alignment are corrected in non-weight-bearing positions or on tiptoe [7, 66]. As shown in Figure 2, the medial longitudinal arch collapses during standing in flexible flatfoot deformity. In typically developing children, arch height often becomes more defined with age, and many cases are asymptomatic and self-limiting [4, 66, 67]. However, in school-aged children, symptomatic flexible flatfoot has been associated with higher pain scores and poorer health-related quality of life, and orthoses are frequently prescribed to address pain and function [68–70]. Consequently, reassurance and periodic follow-up are appropriate for asymptomatic flexible flatfoot, whereas symptomatic cases are typically managed conservatively with education, supportive footwear, stretching when equinus is present, and in-shoe orthoses when pain, fatigue, or functional limitations persist [7, 8, 66, 67]. Contemporary evidence syntheses suggest that orthoses may reduce pain and improve certain functional or radiographic outcomes in older children with symptomatic flatfoot. However, in younger children, the effects are less consistent and appear to vary depending on device design and follow-up duration [71–74].

Figure 2. Flexible flatfoot in a child, showing the collapse of the arch on standing. (Source: Wikimedia Commons, "Children flat feet" (File:Children_flatfeet.jpg), CC BY-SA 3.0, https://commons.wikimedia.org/wiki/File:Children_flatfeet.jpg)

Within pediatric foot orthotics, 3D-printed insoles and other in-shoe devices represent the most frequently reported additive-manufactured application [45, 75–77]. Digitization enables a repeatable workflow in which foot geometry is captured by 3D scanning, while plantar-pressure measurements can be used to localize regions requiring medial support, offloading, or posting [31, 74, 75]. Compared with traditional milling or manual fabrication, 3D printing enables precise and repeatable tuning of orthotic stiffness by modifying arch geometry, shell thickness, and printing parameters (such as infill density, lattice design, and targeted reinforcement), while keeping the patient-specific shape constant for controlled evaluation of different support levels [43, 44, 54, 76, 77]. In pediatric flexible flatfoot, Lee *et al*. reported that pressure-based customized printed insoles were associated with measurable changes in radiographic hindfoot alignment, suggesting that digital customization can translate to objective alignment outcomes [75]. Zhao *et al*. printed multiple insole variants with different arch heights and infill densities and reported changes in center-of-pressure progression and gait-phase measures, illustrating how printing facilitates rapid prototyping across stiffness conditions (Figure 3) [76]. Early clinical evidence also suggests potential advantages in comfort and adherence, which are particularly relevant for children. In an open-access study including a 1-year follow-up of school-age children with symptomatic flexible flatfoot, Hu *et al*. compared ordinary orthopedic insoles with 3D-printed orthopedic insoles and reported longer wearing time in the 3D-printed group, alongside significant pain reduction after follow-up, highlighting comfort as a potential contributor to adherence [74]. Nevertheless, systematic reviews emphasize substantial heterogeneity across studies in scan methods, design features, materials, outcome metrics, and follow-up duration, limiting quantitative pooling and generalizability [45, 78]. Overall, the pediatric literature supports feasibility and measurable biomechanical or alignment changes, but higher-quality comparative trials with standardized clinical and patient-reported outcomes are still needed to define which design parameters provide durable benefit in specific subgroups [45, 74–76].

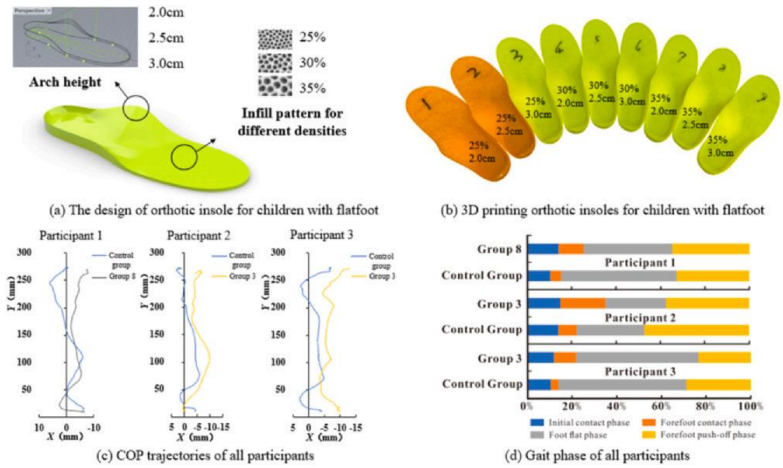

Figure 3. (a) Design of the orthotic insole based on pediatric foot arch morphology. (b) 3D printing of orthotic insoles with different arch heights and infill densities to achieve varying support stiffness. (c) Center-of-pressure (COP) trajectories of all participants during walking. (d) Gait phase characteristics of all participants. (Source: Zhao *et al*., 2023, Design and validation of 3D printed orthotic insoles for children with flatfoot, *Gait & Posture*, https://doi.org/10.1016/j.gaitpost.2023.07.275)

3D-printed Ankle Foot Orthoses for Neuromuscular-related Deformities

Neuromuscular and neuro-developmental disorders such as cerebral palsy (CP), Charcot-Marie-Tooth disease (CMT), and muscular dystrophy commonly result in secondary foot and ankle deformities and abnormal gait patterns. In these patients, ankle-foot orthoses (AFOs) and supramalleolar orthoses (SMOs) are used to stabilize the ankle, improve alignment, reduce energy expenditure, and support functional ambulation [40, 79–82]. In CMT, in-shoe orthoses may be used for symptomatic pes cavus, whereas AFOs are commonly indicated when foot drop or more pronounced gait impairment is present; however, comfort and perceived usefulness substantially influence adherence [11, 20–22, 83]. In spastic CP, orthoses are often integrated with physiotherapy, stretching/serial casting, and botulinum toxin to address equinus gait, and meta-analytic evidence suggests that orthoses can increase ankle dorsiflexion at initial contact compared with control conditions [10, 13, 84, 85]. These clinical drivers make digital design and 3D printing appealing, because devices can be resized and iteratively updated as children grow or as motor patterns evolve [22, 40]. Figure 4a illustrates equinus (toe-walking) gait commonly observed in children with spastic cerebral palsy, while Figure 4b shows the characteristic cavovarus foot deformity associated with Charcot-Marie-Tooth disease.

(a) (b)

Figure 4. (a) Toe walking (equinus gait) in a child, characterized by forefoot contact and limited heel strike during stance. (Source: Wikimedia Commons, “Zehenspitzengang unbehandelt.jpg”, CC BY-SA 4.0, https://commons.wikimedia.org/wiki/File:Zehenspitzengang_unbehandelt.jpg), (b) Foot deformity in Charcot-Marie-Tooth disease, showing muscle atrophy, a high medial longitudinal arch, and hammer toes. (Source: Wikimedia Commons, “Charcot-marie-tooth_foot.jpg”, CC BY-SA 3.0, https://commons.wikimedia.org/wiki/File:Charcot-marie-tooth_foot.jpg).

In pediatric practice, 3D-printed foot and ankle orthoses are most commonly reported in neuromuscular gait disorders where ankle control is central, particularly spastic CP and CMT [11, 22, 64]. For children with spastic CP, Qin *et al*. retrospectively compared customized 3D-printed AFOs with traditional AFOs and reported that the printed devices were lighter and thinner (approximately 124 g vs. 183 g; 1.7 mm vs. 3.0 mm), with modest improvements in walking speed and stride length (Figure 5) [64]. For pediatric CMT, Wojciechowski *et al*. demonstrated that 3D printing can replicate traditional AFO geometry and that redesign using print-enabled structural changes produced devices that were approximately 35% lighter and improved the ankle dorsiflexor moment during loading response, highlighting the potential of digital iteration beyond simple replication [22].

Beyond these pediatric comparisons, engineering and adult clinical studies provide a methodological foundation for printed AFO development, including selective laser sintering (SLS) of nylon-based braces, objective gait and plantar-pressure assessment during fitting, and systematic exploration of stiffness effects [47–49]. Overall, current reviews suggest that 3D-printed AFOs can achieve gait effects broadly comparable to traditionally fabricated AFOs, but pediatric-specific evidence and durability/quality-assurance reporting remain limited [19, 40, 78].

Figure 5. Prototype application and integration of a 3D-printed foot/ankle orthotic system. (A) Custom-fabricated 3D-printed foot orthosis (FO) insole. (B) The insole integrated into a foot/ankle brace with metallic supportive components. (C) Lateral view of the fully assembled ankle-foot orthosis (AFO). (D) Clinical demonstration of the bilateral 3D-printed AFO system worn with standard footwear. (Source: Qin *et al*., 2025, *Frontiers in Pediatrics*, CC BY 4.0, https://doi.org/10.3389/fped.2025.1661098)

3D-printed Foot Abduction Orthoses and Brace Components for Clubfoot

Idiopathic congenital talipes equinovarus (clubfoot, CTEV) is a common congenital musculoskeletal deformity, with a corrected pooled global birth prevalence of about 1.10 per 1,000 births; regional variation is substantial, and the burden is disproportionately high in low- and middle-income settings [9, 62, 86]. Clinically, clubfoot is characterized by cavus, forefoot adduction, hindfoot varus, and equinus (Figure 6) [62, 87]. The first-line standard of care is the Ponseti method, which involves staged manipulation and serial casting. This is commonly followed by percutaneous Achilles tenotomy and prolonged foot-abduction bracing to maintain

correction and reduce the need for extensive surgery [62, 63, 88–90]. Because relapse is strongly associated with poor brace adherence, the design, comfort, and usability of foot-abduction orthoses (FAOs) are clinically consequential and are a major focus of device innovation [91, 92].

Figure 6. Infant with congenital clubfoot (talipes equinovarus). The affected foot is twisted sharply inward and downward. (Source: Wikimedia Commons, CC BY 3.0, https://commons.wikimedia.org/wiki/File:813_Clubfoot.jpg)

For idiopathic clubfoot treated with Ponseti, post-correction FAO use is central to relapse prevention, and objective monitoring studies show that parent-reported brace wear can be inaccurate; lower adherence is associated with higher relapse risk [93, 94]. Traditional boots and bars reduce recurrence more effectively than ankle-foot orthoses, reinforcing the need to maintain abduction during the maintenance phase [95]. However, skin problems, discomfort, and practicality can undermine adherence, motivating alternative brace designs (e.g., dynamic FAOs) intended to improve tolerance [96]. In this context, additive manufacturing has been explored primarily as a means to improve access, fit, adjustability, and instrumentation rather than to replace the Ponseti protocol itself [23, 65, 97, 98].

An open-source 3D-printable infant clubfoot brace has been reported as a low-cost alternative that aims to preserve the functional principles of foot-abduction bracing while enabling distributed manufacturing and local replacement of components as infants grow [23]. More recently, Beldar *et al*. proposed an adjustable clubfoot splint with modular 3D-printed components, allowing correction angles and fit to be adjusted without fully remanufacturing the entire system—an approach aligned with the rapid iteration potential of digital workflows [65]. 3D printing has also enabled rapid prototyping of custom brace geometries and corrective footwear components (e.g., shoe plates, bar connectors, and adjustable interfaces), supporting iterative refinement based on clinician feedback and observed tolerance [97]. In parallel, sensor-integrated bracing concepts illustrate how additive manufacturing can be combined with remote monitoring to quantify adherence, which is a key determinant of long-term outcomes in clubfoot [98]. Overall, published reports suggest that 3D-printed FAO solutions are feasible and may improve access or adjustability, but clinical validation remains limited; relapse prevention still depends on adherence, follow-up capacity, and service delivery models, particularly in resource-constrained settings [9, 86, 91, 93].

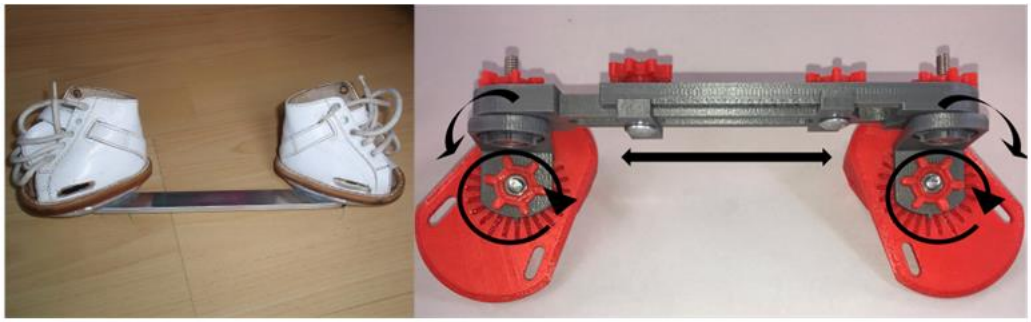

(a) (b)

Figure 7. Examples of traditional and innovative 3D-printed FAOs for clubfoot treatment: (a) Shoes mounted on a Denis Browne bar, a foot abduction brace used in clubfoot treatment, named after British pediatric surgeon Denis Browne (Source: Wikimedia Commons, CC BY-SA 4.0, https://commons.wikimedia.org/wiki/File:Botas.JPG). (b) Open-source 3D-printable infant clubfoot brace design illustrating adjustable components. (Source: Appropedia, "Open-Source Three-Dimensional Printable Infant Clubfoot Brace", Savonen, B., Gershenson, J., Bow, J.K., Pearce, J.M., CC BY-SA 3.0, https://www.appropedia.org/Open-Source_Three-Dimensional_Printable_Infant_Clubfoot_Brace)

COMPARISON OF 3D-PRINTED VS. TRADITIONAL ORTHOSES

Clinical Effectiveness

Current evidence suggests that 3D-printed ankle-foot orthoses (AFOs) can achieve gait outcomes broadly comparable to traditional AFOs, although most studies remain small and short-term [19, 40]. In children with spastic cerebral palsy, a comparative study reported greater improvements in function and spatiotemporal gait parameters with 3D-printed AFOs than with traditional polyethylene AFOs over 3 months. In that cohort, both groups improved, but the 3D-printed group showed larger Gross Motor Function Measure (GMFM) gains (about +6.5 vs. +3.2) and larger increases in cadence and step length [64]. For pediatric neuromuscular disease, 3D printing has been used to replicate and redesign AFOs for children with Charcot-Marie-Tooth disease, enabling matched geometry and iterative modification within a single workflow [22]. For school-age children with symptomatic flexible flatfoot, 3D-printed orthopedic insoles have been reported to reduce pain at follow-up, with adherence benefits in some subgroups. A one-year follow-up study reported pain score reductions of approximately 1-2 points on a 0-10 visual analog scale and longer wearing time for 3D-printed insoles in lighter-weight children compared with traditional insoles [74]. Overall interpretations remain cautious because studies vary in materials, stiffness design, and outcome measures [45]. Traditional custom foot orthoses can already improve pain and balance in children with symptomatic flexible flatfoot, so 3D-printed devices should demonstrate similar benefits under comparable conditions [75, 99]. Clinically, printing is a manufacturing route rather than an intervention in itself, and outcomes depend on orthosis geometry and stiffness as much as on the fabrication method [40, 44].

Patient Comfort, Adherence, and Patient-reported Outcomes

Patient-reported outcomes are increasingly reported, and some AFO studies show higher satisfaction with fit and comfort for 3D-printed devices. However, outcome measures are inconsistent across studies [40, 100]. In pediatric flatfoot, comfort is clinically important because it can translate into longer daily wearing time, which is a practical prerequisite for effectiveness [74]. For bracing in infant clubfoot, low-cost 3D-printed brace concepts exist, but adherence still depends on usability, follow-up, and family support rather than printing alone [23].

Customization, Production Time, and Reproducibility

The practical advantage of additive manufacturing is greater workflow control.

Digital capture and computer-aided design make remakes and incremental resizing easier across follow-up visits [19, 24]. In pediatric AFO fabrication, structured-light scanning has been reported to be faster than plaster casting while achieving comparable shape capture under standardized protocols [18, 27]. Cost is context-dependent. An economic evaluation of wrist orthoses found higher mean costs for 3D-printed orthoses than for low-temperature thermoplastic orthoses, with labor as the main cost driver [101]. Therefore, comparisons should be condition and setting-specific. Both routes can meet similar clinical targets, while printing mainly influences reproducibility, redesign speed, and traceability [19, 26].

CHALLENGES AND FUTURE PERSPECTIVES

Materials and Manufacturing Limitations of the Orthosis

3D printing provides new possibilities for customized pediatric foot orthoses; compared with traditional plaster casting and thermoforming, it enables complex geometries, region-specific stiffness tuning, and lightweight designs [26, 27, 31, 43]. However, there are still many limitations in the orthosis materials and manufacturing processes [25, 26, 78]. Common printable materials include polylactic acid (PLA), polyamides (e.g., PA12 nylon), and thermoplastic polyurethane elastomers (TPU); their mechanical properties and biocompatibility differ [40, 78].

Current Challenges

First, evidence on the long-term durability and material robustness of 3D-printed orthoses remains limited, and durability concerns still need to be addressed [19, 78]. Wojciechowski *et al*. noted that fatigue/durability testing is scarce in existing studies, and only a few studies performed destructive tests and compared material performance [19]. For example, some studies compared materials such as Nylon-11 and Nylon-12 and suggested better damping/deformation tolerance for Nylon-11, whereas glass-fiber-filled Nylon-12 was more prone to failure [19, 102, 103]. Second, small changes in printing parameters (e.g., layer thickness, infill density, and build orientation) can significantly alter mechanical properties, requiring empirical calibration using printed specimens rather than relying only on nominal material data [33, 104]. In addition, surface roughness and dimensional accuracy also affect skin conformity and comfort [26, 28]. 3D-printed orthoses often require post-processing (support removal, edge sanding, heat treatment, etc.) to reduce burrs and improve comfort; for photopolymer resin systems, adequate post-curing and long-term mechanical qualification are important for load-bearing devices [19, 26, 50]. Regarding biocompatibility, many polymers used for 3D-printed orthoses are industrial-grade; certification and evidence for prolonged skin contact can be limited, and irritation risks under sweat/friction may warrant further evaluation [26, 50, 78]. Overall, insufficient strength/durability, structural defects, and surface/finishing issues together constitute the core challenges of the 3D-printed orthosis body.

Future Trends

To address material and process constraints, research is moving toward higher-performance materials and design optimization. First, in terms of materials, developing and evaluating new materials will improve orthosis strength and durability [78]. For example, adopting Nylon-11 or reinforcing/compounding PLA with fibers and elastomers may help balance stiffness and toughness [51, 52, 102, 104]. Meanwhile, cyclic fatigue testing under repeated pediatric loading and biocompatibility standardization are needed to verify service life and ensure long-term contact safety [78]. For post-processing, chemical polishing and antibacterial coatings may be used to improve surface smoothness and biocompatibility, making orthoses more comfortable to wear. Second, in terms of manufacturing processes, improvements in digital design tools may help mitigate the impact of structural defects. By using simulation to optimize internal lattice structures and region-specific thickness, overall strength and durability may improve without excessive weight gain [32, 33]. In addition, modular and hybrid design strategies have been proposed to enhance practical adjustability. By introducing detachable or adjustable components, local stiffness or size

can be fine-tuned without redesigning the entire device. For example, combining traditional heat-adjustable elements with 3D-printed components allows selected modules to be replaced or reprinted as needed, rather than remanufacturing the whole orthosis, thereby improving clinical flexibility [65]. Overall, future work should integrate materials science and design innovation to improve the mechanical reliability and safety of 3D-printed orthoses, providing pediatric patients with lightweight, comfortable, and durable assistive devices.

Variability in Clinical Effectiveness

Different clinical studies report substantial variability in the effectiveness of 3D-printed foot orthoses [40, 45, 100]. Some reports indicate that 3D-printed AFOs often provide better comfort and fit than traditional devices, leading to higher patient satisfaction [40, 78]. However, across populations such as pediatric flexible flatfoot, Charcot-Marie-Tooth disease (CMT), and spastic cerebral palsy, studies report inconsistent degrees of gait improvement and symptom relief [40, 45]. Daryabor *et al*. concluded in a systematic review that 3D-printed insoles may have positive effects on pain/comfort and foot function; however, reports on plantar pressure, center-of-pressure measures, and three-dimensional ankle kinematics and kinetics are inconsistent across studies [45]. For example, in children with flatfoot, some studies found that wearing customized 3D-printed insoles can reduce pain and improve walking comfort in the short-term, but findings on gait biomechanics (e.g., plantar pressure distribution and spatiotemporal parameters) are inconsistent [45, 100]. In neuromuscular populations (e.g., cerebral palsy, stroke, and CMT), 3D-printed AFOs have shown immediate improvements in selected gait parameters compared with no orthosis. Across studies, their functional effects are generally comparable to traditionally fabricated AFOs [40].

Current Challenges

First, most existing studies are limited by small sample sizes and short follow-up durations; many are single-case reports or involve fewer than 10 participants, with follow-up ranging from immediate effects to only a few weeks [40, 45, 100], leading to uncertainty about overall clinical effectiveness. In addition, heterogeneity across study populations represents an inherent challenge. Children and adults differ in neuromuscular control and adherence, and even within pediatric cohorts, unavoidable variability in deformity severity, gait patterns, and body size may influence observed outcomes. Furthermore, differences in adherence and real-world use conditions may further contribute to variability across studies. For example, some studies allow participants to wear orthoses within their usual footwear, whereas others assess gait under barefoot conditions; such differences in wearing protocols can affect gait performance and confound comparisons. Moreover, clinical benefits often require time to accumulate; short-term observation may under- or overestimate effects, and long-term follow-up is needed to evaluate arch remodeling or gait reconstruction. The current literature rarely reports long-term follow-up outcomes for 3D-printed orthoses, limiting understanding of the durability of effects and longer-term functional impact [40, 45, 78]. In summary, small sample sizes, short follow-up durations, population heterogeneity, and differences in adherence and real-world use jointly contribute to variability in reported clinical effects.

Future Trends

To reduce variability in effectiveness research, future improvements are needed in trial design and reporting standards. First, higher-quality controlled studies with larger samples and longer follow-up should be conducted to obtain statistically robust and clinically meaningful evidence. As Pollen *et al*. suggested, areas showing preliminary effectiveness urgently need rigorous randomized controlled trials with larger cohorts and long-term follow-up to confirm durability of benefits [40]. In reporting, there is a call to establish standardized outcome frameworks. Future studies should report indications, orthosis type, key design parameters (e.g., materials and stiffness distribution), printing process/settings, and follow-up schedule in detail [26]. Using unified outcome measures (e.g., standardized gait analysis protocols, plantar pressure metrics, and patient-reported outcome scales) would

facilitate cross-study comparisons and meta-analyses [40, 45]. To account for individual differences, future work may integrate 3D foot data with biomechanical models to predict patient-specific gait effects of different designs. In parallel, subjective feedback and adherence data should be emphasized alongside objective measurements (e.g., pain on a visual analog scale (VAS), activity level, and wearing time) to evaluate clinical relevance comprehensively. In short, future clinical research should pursue standardization and personalization in parallel to reduce evaluation bias and clarify the value of 3D-printed orthoses for different pediatric foot conditions.

Barriers to Clinical Implementation

Although 3D printing shows promise for faster orthosis production and improved fit, real-world clinical implementation still faces multiple barriers [26, 27]. Compared with adults, pediatric patients have unique difficulties in digital shape capture and in providing feedback during orthosis use [27, 28].

Current Challenges

First, acquiring foot morphology data is difficult. Accurate foot anatomy is required for customized orthoses and is typically obtained via 3D scanning. However, young children often have difficulty keeping still during scanning. Even with fast structured-light scanners, movement can create artifacts or incomplete data, reducing downstream design accuracy [28]. In addition, the scanning posture (e.g., weight-bearing standing vs. non-weight-bearing sitting) can substantially influence the final corrective orientation of the orthosis [29]. Currently, there is no unified standard to guide pediatric foot scanning posture and protocols; data standards vary across institutions, causing downstream fabrication differences from the outset [26–28]. Second, the digital design workflow lacks standardization. After obtaining a foot model, CAD software is required for 3D modeling and modification of the orthosis. However, there is still no widely accepted pediatric foot orthosis design paradigm; technicians often rely on personal experience to adjust arch support height, shell thickness, and padding locations [26, 31]. This manual modeling process is subjective, and consistent quality is hard to guarantee across designers and software tools. Without standardized templates and parameter guidance, even the same input foot data can yield highly variable orthosis designs. Third, printing reproducibility and consistency are insufficient. Differences across printers and material batches, as well as small changes in printing parameters (temperature, speed, infill pattern, etc.), can affect orthosis hardness and dimensional accuracy [26, 104]. Without a mature quality control system, printed orthoses may vary slightly from one production run to another. Industry standards in this area have not yet been fully established [26]. Fourth, mechanisms for collecting comfort feedback are insufficient. The clinical value of orthoses is not only deformity correction but also sustained wearing and adherence. A key factor influencing wearing willingness is comfort, including whether the orthosis causes pressure pain, skin friction, or walking inconvenience [100]. Existing practice lacks systematic mechanisms for feedback collection and iterative design; it often relies on subjective reports from patients/caregivers, with long feedback cycles and incomplete information. Such an imperfect feedback system may delay identification and correction of comfort issues, thereby reducing adherence [100]. Finally, workforce and workflow bottlenecks also limit large-scale clinical adoption of 3D-printed orthoses. Clinical teams need cross-disciplinary skills in scanning, modeling, and printing, yet many orthotists and clinicians lack training opportunities. If hospitals attempt to adopt digital workflows, new collaboration models and a clear division of labor between clinical and engineering teams are also needed. Without mature workflow guidance, the expected advantages in rapid delivery may not be realized [26]. In summary, barriers in data acquisition, design standards, production consistency, feedback mechanisms, and workforce training make it challenging for 3D-printed pediatric foot orthoses to transition from laboratory exploration to routine clinical practice.

Future Trends

To promote broader clinical adoption of 3D-printed orthoses, optimization is needed on both technical and managerial levels. First, new

child-friendly foot scanning solutions can be explored. For example, faster scanners or multi-view photogrammetry could reduce acquisition time and improve cooperation; for toddlers unable to stand still, lightweight adjustable fixtures may help stabilize posture during rapid scanning. For standardized scanning protocols, posture and weight-bearing requirements for different pediatric age groups, along with accuracy verification methods, should be defined to ensure reliable digital models [27, 28]. Second, regarding CAD standardization, open design databases and parameter guidelines for pediatric foot orthoses could be developed [29, 32]. By aggregating data from many clinically successful cases, optimized geometries for different conditions can be extracted to enable semi-automated design assistance. For example, software could auto-generate an initial orthosis model based on inputs such as arch height and inversion/eversion angles, allowing technicians to fine-tune it and reducing purely subjective variability. Third, printing and quality-control workflows should be optimized; healthcare institutions should adopt rigorous digital manufacturing quality management systems. This includes regular equipment calibration, material batch control, and verification of key parameter consistency. Manufacturing-style approaches can be adopted, such as adding standard test coupons to each batch to monitor whether hardness and dimensions meet requirements and to enable closed-loop adjustment when deviations occur. In addition, because children often require size adjustments during growth, future orthosis designs may reserve adjustable margins or use modular structures; when children grow or discomfort occurs, modules can be replaced or partially reprinted rather than remaking the entire device [65]. Fourth, a systematic patient feedback and follow-up mechanism should be established. Future digital health platforms could allow parents to regularly report comfort, including redness and pressure pain. These data could be linked with design parameters to help technicians identify which design features cause discomfort and improve the next iteration. Finally, workforce training and service models should be upgraded in parallel. Cross-domain training should be provided so orthotists can master basic 3D scanning and CAD skills while engineers understand foot biomechanics and clinical needs. Hospitals may establish multidisciplinary workflows, for example, rehabilitation physicians prescribe and evaluate, orthotists scan and design, engineers print and post-process, and clinicians fit and validate the device [30]. With a clear division of labor and strengthened training, the efficiency benefits of digital workflows can be fully realized. In summary, future efforts should optimize technical workflows while strengthening clinical integration: overcoming technical bottlenecks in scanning, design, and printing, and establishing patient-centered feedback loops and workforce support. Only in this way can 3D-printed pediatric foot orthoses truly move from experimental exploration to routine clinical practice and benefit more children.

CONCLUSION

3D printing enables pediatric foot orthoses to be produced through a digital workflow that improves traceability and supports efficient remakes during growth. Current pediatric studies suggest that printed insoles and ankle-foot orthoses can achieve short-term biomechanical outcomes comparable to traditionally fabricated orthoses in selected conditions, while clubfoot work mainly focuses on foot-abduction bracing and modular components. The main constraint is that the clinical evidence is still early-stage, with short follow-up and inconsistent reporting of key design and manufacturing details. Progress now depends on standardized reporting and clinical quality assurance. Longer follow-up is needed to evaluate durability and everyday use patterns, so that 3D printing becomes a reliable clinical manufacturing approach.

Acknowledgements

This work was supported by the Fundamental Research Funds for the Central Universities, the Sichuan Science and Technology Program (grant number 2025NSFJQ0020), and the Guangxi Science and Technology Program (grant number AB25069081).

REFERENCES

1. Widhe, T., Aaro, S., Elmstedt, E., Foot Deformities in the Newborn--Incidence and Prognosis, *Acta Orthop Scand*, **1988**, 59, 2, 176–179.
2. Beer, A., Common Foot Deformities in Children, *Orthop Trauma*, **2024**, 38, 6, 343–348, https://doi.org/10.1016/j.mporth.2024.10.001.
3. Rerucha, C.M., Dickison, C., Baird, D.C., Lower Extremity Abnormalities in Children, *Am Fam Physician*, **2017**, 96, 4, 226–233.
4. Uden, H., Scharfbillig, R., Causby, R., The Typically Developing Paediatric Foot: How Flat Should It Be? A Systematic Review, *J Foot Ankle Res*, **2017**, 15, 10, 37, https://doi.org/10.1186/s13047-017-0218-1.
5. Pfeiffer, M., Kotz, R., Ledl, T., Hauser, G., Sluga, M., Prevalence of Flat Foot in Preschool-Aged Children, *Pediatrics*, **2006**, 118, 2, 634–639, https://doi.org/10.1542/peds.2005-2126.
6. Halabchi, F., Mazaheri, R., Mirshahi, M., Abbasian, L., Pediatric Flexible Flatfoot; Clinical Aspects and Algorithmic Approach, *Iran J Pediatr*, **2013**, 23, 3, 247–260.
7. Carr, J.B., Yang, S., Lather, L.A., Pediatric Pes Planus: A State-of-the-Art Review, *Pediatrics*, **2016**, 137, 3, e20151230, https://doi.org/10.1542/peds.2015-1230.
8. Dars, S., Uden, H., Banwell, H.A., Kumar, S., The Effectiveness of Non-Surgical Intervention (Foot Orthoses) for Paediatric Flexible Pes Planus: A Systematic Review: Update, *PLOS One*, **2018**, 13, 2, e0193060, https://doi.org/10.1371/journal.pone.0193060.
9. Smythe, T., Rotenberg, S., Lavy, C., The Global Birth Prevalence of Clubfoot: A Systematic Review and Meta-Analysis, *eClinicalMedicine*, **2023**, 63, 102178, https://doi.org/10.1016/j.eclinm.2023.102178.
10. Klaewkasikum, K., Patathong, T., Woratanarat, P., Woratanarat, T., Thadanipon, K., Rattanasiri, S., Thakkinstian, A., Efficacy of Conservative Treatment for Spastic Cerebral Palsy Children with Equinus Gait: A Systematic Review and Meta-Analysis, *J Orthop Surg Res*, **2022**, 17, 1, 411, https://doi.org/10.1186/s13018-022-03301-3.
11. Scheffers, G., Hiller, C., Refshauge, K., Burns, J., Prescription of Foot and Ankle Orthoses for Children with Charcot–Marie–Tooth Disease: A Review of the Evidence, *Phys Ther Rev*, **2012**, 17, 2, 79–90, https://doi.org/10.1179/1743288X11Y.0000000052.
12. Sanpera, I., Villafranca-Solano, S., Muñoz-Lopez, C., Sanpera-Iglesias, J., How to Manage Pes Cavus in Children and Adolescents?, *EFORT Open Rev*, **2021**, 6, 6, 510–517, https://doi.org/10.1302/2058-5241.6.210021.
13. Sees, J.P., Miller, F., Overview of Foot Deformity Management in Children with Cerebral Palsy, *J Child Orthop*, **2013**, 7, 5, 373–377, https://doi.org/10.1007/s11832-013-0509-4.
14. Evans, A.M., Rome, K., Carroll, M., Hawke, F., Foot Orthoses for Treating Paediatric Flat Feet, *Cochrane Database Syst Rev*, **2022**, 1, 1, CD006311, https://doi.org/10.1002/14651858.CD006311.pub3.
15. International Committee of the Red Cross (ICRC), Physical Rehabilitation Programme, Ankle-Foot Orthosis Manufacturing Guidelines, ICRC, **2006**, 0868/002.
16. Peng, C., Tran, P., Lalor, S., Tirosh, O., Rutz, E., Tuning the Mechanical Responses of 3D-Printed Ankle-Foot Orthoses: A Numerical Study, *Int J Bioprint*, **2024**, 10, 3, 3390, https://doi.org/10.36922/ijb.3390.
17. Dombroski, C.E., Balsdon, M.E., Froats, A., The Use of a Low Cost 3D Scanning and Printing Tool in the Manufacture of Custom-Made Foot Orthoses: A Preliminary Study, *BMC Res Notes*, **2014**, 7, 1, 443–447, https://doi.org/10.1186/1756-0500-7-443.
18. Farhan, M., Wang, J.Z., Warncke, R., Cheng, T.L., Burns, J., Comparison of Accuracy and Speed between Plaster Casting, High-Cost and Low-Cost 3D Scanners to Capture Foot, Ankle and Lower Leg Morphology of Children Requiring Ankle-Foot Orthoses, *J Foot Ankle Res*, **2024**, 17, 3, e70006, https://doi.org/10.1002/jfa2.70006.
19. Wojciechowski, E., Chang, A.Y., Balassone, D., Ford, J., Cheng, T.L., Little, D., Menezes, M.P., Hogan, S., Burns, J., Feasibility of Designing, Manufacturing and Delivering 3D Printed Ankle-Foot Orthoses: A Systematic Review, *J Foot Ankle Res*, **2019**, 12, 1, 11–35, https://doi.org/10.1186/s13047-019-0321-6.
20. Vinci, P., Gargiulo, P., Poor Compliance with Ankle-Foot-Orthoses in Charcot-Marie-Tooth Disease, *Eur J Phys Rehabil Med*, **2008**, 44, 1, 27–31.
21. Zuccarino, R., Anderson, K.M., Shy, M.E., Wilken, J.M., Satisfaction with Ankle Foot Orthoses in Individuals with Charcot-Marie-Tooth Disease, *Muscle Nerve*, **2021**, 63, 1, 40–45, https://doi.org/10.1002/mus.27027.
22. Wojciechowski, E.A., Cheng, T.L., Hogan, S.M., Mudge, A.J., Balassone, D., Menezes, M.P., Little, D.G., Dwan, L.N., Burns, J., Replicating and Redesigning Ankle-Foot Orthoses with 3D Printing for Children with Charcot-Marie-Tooth Disease, *Gait Posture*, **2022**, 96, 73–80, https://doi.org/10.1016/j.gaitpost.2022.05.006.
23. Savonen, B., Gershenson, J., Bow, J.K., Pearce, J.M., Open-Source Three-Dimensional Printable Infant Clubfoot Brace, *JPO J Prosthet Orthot*, **2020**, 32, 2, 149–158, https://doi.org/10.1097/JPO.0000000000000257.
24. Chen, R.K., Jin, Y., Wensman, J., Shih, A., Additive Manufacturing of Custom Orthoses and Prostheses—A Review, *Addit Manuf*, **2016**, 12, 77–89, https://doi.org/10.1016/j.addma.2016.04.002.
25. Choo, Y.J., Boudier-Revéret, M., Chang, M.C., 3D Printing Technology Applied to Orthosis

Manufacturing: Narrative Review, *Ann Palliat Med*, **2020**, 9, 6, 4262–4270, https://doi.org/10.21037/apm-20-1185.
26. Alrasheedi, N.H., Tlija, M., Elloumi, N., Louhichi, B., A Critical Review of 3D Printed Orthoses towards Workflow Implementation in the Clinical Practice, *J Eng Res*, **2025**, 13, 2, 1038–1051, https://doi.org/10.1016/j.jer.2024.01.024.
27. Farhan, M., Wang, J.Z., Bray, P., Burns, J., Cheng, T.L., Comparison of 3D Scanning versus Traditional Methods of Capturing Foot and Ankle Morphology for the Fabrication of Orthoses: A Systematic Review, *J Foot Ankle Res*, **2021**, 14, 1, 2, https://doi.org/10.1186/s13047-020-00442-8.
28. Silva, R., Silva, B., Fernandes, C., Morouço, P., Alves, N., Veloso, A., A Review on 3D Scanners Studies for Producing Customized Orthoses, *Sens*, **2024**, 24, 5, 1373, https://doi.org/10.3390/s24051373.
29. Telfer, S., Gibson, K.S., Hennessy, K., Steultjens, M.P., Woodburn, J., Computer-Aided Design of Customized Foot Orthoses: Reproducibility and Effect of Method Used to Obtain Foot Shape, *Arch Phys Med Rehabil*, **2012**, 93, 5, 863–870, https://doi.org/10.1016/j.apmr.2011.12.019.
30. Baronio, G., Harran, S., Signoroni, A., A Critical Analysis of a Hand Orthosis Reverse Engineering and 3D Printing Process, *Appl Bionics Biomech*, **2016**, 2016, 1–7, https://doi.org/10.1155/2016/8347478.
31. Telfer, S., Pallari, J., Munguia, J., Dalgarno, K., McGeough, M., Woodburn, J., Embracing Additive Manufacture: Implications for Foot and Ankle Orthosis Design, *BMC Musculoskelet Disord*, **2012**, 13, 1, 84, https://doi.org/10.1186/1471-2474-13-84.
32. Cheung, J.T.-M., Zhang, M., Parametric Design of Pressure-Relieving Foot Orthosis Using Statistics-Based Finite Element Method, *Med Eng Phys*, **2008**, 30, 3, 269–277, https://doi.org/10.1016/j.medengphy.2007.05.002.
33. Yeh, C.-H., Lin, K.-R., Su, F.-C., Hsu, H.-Y., Kuo, L.-C., Lin, C.-C., Optimizing 3D Printed Ankle-Foot Orthoses for Patients with Stroke: Importance of Effective Elastic Modulus and Finite Element Simulation, *Heliyon*, **2024**, 10, 5, e26926, https://doi.org/10.1016/j.heliyon.2024.e26926.
34. Davia-Aracil, M., Hinojo-Pérez, J.J., Jimeno-Morenilla, A., Mora-Mora, H., 3D Printing of Functional Anatomical Insoles, *Comput Ind*, **2018**, 95, 38–53, https://doi.org/10.1016/j.compind.2017.12.001.
35. Tofail, S.A.M., Koumoulos, E.P., Bandyopadhyay, A., Bose, S., O'Donoghue, L., Charitidis, C., Additive Manufacturing: Scientific and Technological Challenges, Market Uptake and Opportunities, *Mater Today*, **2018**, 21, 1, 22–37, https://doi.org/10.1016/j.mattod.2017.07.001.
36. Guo, N., Leu, M.C., Additive Manufacturing: Technology, Applications and Research Needs, *Front Mech Eng*, **2013**, 8, 3, 215–243, https://doi.org/10.1007/s11465-013-0248-8.
37. Hale, L., Linley, E., Kalaskar, D.M., A Digital Workflow for Design and Fabrication of Bespoke Orthoses Using 3D Scanning and 3D Printing, a Patient-Based Case Study, *Sci Rep*, **2020**, 10, 1, 7028, https://doi.org/10.1038/s41598-020-63937-1.
38. Mavroidis, C., Ranky, R.G., Sivak, M.L., Patritti, B.L., DiPisa, J., Caddle, A., Gilhooly, K., Govoni, L., Sivak, S., Lancia, M., Drillio, R., Bonato, P., Patient Specific Ankle-Foot Orthoses Using Rapid Prototyping, *J NeuroEng Rehabil*, **2011**, 8, 1, 1, https://doi.org/10.1186/1743-0003-8-1.
39. Walbran, M., Turner, K., McDaid, A.J., Customized 3D Printed Ankle-Foot Orthosis with Adaptable Carbon Fibre Composite Spring Joint, *Cogent Eng*, **2016**, 3, 1, 1227022, https://doi.org/10.1080/23311916.2016.1227022.
40. Pollen, T.N., Jor, A., Munim, F., He, Y., Daryabor, A., Gao, F., Lam, W.K., Kobayashi, T., Effects of 3D-Printed Ankle-Foot Orthoses on Gait: A Systematic Review, *Assistive Technol*, **2025**, 37, 4, 287–303, https://doi.org/10.1080/10400435.2024.2411563.
41. Lunsford, C., Grindle, G., Salatin, B., Dicianno, B.E., Innovations with 3-Dimensional Printing in Physical Medicine and Rehabilitation: A Review of the Literature, *PM&R*, **2016**, 8, 12, 1201–1212, https://doi.org/10.1016/j.pmrj.2016.07.003.
42. Huang, S.H., Liu, P., Mokasdar, A., Hou, L., Additive Manufacturing and Its Societal Impact: A Literature Review, *Int J Adv Manuf Technol*, **2013**, 67, 1191–1203, https://doi.org/10.1007/s00170-012-4558-5.
43. Sterman, Y., Solav, D., Rosen, N., Saffuri, E., Shmilov Zaritsky, L., Custom Orthotic Insoles with Gradual Variable Stiffness Using 3D Printed Spacer Technique, *Virtual Phys Prototyping*, **2024**, 19, 1, e2336151, https://doi.org/10.1080/17452759.2024.2336151.
44. Desmyttere, G., Leteneur, S., Hajizadeh, M., Bleau, J., Begon, M., Effect of 3D Printed Foot Orthoses Stiffness and Design on Foot Kinematics and Plantar Pressures in Healthy People, *Gait Posture*, **2020**, 81, 247–253, https://doi.org/10.1016/j.gaitpost.2020.07.146.
45. Daryabor, A., Kobayashi, T., Saeedi, H., Lyons, S.M., Maeda, N., Naimi, S.S., Effect of 3D Printed Insoles for People with Flatfeet: A Systematic Review, *Assistive Technol*, **2023**, 35, 2, 169–179, https://doi.org/10.1080/10400435.2022.2105438.
46. Chhikara, K., Singh, G., Gupta, S., Chanda, A., Progress of Additive Manufacturing in Fabrication of Foot Orthoses for Diabetic Patients: A Review, *Ann 3D Print Med*, **2022**, 8, 100085, https://doi.org/10.1016/j.stlm.2022.100085.
47. Faustini, M.C., Neptune, R.R., Crawford, R.H., Stanhope, S.J., Manufacture of Passive Dynamic

Ankle–Foot Orthoses Using Selective Laser Sintering, *IEEE Trans Bio-Med Eng*, **2008**, 55, 2, 784–790, https://doi.org/10.1109/TBME.2007.912638.
48. Creylman, V., Muraru, L., Pallari, J., Vertommen, H., Peeraer, L., Gait Assessment during the Initial Fitting of Customized Selective Laser Sintering Ankle Foot Orthoses in Subjects with Drop Foot, *Prosthet Orthot Int*, **2013**, 37, 2, 132–138, https://doi.org/10.1177/0309364612451269.
49. Deckers, J.P., Vermandel, M., Geldhof, J., Vasiliauskaite, E., Forward, M., Plasschaert, F., Development and Clinical Evaluation of Laser-Sintered Ankle Foot Orthoses, *Plast, Rubber Compos*, **2018**, 47, 1, 42–46, https://doi.org/10.1080/14658011.2017.1413760.
50. Melchels, F.P.W., Feijen, J., Grijpma, D.W., A Review on Stereolithography and Its Applications in Biomedical Engineering, *Biomaterials*, **2010**, 31, 24, 6121–6130, https://doi.org/10.1016/j.biomaterials.2010.04.050.
51. Park, S.J., Lee, J.E., Lee, H.B., Park, J., Lee, N.-K., Son, Y., Park, S.H., 3D Printing of Bio-Based Polycarbonate and Its Potential Applications in Ecofriendly Indoor Manufacturing, *Addit Manuf*, **2020**, 31, 100974, https://doi.org/10.1016/j.addma.2019.100974.
52. Türk, D.-A., Einarsson, H., Lecomte, C., Meboldt, M., Design and Manufacturing of High-Performance Prostheses with Additive Manufacturing and Fiber-Reinforced Polymers, *Prod Eng*, **2018**, 12, 2, 203–213, https://doi.org/10.1007/s11740-018-0799-y.
53. Totah, D., Kovalenko, I., Saez, M., Barton, K., Manufacturing Choices for Ankle-Foot Orthoses: A Multi-Objective Optimization, *Procedia CIRP*, **2017**, 65, 145–150, https://doi.org/10.1016/j.procir.2017.04.014.
54. Cherni, Y., Desmyttere, G., Hajizadeh, M., Bleau, J., Mercier, C., Begon, M., Effect of 3D Printed Foot Orthoses Stiffness on Muscle Activity and Plantar Pressures in Individuals with Flexible Flatfeet: A Statistical Non-Parametric Mapping Study, *Clin Biomech*, **2022**, 92, 105553, https://doi.org/10.1016/j.clinbiomech.2021.105553.
55. Ho, M., Nguyen, J., Heales, L., Stanton, R., Kong, P.W., Kean, C., The Biomechanical Effects of 3D Printed and Traditionally Made Foot Orthoses in Individuals with Unilateral Plantar Fasciopathy and Flat Feet, *Gait Posture*, **2022**, 96, 257–264, https://doi.org/10.1016/j.gaitpost.2022.06.006.
56. Dijkshoorn, A., Werkman, P., Welleweerd, M., Wolterink, G., Eijking, B., Delamare, J., Sanders, R., Krijnen, G.J.M., Embedded Sensing: Integrating Sensors in 3-D Printed Structures, *J Sens Sens Syst*, **2018**, 7, 1, 169–181, https://doi.org/10.5194/jsss-7-169-2018.
57. Leal-Junior, A.G., Díaz, C.R., Marques, C., Pontes, M.J., Frizera, A., 3D-Printed POF Insole: Development and Applications of a Low-Cost, Highly Customizable Device for Plantar Pressure and Ground Reaction Forces Monitoring, *Opt Laser Technol*, **2019**, 116, 256–264, https://doi.org/10.1016/j.optlastec.2019.03.035.
58. Bolus, N.B., Ganti, V.G., Inan, O.T., A 3D-Printed, Adjustable-Stiffness Knee Brace with Embedded Magnetic Angle Sensor. In: *2018 40th Annual International Conference of the IEEE Engineering in Medicine and Biology Society (EMBC)*. IEEE, Honolulu, HI, **2018**, 1624–1627, https://doi.org/10.1109/EMBC.2018.8512600.
59. Graham, J., Wang, M., Frizzell, K., Watkins, C., Beredjiklian, P., Rivlin, M., Conventional vs 3-Dimensional Printed Cast Wear Comfort, *Hand*, **2020**, 15, 3, 388–392, https://doi.org/10.1177/1558944718795291.
60. Katt, B., Imbergamo, C., Seigerman, D., Rivlin, M., Beredjiklian, P.K., The Use of 3D Printed Customized Casts in Children with Upper Extremity Fractures: A Report of Two Cases, *Arch Bone Jt Surg*, **2020**, 9, 1, 126-130, https://doi.org/10.22038/abjs.2020.47722.2342.
61. Oud, T., Kerkum, Y., De Groot, P., Gijsbers, H., Nollet, F., Brehm, M.-A., Production Time and User Satisfaction of 3-Dimensional Printed Orthoses for Chronic Hand Conditions Compared with Conventional Orthoses: A Prospective Case Series, *J Rehabil Med Clin Commun*, **2021**, 4, 1–7, https://doi.org/10.2340/20030711-1000048.
62. Cady, R., Hennessey, T.A., Schwend, R.M., Section on Orthopaedics, Diagnosis and Treatment of Idiopathic Congenital Clubfoot, *Pediatrics*, **2022**, 149, 2, e2021055555, https://doi.org/10.1542/peds.2021-055555.
63. Ponseti, I.V., Treatment of Congenital Club Foot, *J Bone Joint Surg*, **1992**, 74, 3, 448–454, https://doi.org/10.2106/00004623-199274030-00021.
64. Qin, C., Luo, X., Yang, Y., Lun, Y., Yang, S., Chen, L., Therapeutic Outcomes of Customized 3D-Printed Ankle-Foot Orthoses in Children with Spastic Cerebral Palsy: A Case Series Study, *Front Pediatr*, **2025**, 13, 1661098, https://doi.org/10.3389/fped.2025.1661098.
65. Beldar, M.K., Ahuja, B.B., Chougule, N.K., Sahoo, K., Mohite, D.D., Design Improvements and Clinical Evaluation of an Adjustable Clubfoot Splint, *Sci Rep*, **2025**, 15, 1, 41946, https://doi.org/10.1038/s41598-025-25876-7.
66. Mosca, V.S., Flexible Flatfoot in Children and Adolescents, *J Child Orthop*, **2010**, 4, 2, 107–121, https://doi.org/10.1007/s11832-010-0239-9.
67. Vergillos Luna, M., Khal, A.-A., Milliken, K.A., Solla, F., Rampal, V., Pediatric Flatfoot: Is There a Need

for Surgical Referral?, *J Clin Med*, **2023**, 12, 11, 3809, https://doi.org/10.3390/jcm12113809.
68. Kardm, S.M., Alanazi, Z.A., Aldugman, T.A.S., Reddy, R.S., Gautam, A.P., Prevalence and Functional Impact of Flexible Flatfoot in School-Aged Children: A Cross-Sectional Clinical and Postural Assessment, *J Orthop Surg Res*, **2025**, 20, 1, 783, https://doi.org/10.1186/s13018-025-06207-y.
69. Kothari, A., Stebbins, J., Zavatsky, A.B., Theologis, T., Health-Related Quality of Life in Children with Flexible Flatfeet: A Cross-Sectional Study, *J Child Orthop*, **2014**, 8, 6, 489–496, https://doi.org/10.1007/s11832-014-0621-0.
70. Žukauskas, S., Barauskas, V., Degliūtė-Muller, R., Čekanauskas, E., Really Asymptomatic? Health-Related Quality of Life and Objective Clinical Foot Characteristics among 5–10-Year-Old Children with a Flexible FlatFoot, *J Clin Med*, **2023**, 12, 9, 3331, https://doi.org/10.3390/jcm12093331.
71. Liu, C., Zhang, H., Li, J., Li, S., Li, G., Jiang, X., The Effects of Foot Orthoses on Radiological Parameters and Pain in Children with Flexible Flat Feet: A Systematic Review and Meta-Analysis, *Front Pediatr*, **2024**, 12, 1388248, https://doi.org/10.3389/fped.2024.1388248.
72. Choi, J.Y., Hong, W.H., Suh, J.S., Han, J.H., Lee, D.J., Lee, Y.J., The Long-Term Structural Effect of Orthoses for Pediatric Flexible Flat Foot: A Systematic Review, *Foot Ankle Surg*, **2020**, 26, 2, 181–188, https://doi.org/10.1016/j.fas.2019.01.007.
73. Li, J., Yang, Z., Rai, S., Li, X., Jiang, G., Pan, X., Tang, X., Effect of Insoles Treatment on School-Age Children with Symptomatic Flexible Flatfoot: A 2-Year Follow-up Study, *Indian J Orthop*, **2022**, 56, 11, 1985–1991, https://doi.org/10.1007/s43465-022-00698-1.
74. Hu, S., Lin, Q., Qiu, L., Liu, Y., Guan, S., Luo, Z., Wang, Y., Wang, X., Effect of Orthotic Insole on Symptomatic Flexible Flatfoot in School-Age Children: Meta-Analysis and 1-Year Follow-up Study, *Biomed Technol*, **2024**, 7, 63–70, https://doi.org/10.1016/j.bmt.2024.08.001.
75. Lee, S.-W., Choi, J.-H., Kwon, H.-J., Song, K.-S., Effect of Pressure Based Customized 3-Dimensional Printing Insole in Pediatric Flexible Flat Foot Patients, *J Korean Foot Ankle Soc*, **2020**, 24, 3, 113–119, https://doi.org/10.14193/jkfas.2020.24.3.113.
76. Zhao, Y., Yan, S., Liu, M., Yang, L., Shi, B., Design and Validation of 3D Printed Orthotic Insoles for Children with Flatfoot, *Gait Posture*, **2023**, 106, S230–S231, https://doi.org/10.1016/j.gaitpost.2023.07.275.
77. Cheng, K.-W., Peng, Y., Chen, T.L.-W., Zhang, G., Cheung, J.C.-W., Lam, W.-K., Wong, D.W.C., Zhang, M., A Three-Dimensional Printed Foot Orthosis for Flexible Flatfoot: An Exploratory Biomechanical Study on Arch Support Reinforcement and Undercut, *Materials*, **2021**, 14, 18, 5297, https://doi.org/10.3390/ma14185297.
78. Atallah, H., Qufabz, T., Bakhsh, H.R., Ferriero, G., The Current State of 3D-Printed Orthoses Clinical Outcomes: A Systematic Review, *BMC Musculoskelet Disord*, **2025**, 26, 1, 822, https://doi.org/10.1186/s12891-025-09070-4.
79. Dailey, A.H., Landers, J., Anderson, S., Dillon, M.P., Exploring the Rationale for Prescribing Ankle–Foot Orthoses and Supramalleolar Orthoses in Children with Cerebral Palsy: A Narrative Synthesis of Rationale Statements, *Prosthet Orthot Int*, **2024**, 48, 3, 290–299, https://doi.org/10.1097/PXR.0000000000000282.
80. Firouzeh, P., Sonnenberg, L.K., Morris, C., Pritchard-Wiart, L., Ankle Foot Orthoses for Young Children with Cerebral Palsy: A Scoping Review, *Disabil Rehabil*, **2021**, 43, 5, 726–738, https://doi.org/10.1080/09638288.2019.1631394.
81. Meyns, P., Kerkum, Y.L., Brehm, M.A., Becher, J.G., Buizer, A.I., Harlaar, J., Ankle Foot Orthoses in Cerebral Palsy: Effects of Ankle Stiffness on Trunk Kinematics, Gait Stability and Energy Cost of Walking, *Eur J Paediatr Neurol*, **2020**, 26, 68–74, https://doi.org/10.1016/j.ejpn.2020.02.009.
82. Dobler, F., Cip, J., Lengnick, H., Alexander, N., Effects of Ankle-Foot Orthoses on Different Gait Patterns in Children with Spastic Cerebral Palsy: A Statistical Parametric Mapping Study, *Prosthet Orthot Int*, **2023**, 47, 5, 449–456, https://doi.org/10.1097/PXR.0000000000000216.
83. Kim, A., Frecklington, M., Philps, A., Stewart, S., The Effect of Ankle-Foot Orthoses on Gait Characteristics in People with Charcot-Marie-Tooth Disease: A Systematic Review and Meta-Analysis, *J Foot Ankle Res*, **2024**, 17, 3, e70003, https://doi.org/10.1002/jfa2.70003.
84. Mathewson, M.A., Lieber, R.L., Pathophysiology of Muscle Contractures in Cerebral Palsy, *Phys Med Rehabil Clin N Am*, **2015**, 26, 1, 57–67, https://doi.org/10.1016/j.pmr.2014.09.005.
85. Horsch, A., Klotz, M.C.M., Platzer, H., Seide, S., Zeaiter, N., Ghandour, M., Is the Prevalence of Equinus Foot in Cerebral Palsy Overestimated? Results from a Meta-Analysis of 4814 Feet, *J Clin Med*, **2021**, 10, 18, 4128, https://doi.org/10.3390/jcm10184128.
86. Smythe, T., Rotenberg, S., Lavy, C., Corrigendum for "the Global Birth Prevalence of Clubfoot: A Systematic Review and Meta-Analysis," *eClinicalMedicine*, **2025**, 80, 103087, https://doi.org/10.1016/j.eclinm.2025.103087.
87. Ponseti, I.V., Campos, J., Observations on Pathogenesis and Treatment of Congenital Clubfoot, *Clin Orthop*, **1972**, 84, 50–60, https://doi.org/10.1097/00003086-197205000-00011.

88. Ganesan, B., Luximon, A., Al-Jumaily, A., Balasankar, S.K., Naik, G.R., Ponseti Method in the Management of Clubfoot under 2 Years of Age: A Systematic Review, *PLOS One*, **2017**, 12, 6, e0178299, https://doi.org/10.1371/journal.pone.0178299.
89. Morcuende, J.A., Dolan, L.A., Dietz, F.R., Ponseti, I.V., Radical Reduction in the Rate of Extensive Corrective Surgery for Clubfoot Using the Ponseti Method, *Pediatrics*, **2004**, 113, 2, 376–380, https://doi.org/10.1542/peds.113.2.376.
90. Halanski, M.A., Davison, J.E., Huang, J.-C., Walker, C.G., Walsh, S.J., Crawford, H.A., Ponseti Method Compared with Surgical Treatment of Clubfoot: A Prospective Comparison, *J Bone Joint Surg*, **2010**, 92, 2, 270–278, https://doi.org/10.2106/JBJS.H.01560.
91. Dobbs, M.B., Rudzki, J.R., Purcell, D.B., Walton, T., Porter, K.R., Gurnett, C.A., Factors Predictive of Outcome after Use of the Ponseti Method for the Treatment of Idiopathic Clubfeet, *J Bone Joint Surg Am*, **2004**, 86, 1, 22–27, https://doi.org/10.2106/00004623-200401000-00005.
92. Colburn, M., Williams, M., Evaluation of the Treatment of Idiopathic Clubfoot by Using the Ponseti Method, *J Foot Ankle Surg*, **2003**, 42, 5, 259–267, https://doi.org/10.1016/S1067-2516(03)00312-0.
93. Sangiorgio, S.N., Ho, N.C., Morgan, R.D., Ebramzadeh, E., Zionts, L.E., The Objective Measurement of Brace-Use Adherence in the Treatment of Idiopathic Clubfoot, *J Bone Joint Surg*, **2016**, 98, 19, 1598–1605, https://doi.org/10.2106/JBJS.16.00170.
94. Griffiths, B., Silver, N., Granat, M.H., Lebel, E., Measuring Foot Abduction Brace Wear Time Using a Single 3-Axis Accelerometer, *Sens*, **2022**, 22, 7, 2433, https://doi.org/10.3390/s22072433.
95. Janicki, J.A., Wright, J.G., Weir, S., Narayanan, U.G., A Comparison of Ankle Foot Orthoses with Foot Abduction Orthoses to Prevent Recurrence Following Correction of Idiopathic Clubfoot by the Ponseti Method, *J Bone Joint Surg Br*, **2011**, 93-B, 5, 700–704, https://doi.org/10.1302/0301-620X.93B5.24883.
96. Garg, S., Porter, K., Improved Bracing Compliance in Children with Clubfeet Using a Dynamic Orthosis, *J Child Orthop*, **2009**, 3, 4, 271–276, https://doi.org/10.1007/s11832-009-0182-9.
97. Vishnu, V.S.A., Zacharia, T., Paul, L., Design and Development of Orthosis for Clubfoot Correction in Infants an Additive Manufacturing Approach, *Mater Today Proc*, **2020**, 27, 2605–2608, https://doi.org/10.1016/j.matpr.2019.11.073.
98. Aroojis, A., Pandey, T., Dusa, A., Krishnan, A.G., Ghyar, R., Ravi, B., Development of a Functional Prototype of a SMART (Sensor-Integrated for Monitoring and Remote Tracking) Foot Abduction Brace for Clubfoot Treatment: A Pre-Clinical Evaluation, *Int Orthop*, **2021**, 45, 9, 2401–2410, https://doi.org/10.1007/s00264-021-05042-0.
99. Molina-García, C., Banwell, G., Rodríguez-Blanque, R., Sánchez-García, J.C., Reinoso-Cobo, A., Cortés-Martín, J., Ramos-Petersen, L., Efficacy of Plantar Orthoses in Paediatric Flexible Flatfoot: A Five-Year Systematic Review, *Children*, **2023**, 10, 2, 371, https://doi.org/10.3390/children10020371.
100. Oerlemans, L.N.T., Peeters, C.M.M., Munnik-Hagewoud, R., Nijholt, I.M., Witlox, A., Verheyen, C.C.P.M., Foot Orthoses for Flexible Flatfeet in Children and Adults: A Systematic Review and Meta-Analysis of Patient-Reported Outcomes, *BMC Musculoskelet Disord*, **2023**, 24, 1, 16–28, https://doi.org/10.1186/s12891-022-06044-8.
101. Von Haller, M., Couchman, L., Honigmann, P., Economic Evaluation of the Manufacturing of 3D-Printed Wrist Orthoses vs Low Temperature Thermoplastic Wrist Orthoses, *3D Print Med*, **2025**, 11, 1, 35–43, https://doi.org/10.1186/s41205-025-00287-6.
102. Salazar, A., Rico, A., Rodríguez, J., Segurado Escudero, J., Seltzer, R., Martin De La Escalera Cutillas, F., Monotonic Loading and Fatigue Response of a Bio-Based Polyamide PA11 and a Petrol-Based Polyamide PA12 Manufactured by Selective Laser Sintering, *Eur Polym J*, **2014**, 59, 36–45, https://doi.org/10.1016/j.eurpolymj.2014.07.016.
103. Cano, A.J., Salazar, A., Rodríguez, J., Effect of Temperature on the Fracture Behavior of Polyamide 12 and Glass-Filled Polyamide 12 Processed by Selective Laser Sintering, *Eng Fract Mech*, **2018**, 203, 66–80, https://doi.org/10.1016/j.engfracmech.2018.07.035.
104. Patel, R., Desai, C., Kushwah, S., Mangrola, M.H., A Review Article on FDM Process Parameters in 3D Printing for Composite Materials, *Mater Today Proc*, **2022**, 60, 2162–2166, https://doi.org/10.1016/j.matpr.2022.02.385.

EUROPEAN RESEARCH AREA

COTANCE NEWSLETTERS

Starting with January 2019, the COTANCE Council has issued a monthly ***COTANCE Newsletter*** with the purpose of **promoting an improved image of leather** to relevant decision makers and domestic stakeholders including Members of the European and National Parliament, Governmental authorities, Ministerial officers, Customers of the leather industry, Brands, Retail chains, Relevant NGOs, Designers, etc. The monthly newsletters present topics that tell the truth about a controversial aspect or a fact that is not well known by the general public to bring about a better understanding of leather and the European leather industry, as well as a positive predisposition to legislate in favor of the leather industry. The newsletters are available in seven languages at https://www.euroleather.com/leather/newsletter, and were also published in the 2019-2024 issues of *Leather and Footwear Journal*.

NEWS 6/2025

The Unknown Part of Europe's Bioeconomy: Leather

Leather may be seen as one of the oldest materials known to humankind — but it proves, nature is always keeping surprises – so leather remains **one of the most innovative** and **one to be taken into account** in today's green transition. If we have to look at the price of leather we have to distinguish between inexpensive and cheap. Real Leather is not cheap, but it embodies the very principles of the **EU Bioeconomy**: circularity, sustainability, and durability.

Because leather is **inherently bio-based, circular, and biodegradable**, it deserves a **central place in Europe's Bioeconomy Strategy**, expected by the end of 2025, and in the forthcoming **EU Circular Economy Act**.

Why Leather Belongs in Europe's Bioeconomy

Image © Leatherbiz.com

Leather stands for:

- **Transform waste into value** — The tanning process upcycles by-products of the food and feed ecosystem that would otherwise become waste, transforming into raw material used to produce goods used in the fashion and lifestyle ecosystem.
- **Store carbon naturally** — keeping CO_2 locked within leather products throughout their - long lifespan.
- **Be repaired and renewed** — for leather there are already repair shops for footwear and leather goods, which allow us to keep products usable over decades.
- **Offer a natural end-of-life** — Leather is biodegradable under the right conditions.
- **Combine tradition and innovation** — The sector blends centuries of European savoir-faire with advanced technologies to enhance sustainability, traceability, and process efficiency – fully aligned with the EU's vision of a climate-neutral, resource-efficient economy.

COTANCE Position Statement on Bioeconomy

What to do for a Truly Circular Future

- Acknowledge and incentivise the use of **animal by-products** in EU bioeconomy and circular policies.
- **Fair and transparent labelling** to protect consumers from misleading claims such as "vegan leather."
- Include leather in **sustainable public procurement** frameworks to promote durable, renewable materials.

Support **R&D, innovation, and skills** to accelerate the green and digital transition of Europe's SMEs.

We call on Europe's Leather value chain and its partners:

Keep leading by example. Continue improving **tanning processes, finishing methods, and material traceability**.

Your innovation — from water reuse to bio-based chemicals and low-impact technologies — is what makes European leather the **gold standard of sustainability and craftsmanship**.

Stay proud, stay innovative, and keep proving that **tradition and technology can go hand in hand** in the green transition.

We call on Citizens and Consumers to:

Choose leather — not just because it's stylish, but because it's **natural, smart, sustainable, and built to last**.

Leather is a material that **ages beautifully, repairs easily, and returns safely to nature**.

By embracing leather in your everyday life — from footwear to furniture — you support European craftsmanship, circular economy, and a more responsible way of living.

Because Leather is not a material of the past

- it's a material for Europe's Future

edited by

COTANCE

In Collaboration with

VDL Verband der Deutschen Lederindustrie e.V.

CURTIDORES ESPAÑOLES
SPANISH TANNERS

A Manifesto for Leather on the Occasion of COP30:

Leather and the Measure of What Matters

In August of this year, UN negotiations once again failed to develop a landmark treaty to end plastic pollution. Insurmountable differences of opinion between those nations seeking reductions in plastic production and those in favour of increasing recycling resulted in yet another deadlock in discussions that have been taking place since 2022. As we see every year with the COP negotiations, resolving differences of opinion and achieving global consensus on how best to protect the planet and people is a huge challenge. A significant factor is the often opposing views of the negotiating parties and their presentation of the evidence given to support those views. The failure of the plastics treaty and the challenges of COP show us the same truth: sustainability debates are skewed by narratives and numbers that obscure reality.

This obfuscation has also blighted perceptions of leather. Leather, durable, repairable, and deeply woven into our cultural identity, is one of humanity's oldest materials. For millennia it has clothed, sheltered, and protected us. And yet, in today's sustainability discourse, leather is largely misunderstood—sometimes vilified, often mismeasured, and rarely recognised for what it truly is: a renewable, circular byproduct of livestock farming. This manifesto seeks to correct that imbalance and to position leather as a positive, renewable biomaterial within a circular economy

The story that is told about leather is distorted. It is often assumed that cattle exist only to produce hides, ignoring their status as a byproduct of the meat and dairy industries. In this sleight of hand, leather's role in creating value from what would otherwise be waste is erased. Leather is often conflated with industrial animal agriculture's impacts—deforestation, methane emissions, water use. Reports and headlines frame leather as a driver of environmental harm, but this is a distortion born of flawed accounting.

Cattle are not raised for hides. They are raised primarily for meat and milk. Hides represent only a small fraction of the animal's economic value; on average, only 1.5%. However, current Life Cycle Assessments (LCA) typically assign disproportionate emissions to hides and the resulting leather. This flawed methodology makes leather appear environmentally costly when, in fact, it is part of a circular system that valorises what would otherwise be waste. Each year millions of hides go unused—discarded into landfills or incinerated—precisely because of reduced demand for leather. To abandon leather is not to save a cow. It is to squander a durable, repairable material and replace it with synthetics derived entirely from fossil fuels.

The reality is that leather, when responsibly tanned, is a natural, renewable biomaterial with an unparalleled lifespan. A well-made leather product lasts decades, is repairable and biodegradable in ways other materials cannot emulate. Leather bridges utility and heritage: a boot that wears in, not out; a bag that can be passed down, not thrown away.

To treat leather as a sustainable material is not to deny its origin in livestock farming, but to recognise that, as long as meat and dairy are produced, hides will exist. The choice is not between leather and no leather but between using hides responsibly or wasting them and replacing them with fossil-based substitutes.

Leather embodies the principles of circularity. Leather extends the value of existing resources, prevents waste, stores carbon and offers durability that reduces consumption over time. Unlike

synthetics, it develops character through age, repair, and reuse. Unlike plastics, it returns to the earth when its life is done.

Moreover, the value of leather is cultural as much as material. It carries histories of craft, artistry, and longevity. It resists the throwaway culture that plastics fuel. In a world awash with fast fashion and disposable products, leather reminds us that quality, function, beauty and respect for resources are still all an option.

Therefore, we, the undersigned organisations, again request the COP to endorse our call to:

- Recognise the cyclical, climate efficient nature of leather and its potential for a positive contribution to reducing the climate impacts of consumer products. In particular, a full and proper impact assessment of the unevidenced claim that leather is a driver of deforestation and the development of reliable measures of the lifespan of materials and products and their impact on consumption are required.
- Support LCA methodologies that accurately account for the environmental impact of all materials, in particular when by-products are compared to determining products, including end of life properties and the consequences of use and substitution.
- In keeping with the aspiration for reduced consumption, greater circularity and reduced waste, to promote ‘slow fashion’, durable bio-based materials and products, and items that can be used many times, repaired and refurbished, and last for years.
- Wherever feasible to encourage the use of natural renewable fibres like leather and reduce unnecessary reliance on fossil-fuel-based materials.

Signatories to the Leather Manifesto

- Alliance France du Cuir (AFC)
- American Leather Chemists Association (ALCA)
- Associação Portuguesa dos Industriais de Curtumes (APIC)
- Association pour l’Assurance Qualité des Fabricants de Bracelets Cuir (AQC)
- Australian Hide Skin and Leather Exporters' Association Inc (ASHLEA)
- Centre for the Brazilian Tanning Industry (CICB)
- Centro Tecnológico das Indústrias do Couro (CTIC)
- Confederation of National Associations of Tanners and Dressers of the European Community (COTANCE)
- Chamber of the Tannery Industry of the State of Guanajuato (CICUR)
- China Leather Industry Association (CLIA)
- Fédération Française des Cuirs et Peaux (FFCP)
- Fédération Française Tannerie Megisserie (FFTM)
- International Council of Hides, Skins and Leather Traders Association (ICSHLTA)
- International Council of Tanners (ICT)
- Is It Leather? (IIL)
- International Union of Leather Technologists and Chemists Societies (IULTCS)
- Leather & Hide Council of America (LHCA)
- Leather Naturally (LN)
- Leather UK (LUK)
- One 4 Leather (O4L)
- Sustainable Leather Foundation (SLF)
- Türkiye Deri Sanayicileri Derneği (TDSD)
- Verband der Deutschen Lederindustrie e.V. (VDL)
- Wirtschaftsverband Häute/Leder (WHL)
- Zimbabwe Leather Development Council (ZLDC)

IULTCS NEWSLETTER

Newsleather

Stay curious, informed and connected

Edition 11, 2025

Welcome

This is the eleventh edition of our scientific newsletter, dedicated to providing the latest updates on research, regulatory developments, technology, and standard methods in the leather industry.

NOTE: This newsletter is in English, Spanish and Portuguese. One version after the other. [LFJ Editor's note: For other language versions please visit www.iultcs.org].

In this issue, we feature an interview with Dr. Kalarical J. Sreeram, a scientist, Director of the Central Leather Research Institute (CLRI), a constituent of the Council of Scientific and Industrial Research (CSIR) in Chennai, India.

IULTCS values its collaboration with Dr. Sreeram, an active member, academic, and Director of CLRI. He leads the institute's efforts in advancing leather science and technology, emphasizing sustainability, innovation, and industry partnerships.

We appreciate Dr. Sreeram's collaboration with IULTCS Newsleather.

Please share your comments and suggestions to secretary@iultcs.org

Kind regards,
Dr. Luis A. Zugno, editor

IULTCS INTERVIEW

Lifeline: Dr. Kalarical J. Sreeram
Director of CSIR-CLRI in Chennai, India

Dr. Sreeram holds a doctorate in leather technology and is focused on environmental sustainability in the leather industry. Since joining CSIR-CLRI in 2002, he has advanced to Chief Scientist and then Director, developing formaldehyde-free fillers and chromium (VI) solutions. Under his leadership, CSIR-CLRI established India's footwear sizing standard and created specialized extreme cold leather gloves. He has over 120 publications, an h-index of 28, and 20 patents, receiving numerous awards such as the CSIR Young Scientist Award and IUR Research Project Plan Certificate of Approval of IULTCS in 2013. Currently, he is the Mission Director for the Waste to Wealth Mission of CSIR and heads the Department of Leather Technology at Anna University.

The CLRI is a constituent laboratory of CSIR. It was established in 1948 and is in Adyar, Chennai. The main area of work is Leather science and technology. Conducts R&D in leather processing, tanning, footwear design, and environmental sustainability. Also offers academic programs in collaboration with Anna University (B.Tech, M.Tech, Ph.D., etc.). https://www.clri.res.in/

IULTCS Question 1: Dr. Sreeram, could you briefly outline CLRI's history and explain why it was established in Chennai?

The Central Leather Research Institute was established in 1948, shortly after India's independence, with the vision that industrial research in leather could serve as a catalyst for social empowerment. This initiative likely drew inspiration from Mahatma Gandhi's 1934 statement highlighting the economic drains associated with the export of raw hides and the need for local expertise in leather processing.

In a 1945 lecture, Prof. BM Das (Superintendent, Bengal Tanning Institute), emphasized the importance of the leather industry and the urgent need for research to enhance its efficiency. His insights, along with a proposal by Dr. Sir A. Lakshmanaswami Mudaliar, the Vice Chancellor of the University of Madras, led to the establishment of the Leather Research Institute. The Government of Madras recognized the significance of these proposals and transferred land to the Ministry of Industry to support the institute's creation at the National level.

Entrusted to the Council for Scientific & Industrial Research, with Prof. BM Das as the first Director, the institute was strategically located to connect academia with a thriving industry. This collaboration has proven successful, transforming the Indian leather sector from mere trading into a robust manufacturing hub for quality leather and leather products. Today, the institute stands as a model of innovation and development within the industry.

Figure 1: Overview of the CLRI building with the India's flag colors effect

IULTCS Question 2: CLRI has a strong team of Analytical Chemistry. Please give us an overview of the analytical capabilities applied to leather.

From its inception, our institute has recognized that leather processing is inherently multidisciplinary. We have brought together experts from various fields, including biologists, chemists, engineers, and technologists, to foster a comprehensive approach. Our analytical chemists have played a crucial role in supporting the industry by developing innovative analytical tools aimed at estimating restricted substances and creating newer methods for the determination and regulation of harmful substances.

Additionally, our work on FT-IR based identification of leather materials versus synthetics is paving the way towards the implementation of an India Leather Mark, enhancing quality assurance in the industry. Today, we take pride in our testing wing, the Centre for Analysis, Testing, Evaluation and Reporting Services (CATERS), which is accredited under ISO 17025:2017 by National Accreditation Board for Testing and Calibration Laboratories (NABL), India. Our scope includes over 150 methods related to the testing of Restricted Substances List (RSLs), ensuring our commitment to quality and safety in leather processing continues to be robust and forward-thinking.

IULTCS Question 3: Please give us an update on the work being developed by the Analytical team on method development for regulatory compliance, with examples.

CSIR-CLRI also holds the Chairmanship of the Chemical Division 17 (CHD17) of Bureau of Indian Standards (BIS), which is responsible for bringing out national test methods and standards. The BIS is also the secretariat for ISO TC 120, which brings out international test methods and standards in association with IULTCS. Either by adopting the ISO methods or where needed developing our own methods, the institute has contributed significantly to developing methods for regulatory compliance.

In the 1980s, we were pioneers in establishing protocols for the determination of pentachlorophenol, and in the 1990s, we focused our efforts on azo compounds, with our methods being validated against the German methods. One of our landmark contributions was the development of a new methodology for the unequivocal determination of chromium (VI) through chromatography. Most recently, we introduced a streamlined method for determining hydroxyproline content in leather, which simplifies earlier, more cumbersome procedures.

Figure 2: CLRI-Centre for Analysis, Testing, Evaluation and Reporting Services (CLRI-CATERS)

IULTCS Question 4: CLRI also develops new technologies. Please give us an update on the new developments in leather technology and science.

One of the significant contributions of CSIR-CLRI has been the IUE Guidelines for Best Practices in Sustainable Leather Manufacturing. At the beginning of this millennium, the institute aimed to initiate a paradigm shift from chemical processes to bioprocessing in leather production by introducing enzymes for fiber opening and unhairing. Our research on cyclic tetrameric species found in wastewater after chrome tanning led to the development of high-exhaust basic chromium sulfate.

Today, by utilizing the inherent water present in the leather, we have developed a waterless chrome tanning technology that has been adopted by approximately 180 tanneries in India and

abroad (Patent EP3430174B1). Our focus on making the leather industry more environmentally friendly has resulted in simpler technologies that reduce emissions and add value to waste materials.

In terms of process technologies, one of our major contributions has been the effective use of goat skins and buffalo hides available in India for high-value leather applications. We have developed a method for creating leather for gloves that can withstand extremely cold climatic conditions.

IULTCS Question 5: What research and development areas are CLRI currently pursuing in biotechnology, environmental science, life cycle assessment (LCA), and sustainability?

The institute is actively working on a comprehensive examination of the carbon footprint associated with both conventional and innovative leather processing technologies. Our goal is to achieve a zero-carbon footprint from gate to gate of leather production by adopting two key concepts: cleaner processing and value addition to solid wastes.

One of our recent projects, which has garnered significant attention, involves the preparation of protein syntans as well as those combined with phenol, melamine, or acrylates from chrome shavings. This innovative approach not only contributes to waste reduction but also enhances the value of by-products in the leather manufacturing process.

On the circularity front, we have successfully implemented zero liquid discharge systems across Tamil Nadu, India. Collaborating with our sister laboratory, CSIR-CSMCRI, we have transformed sodium chloride from the reverse osmosis rejects of our Common Effluent Treatment Plants into high-purity salt suitable for the chloralkaline industry. Additionally, we have repurposed black liquor from the paper and pulp industry, which contains degraded lignin, into retanning agents for leather production.

In the realm of biotechnology, our researchers are exploring the creation of collagen-like peptides with the potential for developing leather-like materials from these assembled peptide structures. This groundbreaking concept, reminiscent of producing skin in a laboratory setting, holds promise for applications beyond leather, particularly in biomedical fields. Furthermore, we are investigating the conversion of unused hides/skin components into collagen hydrolysates and gelatin, which could find uses in packaging, cosmetics, and potentially in the future, biomedical scaffolds. Through these diverse and innovative research endeavors, we aim to pave the way for a sustainable and eco-friendly leather industry while advancing scientific knowledge and applications across various sectors.

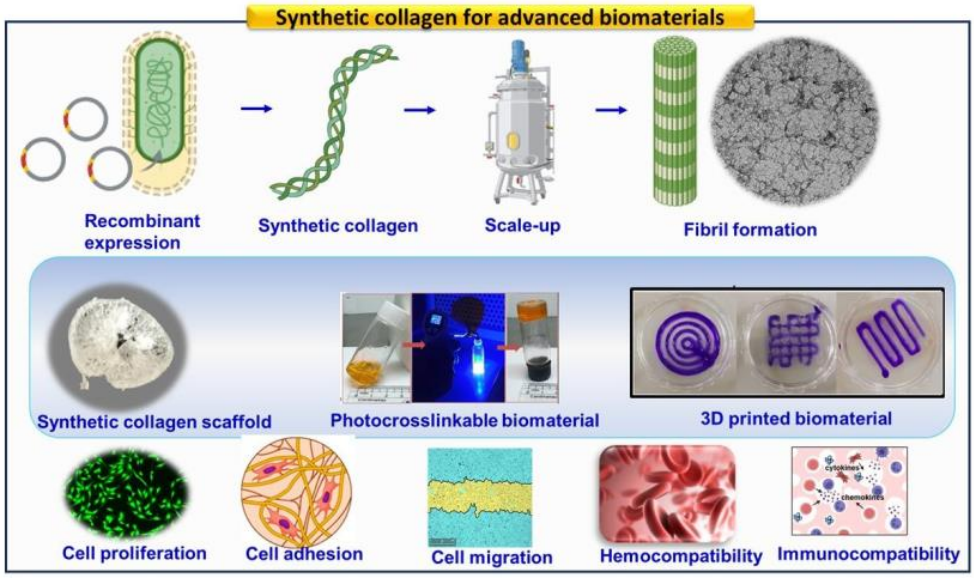

Figure 3: Developing synthetic collagen with multiple applications

IULTCS Question 6: CLRI also collaborates with Anna University and the University of Madras. Please give us an overview of the Bachelor, Master and PhD programs.

Our institute is dedicated to shaping the future of leather and footwear science, offering a robust educational framework for aspiring professionals in the industry. The leather education at Chennai dates back to 1945 and the presence of the university and the institute as adjoining campuses provides a strong academy – research collaboration.

Currently, we offer Bachelor of Technology (B.Tech), Master of Technology (M.Tech), and Ph.D. programs in leather and footwear science, with our esteemed scientists serving as honorary professors at Anna University. Admissions, along with foundational courses in chemistry, physics, biotechnology, and engineering, are managed by the university, while we specialize in leather-related subjects.

In a significant enhancement to our curriculum, B.Tech students can now tailor their educational journey by selecting from various specializations. Options include: a) Leather Science: Prepare for advanced studies with pathways to Master's and Doctorate degrees in leather science, b) Footwear Science: Equip yourself for careers in the footwear industry, c) International Affairs and Marketing: Gain insights into the global leather business landscape, and d) Environmental Management: Learn sustainable practices and waste management to promote circularity in the industry.

For our M.Tech (Leather & Footwear) Program, we welcome undergraduates with degrees in leather, chemistry, mechanical engineering, and production engineering, offering them a chance to deepen their expertise. We are proud to report an impressive 100% campus placement rate for our B.Tech graduates, along with various scholarship opportunities available.

Additionally, our institute is collaborating with the Government College of Engineering and Leather Technology in Kolkata and Harcourt Butler Technological University in Kanpur to provide guest lectures that enhance their curriculum. We have also fine-tuned educational programs for universities in Addis Ababa, demonstrating our commitment to global collaboration.

As we look to the future, our vision is clear: to establish our institute as the premier educational hub for leather science worldwide. We would be happy to explore potential collaborations with the International Union of Leather Technologists and Chemists (IULTCS) and its member bodies to advance this goal.

Figure 4: Interaction with young administrators to appraise them of relevance of leather trade for employment and exports

IULTCS Question 7: A noted challenge for the leather industry globally is the shortage of professionals with formal education in leather technology. How many individuals graduated in leather-related fields in Chennai in 2024?

The global challenge of a shortage of professionals with formal education in leather technology is, in my opinion, a significant reason for the misinformation and negative publicity attributed to our sector. In response, our institute has been making efforts to develop the next generation of professionals who will advance the industry in a professional manner.

Through our B.Tech program in collaboration with Anna University, we have an intake of 60 students each year. This four-year program produces 60 graduates in leather technology annually. After accounting for about 20 students who choose other career paths, approximately 40 undergraduates are available to enter the leather industry. Additionally, there are usually 3 to 5 graduates at the postgraduate level specializing in leather chemicals and the leather and footwear industries.

We also offer a Post Graduate Diploma in leather processing and lifestyle accessories through Academy of Scientific and Innovative Research (AcSIR), designed for individuals from various educational backgrounds who aspire to pursue a career in the leather industry. This course is particularly popular among industry leaders who want to prepare their next generation as professionals before they take over the reins of the business.

In addition to these programs, we conduct tailor-made certificate courses, executive training programs, and diplomas tailored to industry needs. One of our newer initiatives aims to enhance professionalism in the sector by offering customized upskilling programs for existing employees, which is gaining popularity within the industry.

IULTCS Question 8: Is CLRI currently working on projects to replace chrome tanning for compostable leather?

To some extent, we at the institute still believe that chromium is not a significant culprit if managed properly. This belief is based on fundamental studies we conducted about three decades ago regarding the oxidation states of chromium and its role in apoptosis and necrosis. However, the scarcity of chromite ores available for developing chromium-based tanning agents is one reason we are exploring alternatives beyond chromium. We are looking forward to launching chromium-free silicate gels as a substitute for chromium tanning. Additionally, we are collaborating with industries such as tea, cashew nut, and areca nut to develop tannins that can be used for tanning while remaining outside the scope of the European Union Deforestation Regulation (EUDR).

IULTCS Question 9: What information or guidance would you like to share with young IULTCS members regarding leather education, leather science, and applied technology?

Many of us, including myself, entered this sector without a clear understanding of what leather science entails. However, as we delve deeper into the world of leather, the skin, and the remarkable protein collagen, we become increasingly passionate about it. Leather offers opportunities for every branch of science to contribute meaningfully. What we need is a mindset that appreciates high-quality leather.

Every young professional in this sector can take pride in our efforts to ensure a sustainable future by transforming waste from the meat industry into a valuable product. We should ask ourselves: if leather production did not exist, what cleaner alternatives would we have for covering our feet?

It is essential for universities near tannery clusters to at least offer elective courses on leather making, as it serves as a tangible example of chemistry and biology in action. If we could redefine leather education from being process-oriented to focusing on achieving specific properties of end products, and understanding the chemistry involved in treating collagen fiber bundles, courses would become far more engaging and appealing.

To move forward, I believe we should establish a leather education hub led by the IULTCS, in collaboration with institutions like mine and the industry, to develop a global curriculum. Additionally, we might consider offering a course on how leather contributes to social upliftment and environmental protection for students of mass communication and journalism.

Though a little unconnected with the topic, CSIR-CLRI now organizes institutional visits for school and college students, programs such as one day as a scientist and open house for the public to understand and appreciate leather as a material for lifestyle commodities. Our effort to hold leather product sales by brands that have been created by our alumni in the institute premises have been well received by the local community. In essence, not only should we learn to appreciate leather, we need to educate others to do the same.

Figure 5: Empowering Women through Leather: Training Program for Rural Women

IULTCS Question 10: In your opinion how the leather education and leather production will evolve in India on the next 10 years?

Though a topic that could create a storm in many minds, I am strong believer that we only have that much raw material globally that we can cater to niche products. As per the statistics available to me, we do not have enough hides/skins to cover every foot in the world with a pair of shoes, which then opens up scope for nonleather materials to come into the footwear sector. The future leather industry needs to articulate the leather properties very well and occupy those niche segments that other fabrics may not be able to in the recent future, such as automotive leathers. Thus, moving of leather industry towards a niche lifestyle commodity manufacturer is inevitable, and we would have to take other fabrics along as partners in the journey, rather than as competitors.

The industrial segment in India would be prominently occupied by those who can make sufficient profits from their leather and product trade that they can not only make niche leather but also manage the environmental aspects of the trade.

IULTCS NEWSLETTER

Newsleather

Stay curious, informed and connected

Edition 12, 2025

Welcome

This is the twelfth edition of our scientific newsletter, dedicated to providing the latest updates on research, regulatory developments, technology, and standard methods in the leather industry.

NOTE: This newsletter is in English, Spanish, Portuguese and Turkish. One version after the other. [LFJ Editor's note: For other language versions please visit www.iultcs.org].

In this issue, we feature an interview with Dr. Wen Huitao, R&D Director of Xingye Leather Technology Co., Ltd. (referred as Xingye), located in Jinjiang City, Fujian Province, China.

IULTCS appreciates working with Dr. Huitao, CLIA member and Xingye's R&D Director, who drives the tannery's progress in sustainable, innovative leather science and technology.

We extend our sincere thanks to Dr. Huitao for his valuable contributions to IULTCS Newsleather.

Please share your comments and suggestions to secretary@iultcs.org

Subscribe to the Newsleather here: https://bit.ly/3NsXNeL

Kind regards,
Dr. Luis A. Zugno, editor

IULTCS INTERVIEW

Lifeline: Dr. Wen Huitao
R&D Director of Xingye, Jinjiang City, Fujian Province, China

Dr. Wen Huitao holds a doctoral degree in Leather Chemistry and Engineering from Sichuan University and is a senior engineer and innovation engineer.

He began his career in 2003 and joined Xingye in 2013, where he is in charge of technology research and innovation management. He has developed a series of new technologies for multifunctional high-performance ecological leather and enabling the resource utilization of leather waste. He has obtained more than 80 patents in leather field.

KINGYE TECHNOLOGY
兴业科技

In this period, the National Enterprise Technology Center and the Provincial-level Key Laboratory were established. Currently, he is the person in charge of these innovative platforms.

Xingye is one of the leading enterprises in China's tanning industry; recognized as one of the China Top 500 Private Enterprises and 100 Key Industrial Enterprises in Fujian Province. The company engaged in mid-to-high-end full-grain leather and has established a product layout with three main series of Nappa, natural milled

and special effect leather, which are widely used in such areas as footwear, furniture, automotive, bags and suitcases, etc. https://www.xingyeleather.com/en/

IULTCS Question 1: Dr. Huitao, please tell us a brief history of the Xingye tannery, telling us why it was founded and why in Fujian.

Xingye Leather, founded in 1992 in Jinjiang, Fujian, initially focused on premium cowhide processing for China's footwear industry, leveraging coastal ports for raw material imports. By the 2000s, it adopted eco-friendly tanning to meet EU standards, attracting global clients like Nike and Adidas, while listing on the Shenzhen Stock Exchange in 2012 to fund R&D and automation. Expanding into automotive leather and functional materials, the company later pioneered zero-waste production (95% byproduct recycling) and AI-driven quality control, earning titles like National Green Factory (2020). Today, it produces over 150 million square feet of leather annually for 500+ brands across 40 countries, blending sustainability with innovation to lead China's shift to high-value manufacturing.

Figure 1: Main building of Xingye Leather

IULTCS Question 2: Please give us an overview of the production today, indicating the types of leather produced (% of each type), and the percentage of leather produced from raw, and percentage bought as wet blue. If possible, indicate the source of wet blue purchased.

Xingye focuses on middle and high-end full-grain cow leather. So far it has three wellknown lines in Nappa leather, natural milled leather, and special effect leather, which are widely used in the fields of shoes, bags, and belts (70%), automotive interiors (25%), and others such as furniture (5%). Xingye has an annual production capacity of over 150 million square feet of finished leather, 90% of which are processed from raw hides, and 10 % are processed from wet blue. The raw hides of cattle are mainly sourced from the United States, Europe, Brazil, and other countries.

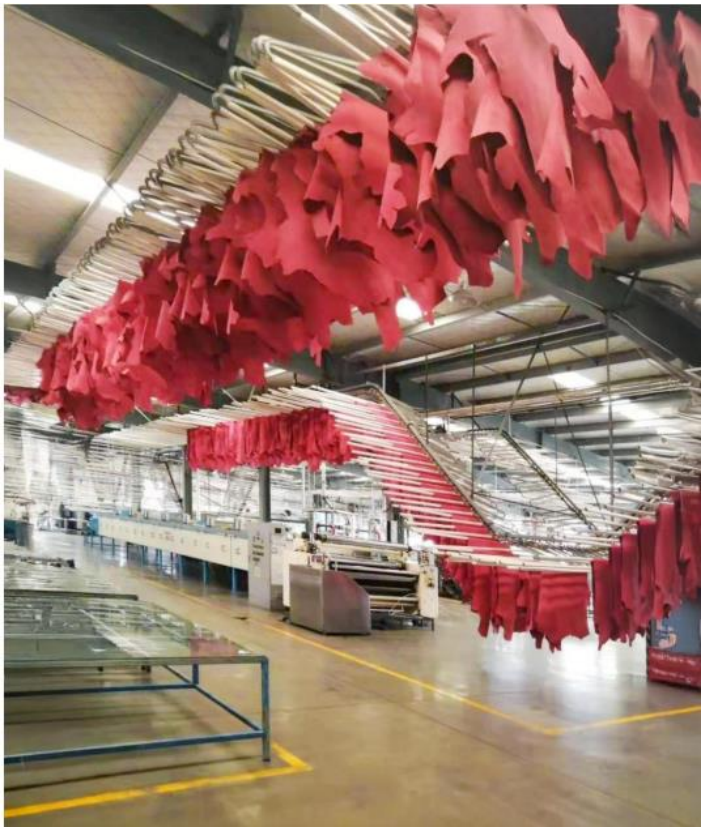

Figure 2: Detail of the air-drying racks in the tannery

IULTCS Question 3: Please give us an overview of the series of R&D laboratories indicating the type of capabilities of each lab and staffing.

Xingye Leather's series of laboratories include the National Technology Center, the Provincial Key Laboratory, the Postdoctoral Workstation, and the Testing Laboratory, and each equipped with one supervisor and several technical personnel. The technology center focuses on technology research and development, and the staff are grouped according to process modules (tanning group, dyeing and finishing group, coating group, etc.), and each group is equipped with engineers and technicians, and focuses on solving practical problems. The Provincial Key Laboratory focuses on basic research, such as tanning mechanism research, with research personnel and senior technicians. The Postdoctoral Workstation is positioned for cutting-edge research, such as exploring disruptive technologies such as intelligent leather (such as shoe upper leather embedded with flexible sensors) and bio-based materials. The Testing Laboratory is responsible for product performance testing, implementing international standards (ISO, ASTM) certification, covering physical properties (wear resistance, tensile strength), chemical safety (VOCs, formaldehyde), and functional testing (waterproof, antibacterial), and is composed of professional testing personnel.

The research achievements of provincial key laboratories and postdoctoral workstations (such as new tanning agents) are evaluated by the technical committee and transferred to the technical center for pilot testing. The performance is confirmed by the testing center, forming a closed loop of "basic research technology development product verification".

IULTCS Question 4: Xingye has 98 invention patents. Please give us an overview of the types of patents you have and how many are being used in your manufacturing industry today.

Xingye Leather’s 98 invention patents are systematically categorized into four strategic fields, reflecting its R&D priorities in sustainability, quality, functionality, and circular economy. Approximately 75% (73 patents) are actively integrated into manufacturing processes, while the remaining 25% (25 patents) support long-term innovation pipelines or strategic IP reserves.

Figure 3: Overview of one of the analytical labs at Xingye

IULTCS Question 5: Please describe your process of water reuse rate above 50% by using Multi Medium Technology, Ultrafiltration and Reverse Osmosis.

Xingye Leather attaches great importance to water conservation, emission reduction, and circular utilization. Based on the selection of water-saving processes and waste liquid recovery (Soaking, Liming, Tanning), advanced technologies such as ultrafiltration and reverse osmosis membrane treatment are utilized to establish a reclaimed water reuse system, achieving a reclaimed water reuse rate of over 50%.

(1) A multi-media filter is installed at the drainage inlet of the existing biochemical treatment system. The multi-media filter adopts a carbon steel lined rubber tank body, in which different filtering materials such as pebbles and quartz sand are placed in layers. When wastewater passes through the filter material, impurities such as colloids, sediment substances, and bacterial colonies remaining during the biochemical precipitation process are intercepted through collision and adhesion on the surface of the filter material, forming a filter cake layer that facilitates their removal.

(2) The fully automatic ultrafiltration system operates in full capacity filtration mode, and all produced water enters the ultrafiltration water tank. The fine colloidal pollutants contained in the wastewater are trapped on the outer surface of the membrane fibers. A filter bag type safety filter is installed before the ultrafiltration system enters the membrane to intercept large residual floating debris, permeable filter materials, and other impurities that may remain during the pretreatment process, preventing these impurities from damaging the membrane layer.

(3) The reverse osmosis system also adopts fully automatic control, filters the produced water, adds chemicals, shuts down for flushing, and performs online CIP cleaning according to the program. The regenerated water obtained after the above process can be reused in the production process.

Figure 4: Detail of the ultrafiltration equipment

IULTCS Question 6: Xingye has developed a "sulfur free hair saving unhairing technology". Please comment on this technology, as it is important for the IULTCS community.

"The high pH sulfur free hair removal technology based on composite enzymes" developed by Xingye Leather adopts a composite system of alkaline protease and keratinase. The former hydrolyzes collagen in the hair follicle basement membrane, while the latter specifically degrades keratin in the hair root sheath. Through enzymatic coordination, selective hair removal and broad-spectrum adaptability are achieved. By using a high pH to enhance enzyme activity and expand hair follicles, the penetration of enzyme molecules is accelerated, and the hair removal rate is improved. Through the collaborative innovation of complex enzymes and a high pH environment, sulfide pollution caused by hair removal can be eliminated from the source.

Sulfide wastewater needs to be treated separately, while sulfur free wastewater is treated as general wastewater, reducing treatment costs; At the same time, the COD/BOD load of the wastewater decreases, reducing the amount of sludge generated, which meets the emission reduction requirements under the global "dual carbon" target.

Due to the difficulty in controlling the enzymatic hair removal process, it has not yet been widely used. However, it is believed that with the application of intelligent equipment and artificial intelligence, the control of enzymatic hair removal will no longer be a problem, and it is expected to be widely used at that time.

IULTCS Question 7: For the IULTCS members it will be valuable if you can explain the policy of five-water separation and treatment.

Five-water separation and treatment refer to the separate collection and treatment of chromium containing wastewater, sulfur-containing wastewater, other production wastewater, domestic sewage, and rainwater generated during the leather making process by Xingye Leather. For example, chromium containing wastewater and sulfurcontaining wastewater are treated with dechroming and desulfurization respectively, then separately recycled. Other wastewater production and domestic sewage are treated through a comprehensive wastewater treatment system. After separate collection, rainwater is discharged into the urban rainwater pipe network. Separate treatment can not only reduce the amount of wastewater treatment, but also recycle it through professional methods, which has better economic efficiency.

IULTCS Question 8: How do you characterize the "Ecological Tanning Technology?". Which parameters are measured to compare with regular leather? Please indicate comparative values.

Ecological Tanning Technology, or Ecological Leather-making, means the leathermaking process is more ecological and has a reduced impact on the environment. For example, using leather chemical materials from natural products with low chromium, sulfur, and organic solvents can reduce carbon emissions during the leather-making process by more than 20%. Leather made in this

way has low contents of heavy metals and volatile organic compounds. Our objective is to eliminate harmful substances from the leather-making process and to guarantee that finished leather products are free from materials that could pose risks to human health. Despite market and customer challenges, we remain committed to achieving our goals.

IULTCS Question 9: On leather waste resource utilization technologies, please give more details on the utilization of solid waste in tanning.

Leather solid waste includes chromium-free solid waste such as cow hair, meat residue, and scraps, chromium containing solid waste such as shavings, grinding ash, and scraps, as well as chromium containing sludge obtained from the treatment of chromium containing wastewater. Solid waste without chromium is relatively easy to handle, and proteins can be extracted through physical or chemical methods for industrial products such as feed, fertilizers, adsorbent materials, functional fillers, etc. Solid waste containing chromium is relatively difficult to treat, and can be processed into regenerated leather through defibrillation, chromium can be recovered through dechroming, or heat can be obtained through incineration. Leather sludge is treated harmlessly by third-party institutions.

IULTCS Question 10: Dr. Huitao, you mentioned that the Provincial Key Laboratory focuses on basic research, such as tanning mechanism research. Please give us an overview of the work being done by this group.

At present, our laboratory is conducting research and development on ecological leather, such as attempting to use all natural materials instead of chemical products from petroleum, to produce fully natural leather. We are also researching functional leather products, with the latest research focusing on developing leather products that can be used as skin for human walking robots, in order to give future home robots a better appearance. In terms of waste resource utilization, we have attempted to introduce special equipment such as subcritical and microwave, as well as graphene and nanomaterials, in order to explore better resource utilization methods. The goal of the laboratory is to hope that leather can achieve better development and have a better future.

INSTRUCTIONS FOR AUTHORS

Publication Ethics and Malpractice Statement

Leather and Footwear Journal publishes articles reviewed by two independent reviewers selected by the Editorial Board. The Publication Ethics and Malpractice Statement for *Leather and Footwear Journal*, based on COPE's Best Practice Guidelines for Journal Editors, clearly outlines standards of expected ethical behavior for all parties involved in the act of publishing (the author, the journal editor(s), the peer reviewer and the publisher) and is available on the journal's website, https://www.revistapielarieincaltaminte.ro.

Open Access Statement

Leather and Footwear Journal is a peer reviewed, open access journal. All articles published open access will be immediately and permanently free for everyone to read, download, copy and distribute, under the provisions of a Creative Commons Attribution (CC BY) which lets others distribute and copy the article, create extracts, abstracts, and other revised versions, adaptations or derivative works of or from an article (such as a translation), include in a collective work (such as an anthology), text or data mine the article, even for commercial purposes, as long as they credit the author(s), do not represent the author as endorsing their adaptation of the article, and do not modify the article in such a way as to damage the author's honor or reputation.

Open Access Publication Fee

Leather and Footwear Journal requires article processing charges of 200 EURO per article, for accepted manuscripts, payable by the author to cover the costs associated with publication. There are no submission charges.

Author Rights

The copyright for all articles published in *Leather and Footwear Journal* shall remain the property of the author(s). The copyright on the layout and final design of the articles published in *Leather and Footwear Journal* belongs to INCDTP – Division: Leather and Footwear Research Institute and cannot be used in other publications.

Presentation of Papers

The scientific papers should be presented for publishing in English only. The text of the article should be clear and precise, as short as possible to make it understandable. As a rule, the paper should not exceed fifteen pages, including figures, drawings and tables. The paper should be divided into heads and chapters in a logical sequence. Manuscripts must meet high scientific and technical standards. All manuscripts must be typewritten using MS Office facilities, single spaced on white A4 standard paper (210 x 297 mm) in 11-point Times New Roman (TNR) font.

Paper Format

Title. Title (Centered, 12 pt. TNR font) should be short and informative. It should describe the contents fully but concisely without the use of abbreviations.
Authors. The complete, unabbreviated names should be given (Centered, 10 pt. TNR font), along with the affiliation (institution), city, country and email address (Centered, 9 pt. TNR font). The author to whom the correspondence should be addressed should be indicated, as well as email and full postal address.
Abstract. A short abstract in a single paragraph of no more than 200-250 words must accompany each manuscript (8 pt. TNR font). The abstract should briefly describe the content and results of the paper and should not contain any references.
Keywords. Authors should give 3-5 keywords.

Text

Introduction. Should include the aims of the study and results from previous notable studies.
Materials and Methods. Experimental methods should be described clearly and briefly.
Results and Discussions. This section may be separated into two parts. Unnecessary repetition should be avoided.
Conclusions. The general results of the research are discussed in this section.
Acknowledgements. Should be as short as possible.
References. Must be numbered in the paper, and listed in the order in which they appear.

Diagrams, Figures and Photographs should be constructed so as to be easy to understand and should be named "Figures"; their titles should be given below the Figure itself. The figures should be placed immediately near (after or before) the reference that is being made to them in the text. Figures should be referred to by numbers, and not by the expressions “below” or “above”. The number of figures should be kept to minimum (maximum 10 figures per paper).
Tables. Should be numbered consecutively throughout the paper. Their titles must be centered at the top of the tables (10 pt. TNR font). The tables text should be 9 pt. TNR font. Their dimensions should correspond to the format of the Journal page. Tables will hold only the horizontal lines defining the row heading and the final table line. The tables should be placed immediately near (after or before) the reference that is being made to them in the text. Tables should be referred to by numbers, and not by the expressions “below” or “above”. The measure units (expressed in International Measuring Systems) must be explicitly presented.
Formulas, Equations and Chemical Reactions should be numbered by Arabic numbers in round brackets, in order of appearance, and should be aligned left. The literal part of formulas should be in Italics. Formulas should be referred to by Arabic numbers in round brackets.
Nomenclature. Should be adequate and consistent throughout the paper, should conform as much as possible to the rules for Chemistry nomenclature. It is preferable to use the name of the substances instead of the chemical formulas in the text.
References should be numbered consecutively throughout the paper in order of citation in square brackets; the references should list recent literature also. Footnotes are not allowed. If the cited literature is in other language than English, the English translation of the title should be provided, followed by the original language in round brackets. Example: Handbook of Chemical Engineer (in Romanian), vol. 2, Technical Press, Bucharest, **1951**, 87.
We strongly recommend that authors cite references using DOIs where possible. DOIs are persistent links to an object/entity and can be used to cite and link to any article existing online, even if full citation information is not yet available. DOIs should always be displayed as full links. Example: Onem, E., Cin, G., Alankus, A., Pehlivan, H., Mutlu, M.M., Utilization of Chestnut Shell Wastes as a Dyeing Agent for Leather Industry, *Leather and Footwear Journal*, **2016**, 16, 4, 257-264, https://doi.org/10.24264/lfj.16.4.1.
Citation of Journal Articles: all authors' names (surname, name initials), abbreviated journal title, year, volume number, issue number, full page reference, e.g.: Helissey, P., Giorgi–Renault, S., Renault, J., *Chem Pharm Bull*, **1989**, 37, 9, 2413-2425.
In case the reference is not cited in original, the author(s) should also list the original paper that has been consulted.
Citation of Books: authors' full name and name (initials), title of the book, issue number in Arabic numbers, publishing house, editors' names (if present), city where the book has been published, year of publication, the page(s) containing the text that has been cited.
Citation of Patents: all authors' names (surname, name initials), or company's name, country and patent number, date of issuance.

Paper template is available for download on the journal's website, https://www.revistapielarieincaltaminte.ro.

Manuscript Submission

By submitting your manuscript to be considered for publishing in *Leather and Footwear Journal* you are giving consent to processing personal data for administration and publication purposes. Our Privacy Policy is available on the journal's website.
Manuscripts should be submitted in electronic format by email to the following address:

Dana Gurău, Editor-in-chief
INCDTP - Leather and Footwear Research Institute (ICPI)
93 Ion Minulescu St., code 030215, Bucharest, Romania
Phone: +4021-323.50.60; Fax: +4021-323.52.80.
E-mail: jlfjournal@gmail.com

INCDTP - SUCURSALA INSTITUTUL DE CERCETĂRI PIELĂRIE ÎNCĂLŢĂMINTE

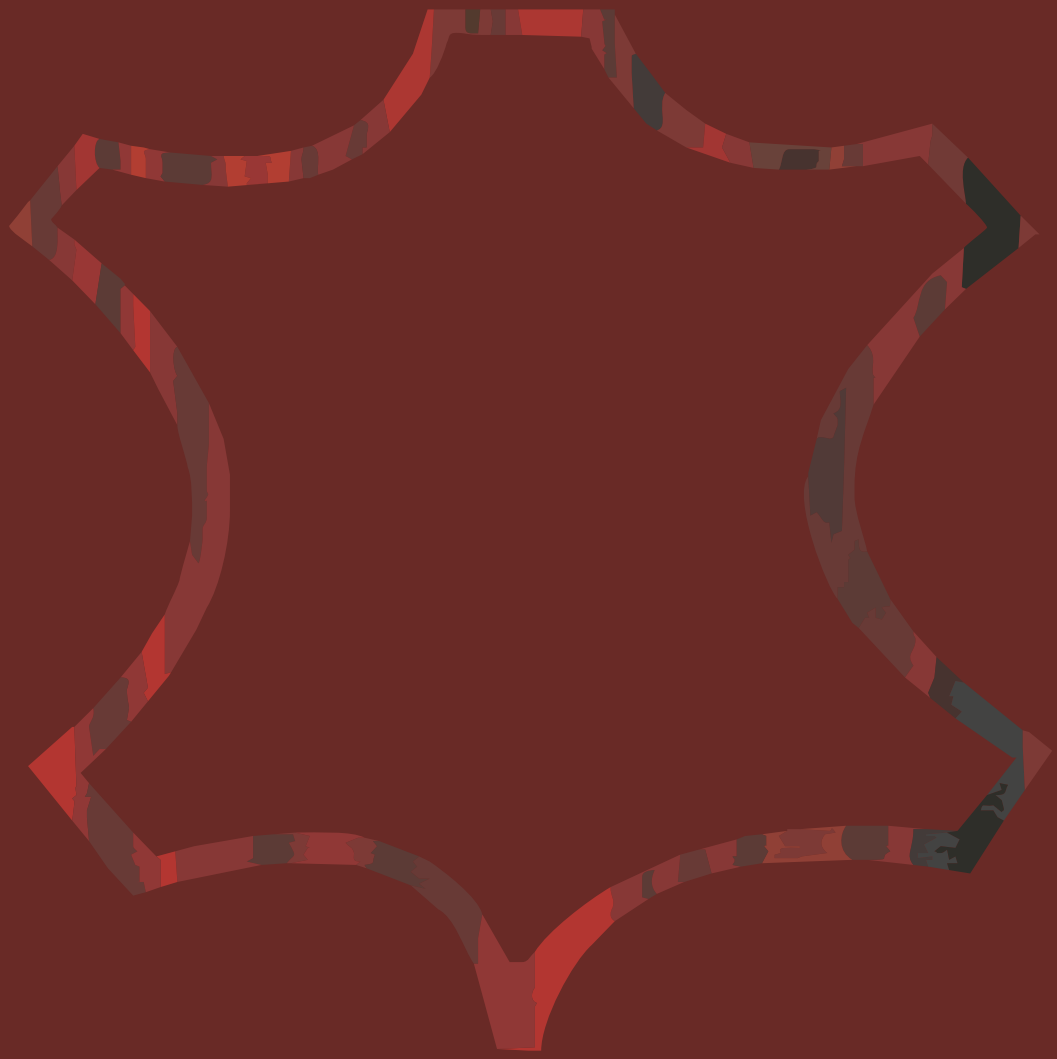

ISSN 1583-4433